

Hoai Jaclyn Hallam

2019

**The Dissertation Committee for Hoai Jaclyn Hallam Certifies that this is the approved  
version of the following dissertation:**

**CHARACTERIZATION OF GENETIC REASSORTMENT AND  
RECOMBINATION POTENTIALS BETWEEN ARUMOWOT VIRUS AND  
MP-12 VACCINE STRAIN**

**Committee:**

---

Tetsuro Ikegami, PhD, Mentor

---

Alan Barrett, PhD

---

Alexander Freiberg, PhD

---

Chad Mire, PhD

---

Hideki Ebihara, PhD

---

**CHARACTERIZATION OF GENETIC REASSORTMENT AND  
RECOMBINATION POTENTIALS BETWEEN ARUMOWOT VIRUS AND  
MP-12 VACCINE STRAIN**

**by**

**Hoai Jaclyn Hallam, B.S, MPH**

**Dissertation**

Presented to the Faculty of the Graduate School of

The University of Texas Medical Branch

in Partial Fulfillment

of the Requirements

for the Degree of

**Doctor of Philosophy**

**The University of Texas Medical Branch**

**March, 2019**

## **Dedication**

This work is dedicated to my husband, Steven, and son, William, and to my parents, Hong Dang and Hai Ly, for their endless inspiration, love, and support.

## **Acknowledgements**

Tetsuro Ikegami

Nandadeva Lokugamage

Shoko Nishiyama

Olga Slack

Masami Wada

Alan D. Barrett

Alexander Freiberg

Robert B. Tesh

Chad E. Mire

Terry L. Juelich

Jennifer K. Smith

David Perez

Lihong Zhang

John C. Morrill

**Mayo Clinic**

Hideki Ebihara

**The University of Texas at El Paso**

Douglas M. Watts

George Bettinger

**BioRad**

Raymond Miller

# Characterization of genetic reassortment and recombination potentials between Arumowot Virus and MP-12 vaccine strain

Publication No. \_\_\_\_\_

Hoai Jaclyn Hallam, PhD

The University of Texas Medical Branch, 2019

Supervisor: Tetsuro Ikegami, BVSc, PhD

**Abstract:** Rift Valley fever virus (RVFV) is a zoonotic arbovirus that causes significant morbidity and mortality in both humans and animals. In humans, the disease manifests itself as febrile illness, hemorrhagic fever, encephalitis, or retinitis. In animals, RVFV causes high rates of abortions and fetal malformations. Since the first Rift Valley fever (RVF) outbreak in 1930, there have been several major outbreaks across Africa and the Middle East. Effective control of RVF outbreaks via vaccination is important for both endemic and non-endemic countries. In some countries in Africa, inactivated and/or live-attenuated vaccines have been available for vaccinations of susceptible ruminants. In the U.S., a live-attenuated MP-12 vaccine strain was conditionally licensed for animal use, whereas it is also an Investigational New Drug for clinical trials. Upon the field trials of live-attenuated RVF MP-12 vaccine, potential formations of reassortant or recombinant strains between a vaccine strain and circulating pathogenic RVFV strains or other phleboviruses should be characterized. My central hypothesis is that genetic reassortment or recombination between two phleboviruses can occur when a loss or swap of gene element does not deteriorate the viability of resulting viruses. The overall objective of this study is to analyze genetic reassortment or recombination between RVFV MP-12 strain and AMTV, using co-infection assays and reverse genetics. The long-term goal is to establish a universal method to develop a novel pseudotype chimeric virus system applicable for most pathogenic phleboviruses. To address the central hypothesis, the following three aims are proposed. **Specific Aim 1:** Characterization of genetic reassortment between MP-12 strain and the genetic variant, rMP12-GM50, and between MP-12 strain and Arumowot virus, **Specific Aim 2:** Characterization of the attenuation and protective efficacy of rMP12-GM50 strain in mice, and **Specific Aim 3:** Characterization of recombinant MP-12 strain with AMTV genetic elements. Overall, the study will characterize potential occurrence of interspecies reassortment and recombination between RVFV and AMTV, and evaluate the significance of the presence of AMTV in RVF vaccination in endemic countries.

## TABLE OF CONTENTS

List of Tables .....	9
List of Figures .....	10
List of Abbreviations .....	13
Chapter 1 Introduction .....	17
Classification of phleboviruses .....	17
Genome structure and gene function .....	17
Rift Valley Fever .....	22
Mosquito-borne phleboviruses in Africa .....	27
Transmission of RVFV and AMTV .....	29
Viral life cycle of RVFV .....	30
RVF vaccines and the candidates .....	31
Specific Aims .....	33
Chapter 2 Characterization of genetic reassortment between MP-12 strain and the genetic variant, rMP12-GM50, and between MP-12 strain and Arumowot virus .....	36
Introduction .....	36
Material and methods .....	38
Results .....	48
Discussion .....	61
Chapter 3 Characterization of the attenuation and protective efficacy of rMP12-GM50 strain in mice .....	65
Introduction .....	65
Material and methods .....	66
Results .....	79

Discussion.....	77
Chapter 4 Characterization of recombinant MP-12 strain with AMTV genetic elements .....	80
Introduction.....	80
Material and methods.....	82
Results.....	89
Discussion.....	98
Chapter 5 Epilogue.....	103
Bibliography .....	107
Vitae .....	124

## **List of Tables**

Table 4.1	Summary of rMP-12 Chimeric Strain rescue result.....	90
-----------	--	----

## List of Figures

Figure 1.1: Rift Valley fever phlebovirus virion and genome structure.....	22
Figure 1.2: RVFV distribution in Africa.....	24
Figure 1.3: AMTV distribution in Africa.....	29
Figure 2.1: Indirect fluorescent assay to test the infectivity of rMP-12, rMP-GM50, and AMTV in C6/36 cells .....	42
Figure 2.2: PCR-RFLP analysis to genotype L-, M-, and S-segments of rMP-12 and rMP12-GM50 strains .....	44
Figure 2.3: RT-PCR analysis to genotype of L-, M-, and S-segments of the rMP-12 strain and AMTV.....	46
Figure 2.4: Changes in codon pair bias and codon usage in rMP12-GM50 strain.	50
Figure 2.5: Replication kinetics of rMP-12 and rMP12-GM50 in Vero cells and MRC-5 cells .....	51
Figure 2.6: Replication of the M-segment minigenomes of RVFV and AMTV in relation to co-expression of RVFV N and L proteins .....	53
Figure 2.7: Minigenome assays with expressions of N and L proteins derived from AMTV or RVFV .....	55
Figure 2.8: Minigenome assays with expressions of N, L, and Gn/Gc proteins derived from AMTV or RVFV.....	57

Figure 2.9: Reassortant formation between rMP-12 and rMP12-GM50 strains, or between rMP-12 and AMTV .....	59
Figure 3.1: Survival of mice infected with the parental rZH501 strain of Rift Valley fever virus or its reassortants with the rMP12-GM50 strain.....	71
Figure 3.2: Protective efficacy experiment 1: vaccination via subcutaneous route	73
Figure 3.3: Titers of Plaque Reduction Neutralization Test (PRNT <sub>80</sub> and PRNT <sub>50</sub> ) and clinical signs of disease observed in each mouse vaccinated via the subcutaneous route.....	74
Figure 3.4: Protective efficacy experiment 2: vaccination via subcutaneous or intramuscular route .....	76
Figure 4.1: Comparison of the terminal 3' and 5' ends of AMTV and MP-12.....	82
Figure 4.2: Rescued chimeric strains genome.....	85
Figure 4.3: Replication kinetics of chimeric strains in Vero and C6/36 cells.....	91
Figure 4.4: Viral RNA accumulation of chimeric MP-12 viruses (rMP-12 vs rMP12/GFP-AM-LUTR).....	93
Figure 4.5: Viral RNA accumulation of chimeric MP-12 viruses (rMP-12 vs rMP12-AM-SUTR).....	94
Figure 4.6: Alteration of L, M, S RNA ratios in virions via UTR exchanges.....	96
Figure 4.7: The replication kinetics of rMP-12, rMP12-AMTVNSs, or rMP12-ΔNSs <sub>16/198</sub> in MRC-5 and Hepa1-6.....	97

Figure 4.8: Induction of interferon- $\beta$  mRNA in MRC-5 cells or Hepa1-6 ..... 98

## List of Abbreviations

AMTV	Arumowot Virus
BHQ	Black Hole Quencher
BUNV	Bunyamwera virus
CAT	Chloramphenicol acetyltransferase
cDNA	Complementary DNA
cRNA	Complementary RNA
dpi	Days post infection
dpv	Days post vaccination
DI	Defective-interfering
DC-SIGN	Dendritic cell-specific intercellular adhesion molecule-3-grabbing non-integrin
DIVA	Differentiation of Infected from Vaccinated Animals
ddPCR	Droplet digital polymerase chain reaction
DMEM	Dulbecco's modified minimum essential medium
ER	Endoplasmic reticulum
eIF2 $\alpha$	Eukaryotic initiation factor 2
FBS	Fetal bovine serum
fLuc	Firefly luciferase
FFA	Focus-forming Assay
FFU	Focus-forming Unit
GFV	Gabek Forest virus
GM50	Gene marker 50

GAPDH	Glyceraldehyde 3-phosphate dehydrogenase
GORV	Gordil virus
GFP	Green fluorescent protein
HEX	Hexachloro-Fluorescein
HRP	Horseradish peroxidase
hpi	Hour post infection
hpt	Hour post transfection
IFA	Indirect fluorescent assay
IACUC	Institutional Animal Care and Use Committee
IRF3	Interferon regulatory factor 3
IGR	Intergenic region
i.m.	Intramuscular
i.p.	Intraperitoneal
LACV	La Crosse virus
L-segment	Large segment
MDA-5	Melanoma differentiation-associated protein 5
M-segment	Medium segment
mRNA	Messenger RNA
MEM	Minimum essential medium
MOI	Multiplicity of infection
NSs	Non-structural S protein
NF- $\kappa$ B	Nuclear factor- $\kappa$ B
N	Nucleoprotein

ODRV	Odrenisrou virus
ORF	Open reading frames
RFLP	PCR-restriction fragment length polymorphism
PFU	Plaque forming units
PRNT <sub>50</sub>	Plaque reduction neutralization test 50
PRNT <sub>80</sub>	Plaque reduction neutralization test 80
PTV	Punta Toro virus
rMP-12	Recombinant MP-12
rLuc	Renilla luciferase
RVF	Rift Valley fever
RVFV	Rift Valley fever phlebovirus
RIG-I	retinoic acid-inducible gene 1
L protein	RNA-dependent RNA polymerase
SAFV	Saint Floris virus
SFNV	Sandfly fever Naples phlebovirus
SFSV	Sandfly fever Sicilian virus
Ser	Serine
SAP30	Sin3A Associated Protein 30
S-segment	Small segment
s.c.	subcutaneous
TOSV	Toscana virus
TF	Transcription factor
TPB	Tryptose phosphate broth

U.S.A	United States of America
UTMB	The University of Texas Medical Branch at Galveston
UTR	Untranslated regions
vRNA	Viral RNA
VLP	Virus-like particles
YY1	Yin Yang 1

## CHAPTER 1: Introduction

### Classification of phleboviruses

According to the International Committee on Taxonomy of Viruses in 2018, the *Bunyavirales* order consists of twelve families: *Arenaviridae*, *Cruliviridae*, *Fimoviridae*, *Hantaviridae*, *Myxoviridae*, *Nairoviridae*, *Peribunyaviridae*, *Leishbuviridae*, *Phasmaviridae*, *Phenuiviridae*, *Tospoviridae*, and *Wupedeviridae*, encompassing 300 species and 45 genera, including highly pathogenic species that lack effective vaccines for the prevention of outbreaks. *Phlebovirus* is one of the 14 genera within the family *Phenuiviridae*. As of current, there are 10 species assigned under the genus *Phlebovirus*: *Bujaru*, *Candiru*, *Chilibre*, *Frijoles*, *Punta Toro*, *Rift Valley fever*, *Salahabad*, *Sandfly fever Naples*, *Mukawa*, and *Uukuniemi phleboviruses*. There are also unclassified phleboviruses, which are not assigned to any species. Those viral members could be grouped into similar representative phlebovirus species, via genetic or serologic relation to one another. The phlebovirus genome is comprised of tripartite single-stranded RNA with negative or ambi-sense polarity. Among phleboviruses, Rift Valley fever virus (RVFV) is classified as a Category A Priority Pathogen by the National Institutes of Health in the United States of America (U.S.A), due to the grave economic and health consequences upon introduction into the U.S.A, and an overlap Select Agent by the U.S. Department of Health and Human Services, and U.S. Department of Agriculture<sup>1</sup>.

### Genome structure and gene functions

The genome of phleboviruses is comprised of Small (S), Medium (M), and Large (L) RNA segments. The S segment encodes two open reading frames (ORF) that encode the nucleoprotein

(N) and the non-structural (NSs) protein in an ambi-sense manner. Termination of mRNA synthesis occurs within the intergenic region (IGR), which is located between the two ORFs in the S-segment, or within the 5' untranslated regions (UTR) of the M- or L- RNA segments<sup>2-4</sup> (Fig. 1.1). The 3' and 5' termini of each viral RNA segment are complementary and form a stable pan-handle structure, which serves as a signal for the encapsidation of viral RNA with N protein, viral RNA replication, and viral mRNA transcription<sup>5</sup>.

The viral-sense and anti-viral sense S-segment encode N mRNA and NSs mRNA, respectively. The N protein is the nucleocapsid protein and is the most abundant viral protein in the virion and is the major structural component of the RNP complex. It has a molecular weight of roughly 27-kDa and forms hexamers through interactions with its N terminus. The N terminus is thus important for the oligomerization of the N protein, where the extension of the N-terminal arm interacts with the hydrophobic pocket of the adjacent subunit thus mediating an inter-molecular interaction crucial for hexamer formation<sup>6</sup>. In the monomeric form, however, the N-terminal arm makes an intra-molecular interaction and binds to its own hydrophobic core. In addition to preventing oligomerization, this monomeric structure also covers the RNA binding cleft, so that it does not bind to viral RNA. Each N subunit has been described to accommodate up to 6 bases, thus one hexamer can hold 36 bases<sup>6</sup>. Overall, the N protein plays an important role in protecting the viral RNA through encapsidation, as well as an active role in viral transcription, replication, and packaging.

The RVFV NSs protein is estimated to be 31-kDa in size and is considered the major virulence factor that plays an important role in viral evasion from the host innate immunity. The NSs protein is present in both the nucleus and cytoplasm of RVFV-infected cells and forms filamentous structures in the nucleus. The stable core domain of RVFV NSs (residues 83–248) is

responsible for the formation of this filamentous structure as well nuclear translocation<sup>7</sup>. RVFV NSs protein is a type-I IFN antagonist, and cells infected with RVFV fails to up-regulate IFN- $\beta$  mRNA<sup>8,9</sup>. Le May et al. demonstrated that the NSs protein binds to the Sin3A Associated Protein 30 (SAP30) and subsequently prevents the activation of the IFN- $\beta$  promoter through its interaction with a transcription factor, Yin Yang 1 (YY1) protein<sup>10,11</sup>. In the presence of this NSs-SAP30-YY1 complex, the cAMP-response element-binding protein-binding protein cannot be recruited to the IFN- $\beta$  promoter, and subsequent acetylation of histone K8H4 or K14H3 cannot occur. RIG-I, however, is still shown to be activated and nuclear translocation of interferon regulatory factor 3 (IRF3), nuclear factor- $\kappa$ B (NF- $\kappa$ B), and activator protein 1 still occurs<sup>12</sup>. Thus, RVFV NSs protein inhibits the upregulation of the IFN- $\beta$  promoter downstream of the activation of transcription factors. Le May et al. also demonstrated that the RVFV NSs protein inhibits general cellular transcription activity by interacting with transcription factor (TF) IIH components, specifically, the p44 and p62 subunits<sup>13</sup>. TFIID is a major component of the transcription pre-initiation complex, and promotes transcription by opening the promoter site and activating cellular RNA Polymerase II through phosphorylation of its carboxyl-terminal domain. Ten different subunits comprise TFIID; cdk7, MAT1, cyclin H, XPB, XPD, p8, p34, p44, p52, and p62<sup>14</sup>. The NSs protein binds to the p44 subunit and sequesters it from the assembly site of TFIID, thus preventing and interrupting the TFIID complex assembly. In contrast, the NSs protein causes the post-translational degradation of the p62 subunit, through the E3 ligase complex, which consists of cullin 1, Skp1, and FBXO3. Another function of the RVFV NSs protein is the degradation of PKR<sup>15,16</sup>. Pathogen recognition receptors, including RIG-I (retinoic acid-inducible gene 1), TLR (toll-like receptor)-3, and MDA-5 (melanoma differentiation-associated protein 5); can recognize viral RNA and induce IFN- $\beta$  gene expression through the activation of transcription factors, such as IRF3 and

NF- $\kappa$ B. The induced IFN- $\beta$  protein then up-regulates IFN- $\alpha$  and interferon-stimulated genes. Both endogenously expressed PKR and transcriptionally-induced PKR via IFNs can inhibit host and viral translational initiation via the phosphorylation of its substrate protein, eukaryotic initiation factor 2 (eIF2 $\alpha$ ). Activation of PKR occurs when it binds to dsRNA or the 5' triphosphated ssRNA at the N-terminal domain, causing a structural change that results in an activated kinase<sup>17</sup>. The phosphorylated eIF2 $\alpha$  then forms a stable complex with eIF2B, which is required for the conversion of eIF2-GDP to eIF2-GTP, and thus, the sequestration of eIF2B leads to the cessation of translational initiation. Similar to the degradation of the p62 subunit, the degradation of PKR occurs through the E3 ligase complex, consisting of cullin 1, Skp1, and FBXW11. The RVFV NSs protein forms two different E3 ligase complexes and promotes the degradation of p62 or PKR through different F-box proteins. In addition to RVFV NSs protein, Toscana virus (TOSV) NSs protein is also shown to promote the degradation of PKR<sup>15,16,18</sup>. TOSV NSs protein localizes in the cytoplasm and inhibits the nuclear localization of IRF3. TOSV NSs protein also interacts with RIG-I or PKR, and promotes the degradation of RIG-I and PKR via the proteasome pathway<sup>18,19</sup>. Other NSs proteins, such as Bunyamwera virus (BUNV), La Crosse virus (LACV), Punta Toro virus (PTV), SFSV, or Severe Fever with Thrombocytopenia Syndrome virus have also been reported to inhibit the induction of IFN- $\beta$  mRNA.

The RVFV M-segment encodes a single ORF for a precursor polyprotein that is co-translationally cleaved into the 78kD, NSm, Gn and Gc proteins by cellular signal peptidases<sup>20</sup>. Five in-frame AUGs initiation codons are located in the preglycoprotein region, and is involved in the biogenesis of precursor polyproteins through a leaky scanning mechanism. Initiation of translation at the first AUG codon leads to the synthesis of an 78kD-Gc precursor where cleavage leads to the production of the 78kDa protein and Gc. Initiation of translation from the second AUG

leads to the synthesis of an NSm-Gn-Gc precursor and after cleavage, it generates the NSm, Gn, and Gc protein. The third, fourth and fifth AUG are not dominantly utilized when the 1<sup>st</sup> and 2<sup>nd</sup> AUGs are available, whereas they also contribute to Gn and Gc expression, if upstream AUGs are not available due to mutations or truncations. The 78kD protein and NSm are dispensable for viral replication in host cells, whereas the Gn and Gc together constitute the viral glycoproteins that are found in the envelope of mature virions (Fig. 1.1). The RVFV 78kD protein is reported to be a structural protein that is incorporated into matured virions from infected C6/36 mosquito cells, but not from Vero cells<sup>21</sup>. The 78kD protein also plays a role in efficient viral dissemination in mosquitoes through an unknown mechanism<sup>22-24</sup>. RVFV NSm proteins localize to the mitochondrial outer membrane and delay apoptosis in mammalian cells<sup>25,26</sup>.

The L-segment encodes the RNA-dependent RNA polymerase (L protein) that functions in both viral RNA replication and transcription. The L protein is packaged into virions with viral RNP and is responsible for genomic RNA replication, which begins with the synthesis of complementary-sense (positive-sense) copies of the genome (cRNA), which are then copied into viral-sense (negative-sense) RNA (vRNA). Unlike viral mRNA synthesis, neither cRNA nor vRNA synthesis requires an oligonucleotide cap primer. N encapsidation of vRNA, however, is required for viral RNA replication and transcription<sup>27</sup>. Viral mRNA transcription occurs through a cap-snatching mechanism where the L protein, through its endonuclease activity, cleaves capped host mRNA and uses it as a primer to initiate mRNA synthesis<sup>28,29</sup>.

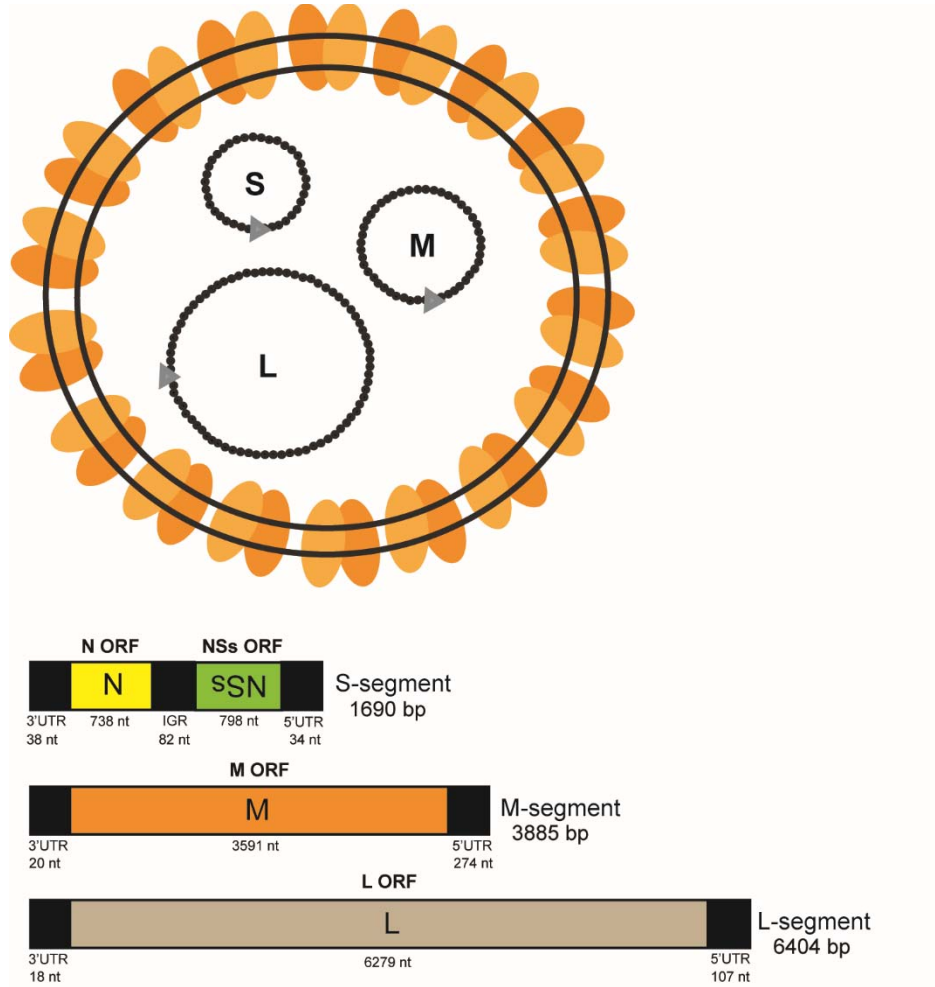


**Figure 1.1: Rift Valley fever phlebovirus virion and genome structure**

The virion of RVFV contains the RNP, which consists of the viral genomic RNA encapsidated with the nucleoproteins (N). The L protein is also packaged within mature virion to initiate primary transcription and replication after infection. RVFV has a lipid bilayer that contains the viral glycoproteins Gn and Gc (shown in orange in the top panel). The genome of phleboviruses is comprised of three negative- or ambi-sense RNA segments named Small (S), Medium (M), and Large (L). The S segment encodes two open reading frames (ORFs) that encode the N and the non-structural (NSs) protein in an ambi-sense manner (Bottom panel). Termination of mRNA synthesis occurs within the intergenic region (IGR), or within the 5' untranslated regions (UTR) of the M- or L- RNA segments (shown in black in the bottom panel). The 3' and 5' termini of each viral RNA segment are complementary and form a stable pan-handle structure, which serves as a signal for the encapsidation of viral RNA with N protein, viral RNA replication, and viral mRNA transcription.

## Rift Valley fever

RVFV is transmitted by mosquitoes, and causes significant morbidity and mortality in both animal and human hosts. Floodwater *Aedes* spp. mosquitoes play an important role in the viral maintenance of RVFV. Ideal conditions for hatching of floodwater *Aedes* spp. mosquito eggs are

established during periods of heavy rainfall or irrigation. An increase of infected mosquitoes can lead to an amplification of RVFV in ruminants and mosquitoes, which subsequently triggers outbreaks of RVF in endemic areas. In ruminants, such as sheep, cattle, and goats, RVFV causes high rates of spontaneous abortions and fetal malformations<sup>30</sup>. Human transmission of RVFV occurs through direct contact with bodily fluids or aerosols derived from infected animals or from the bite of an infected mosquito. The disease, Rift Valley fever (RVF), is characterized by febrile illness, hemorrhagic fever, encephalitis, or retinitis in humans. Since the first RVF outbreak in Kenya in 1930, there have been several major outbreaks, including in Egypt in 1977-1978, resulting in an estimated 20,000 to 200,000 infections and 600 deaths<sup>31</sup>. Outbreaks of RVF have been predominantly reported in sub-Saharan Africa, but have spread into Egypt, Madagascar, and the Arabian Peninsula (Fig.1.2). In 2000, a large outbreak of RVFV occurred in Saudi Arabia and Yemen and resulted in 886 reported cases with a case fatality rate of 13.9%<sup>32</sup>. Effective control of RVF outbreaks is important not only in endemic countries but also in non-endemic countries due to the potential introduction of RVFV. In Africa, inactivated vaccines, and live-attenuated vaccines [i.e., the Smithburn vaccine from the Onderstepoort Biological Products (OBP) or the Kenya Veterinary Vaccines Production Institute (KEVEVAPI); the Clone 13 vaccine from the OBP] are available for vaccination of susceptible ruminants in registered countries. The latter provides prolonged protective immunity in ruminants with a single dose. The Smithburn vaccine retains significant residual virulence (e.g., fetal malformation or abortion) and formed a reassortant strain with circulating pathogenic RVFV in a human. It is thus important to evaluate potential formation of genetic reassortants via any live-attenuated RVF vaccine, which is used in field trials.

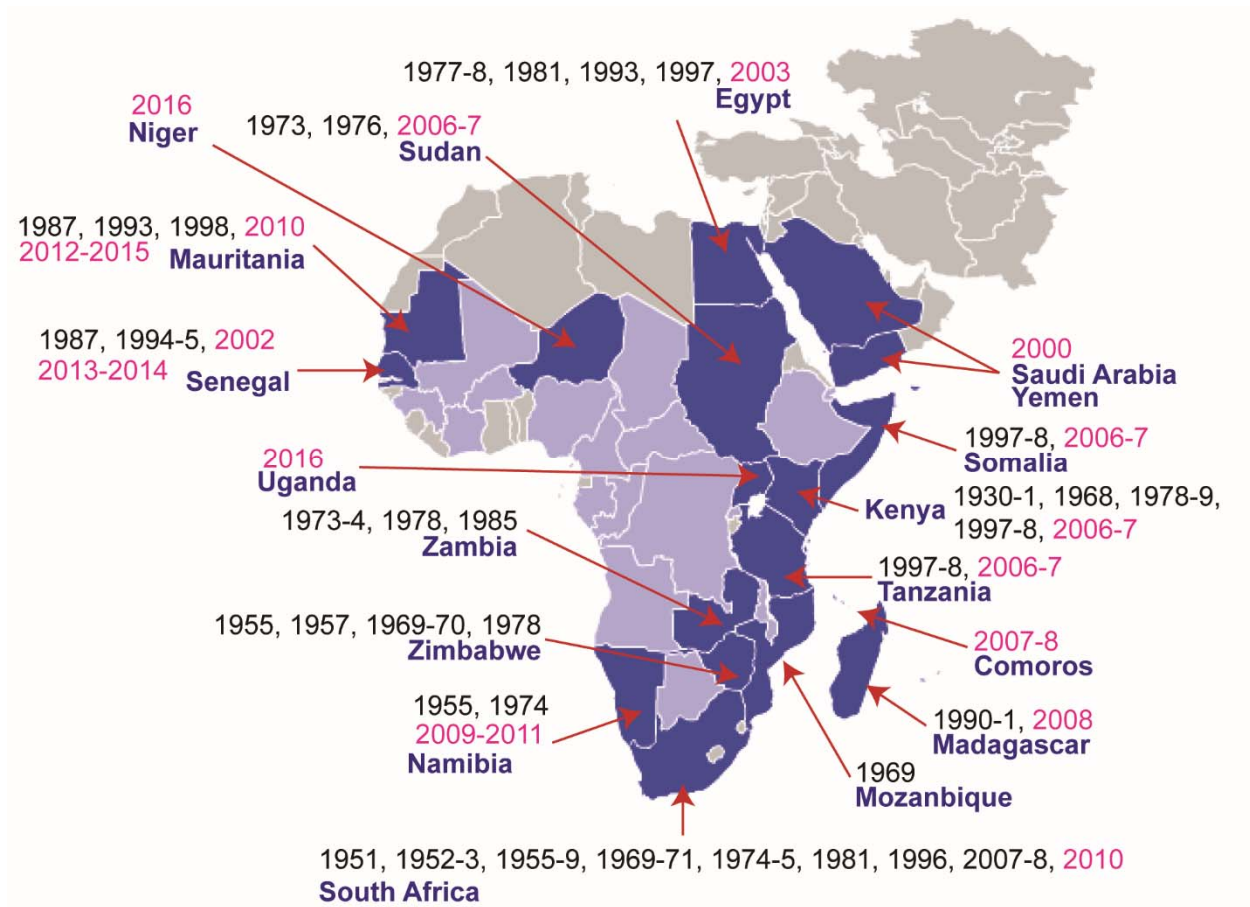


**Figure 1.2: Rift Valley Fever Virus Distribution in Africa**

Map illustrating endemic regions for RVFV. Countries shown in dark blue represents reported outbreaks of RVFV. The year for each reported outbreak in the respective country is also shown. Countries shown in light blue represent regions where RVFV has been isolated.

During the RVF outbreak in 1930, RVF was characterized by high rates of abortions and fetal malformations in pregnant ewes, and high mortality in newborn lambs<sup>33</sup>. The susceptibility of sheep to RVFV is largely age-dependent, and the mortality rate in RVFV-infected newborn lambs is 95 to 100%, whereas in adult sheep it is approximately 20%<sup>34</sup>. Symptoms, which include elevated body temperature (40–42°C), loss of appetite, and decreased physical activity, have been reported to occur 12 to 18 hours before death<sup>34</sup>. Lethal fulminant liver necrosis can occur in infected lambs, as the disease progresses<sup>35</sup>. Older sheep are less susceptible to RVFV,<sup>36</sup> and the disease is characterized by lethargy, nasal discharge, viremia, fever, and diarrhea<sup>34</sup>. More severe

clinical signs of diseases include widespread rash and bruising in hairless areas, bleeding from nares, and bloody diarrhea<sup>37,38</sup>. RVFV can also cause disease in other animals including cattle, goats, camels, ferrets, dogs, and cats<sup>33,34,39–43</sup>. Interestingly, in the case of the latter two animals, dogs and cats did not display any signs of disease yet had detectable viremia and neutralizing antibody after exposure through the aerosol route<sup>42</sup>. Other animals, such as birds and reptiles were described to be refractory, while other livestock species such as pigs and horses, were reported to be resistant to RVFV infection<sup>44</sup>. The mechanism of species-specific susceptibility to RVFV infection is unknown to date.

Humans infected with RVFV generally exhibit a self-limiting febrile illness<sup>33,39,45–49</sup>. Symptoms, which may vary among patients, begin to manifest after an incubation period of 4-6 days; i.e., chills, malaise, dizziness, weakness, severe headache and/or sensation of fullness in the liver<sup>39,45,47</sup>, which is then followed by a decrease in blood pressure, elevated body temperature (38.8–39.5°C), muscle aches, shivering, insomnia, and constipation<sup>33,39,47–49</sup>. Other symptoms such as nosebleeds, impaired taste, photophobia, and vomiting and/or diarrhea have also been reported<sup>33,39,47–49</sup>. Patients have been shown to improve several days after the onset of symptoms, whereas a resurgent fever with severe headaches has been reported to occur in some patients within a few days after initial recovery<sup>33,39,48,49</sup>. This secondary febrile phase can last between a few days to up to 10 days. In the convalescent period, patients may still experience continuous pain in the legs, lasting up to 2 weeks<sup>33,47</sup>. Additionally, patients may develop massive blood clots in the coronary artery, malaise, frequent headaches, weakness, a sense of disequilibrium, and pain when moving the eyes<sup>48</sup>. Viremia is normally detected during the febrile period, and antibodies specific to RVFV usually develop by the fourth day after onset. This antibody response is able to subsequently neutralize and eliminate RVFV infection<sup>33,39,46,47,49</sup>.

The development of hemorrhagic disease is often seen in fatal RVF cases<sup>50,51</sup>. Symptoms start abruptly and include, fever, shivering, headaches, body aches, and nausea. These cases may also include bruising in the limbs and/or eyelids; bleeding in the mouth and/or gastrointestinal tract; vomiting blood; and bloody diarrhea<sup>51</sup>. Other reported symptoms may include a raised rash on the upper body, throat pain, jaundice, and/or enlargement of both the liver and the spleen<sup>51,52</sup>. Although death can be delayed for up to 17 days after the onset of symptoms, it usually occurs within 3–6 days. An acute hepatic injury is also thought to play a role in human deaths caused by RVFV infection, as widespread liver necrosis has been observed in autopsies<sup>50,52</sup>.

Another serious outcome of patients infected with RVFV is viral infection in the central nervous system, which usually develops one to two weeks after the onset of symptoms. Symptoms usually include fever, confusion, temporal blindness, and paralysis<sup>53–55</sup>. Indicative of meningeal inflammation or meningoencephalitis is increased white blood cell count found in the cerebrospinal fluid<sup>53</sup>. Hemorrhage and inflammation in both eyes have also been documented in RVF-induced encephalitis<sup>53</sup>. Focal necrosis associated with perivascular cuffing with infiltrations of macrophages and lymphocytes was demonstrated in histopathological examinations of encephalitic brains<sup>55</sup>.

RVFV can also cause retinopathy or maculopathy, resulting in blurred vision and/or loss of highly susceptible central vision. Vision changes can affect one or both eyes and can occur immediately or weeks to months after the onset of symptoms<sup>56–58</sup>. In some patients, obstruction or blockage of the retinal arteries, irritation and swelling of the middle layer of the eye, and even detachment of the retina can occur<sup>56,58–60</sup>. In a few patients, partial improvement in vision is seen after several months while in other, however, scarring of the central retina causes permanent blindness or impaired vision<sup>56–59</sup>.

As can be seen, clinical symptoms of RVF vary widely among patients in different outbreaks. Additionally, the determinant of host susceptibility to induce hemorrhagic fever or encephalitis in humans has not been identified or characterized. It is also unknown through which mechanisms RVFV causes diseases such as neurological disorders, vision loss or thrombosis in the presence of protective antibodies.

### **Mosquito-borne phleboviruses in Africa**

In Burkina Faso, serological studies revealed that local sheep had antibodies specific to not only RVFV, but also other related phleboviruses such as Arumowot virus (AMTV), Odrenisrou virus (ODRV), Gabek Forest virus (GFV), Saint Floris virus (SAFV), and Gordil virus (GORV)<sup>61</sup>. Among those phleboviruses, AMTV and ODRV are transmitted by mosquitoes and are phylogenetically grouped into the Salehabad species complex. AMTV is transmitted by *Cx. antennatus*, one of the highly competent vectors for RVFV, and thus, co-infection of RVFV and AMTV is expected to occur in mosquitoes<sup>62-64</sup>. Although RVFV can form reassortant strains via co-infection with different RVFV strains<sup>65</sup>, there has been no evidence of interspecies reassortment between RVFV and other phleboviruses. Ngari virus, which was isolated from patients during an RVF outbreak in Kenya, Somalia, and Tanzania between 1997 and 1998, was found to be a reassortant strain, which encoded the M-segment of Batai virus and the L-, and the S-segments of Bunyamwera virus, both of which are within the *Orthobunyavirus* genus of the *Peribunyaviridae* family<sup>66,67</sup>. Accordingly, the identification and characterization of interspecies genetic reassortment upon vaccination using live-attenuated RVFV strains in endemic countries is considered important. In the U.S., a live-attenuated MP-12 vaccine strain is conditionally licensed for veterinary use in ruminants, and is also an Investigational New Drug under clinical trials in humans.

There are no evidence of human or animal diseases associated with AMTV infections. AMTV is predominantly present in Africa, and past isolation of AMTV includes rodents from Nigeria, the Kurrichane Thrush (*Turdus libonyanus*), which is a species of birds, from the Central African Republic (CAR), and mosquitoes from Sudan<sup>68,69</sup> (Fig. 1.3). Evidence of seroprevalence was demonstrated in sheep in Burkina Faso and in humans in Sierra Leone, Sudan, Egypt, and Somalia<sup>61,69</sup>. There have been few pathological studies of AMTV in animals. Swanepoel et al. inoculated AMTV into sheep, and demonstrated transient mild fever without signs of viremia<sup>70</sup>. Tesh et al. demonstrated transient viremia with titers around  $10^5$ - $10^7$  plaque forming units (PFU)/mL in Syrian hamsters after three days post infection with AMTV via s.c. All hamsters survived without developing any severe sequelae<sup>71</sup>. In addition to AMTV, Tesh et al. also demonstrated viremia in hamsters with other phleboviruses such as Chagres, and Gabek Forest viruses. Arumowot and Chagres viruses produced nonfatal infections in hamsters via s.c. with  $10^{5.4}$  PFU and  $10^{3.0}$  PFU, respectively. In contrast, Gabek Forest virus infection via s.c. with  $10^{4.6}$  PFU, was fatal in hamsters. Interestingly, in hamsters previously infected with AMTV and/or Chagres virus, Gabek Forest infection was less severe. This indicated some level of cross-protection between these strains.

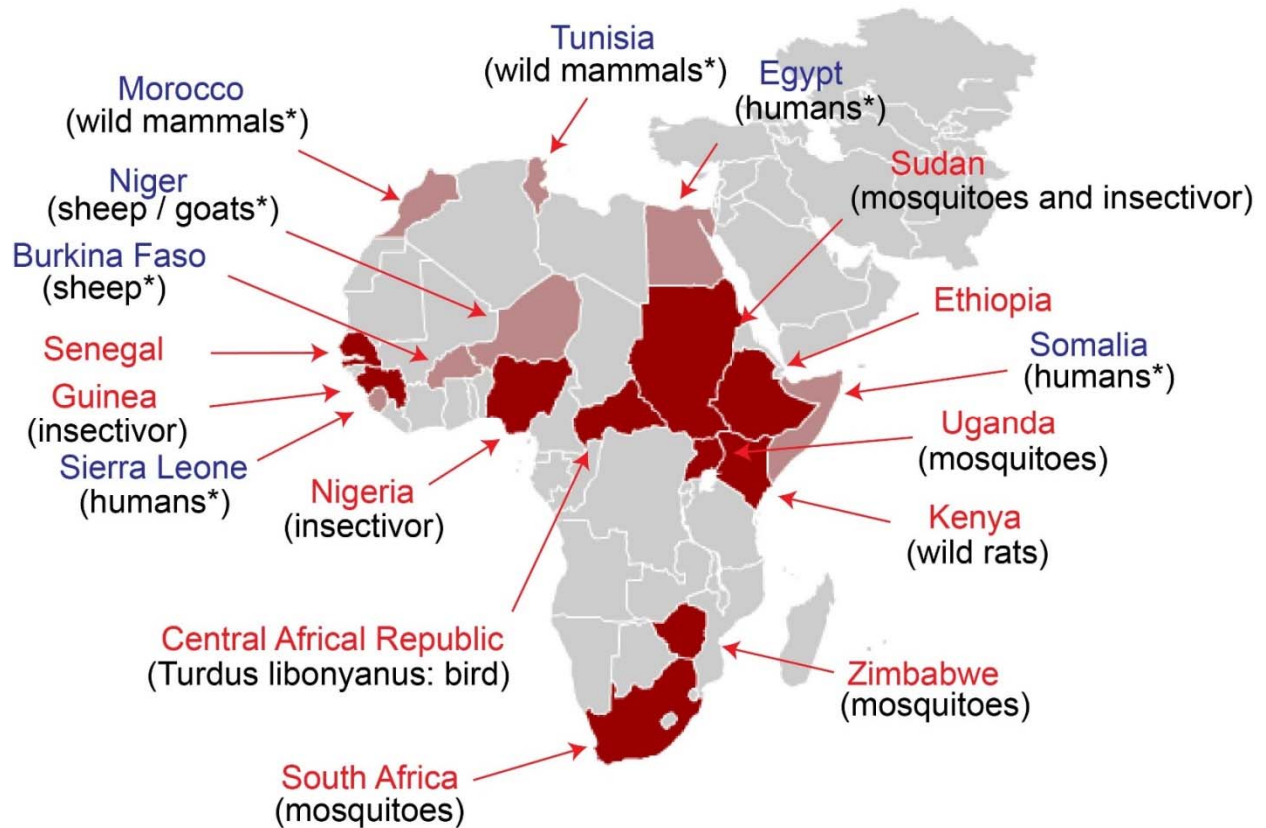


**Figure 1.3: Arumowot Virus Distribution in Africa**

Map illustrating countries where AMTV has been isolated (red) or circulating due to serological evidence (light red). Asterisk indicates seropositive.

### Transmission of RVFV and AMTV

RVFV is transmitted through the bite of an infected mosquito or through direct contact with bodily fluids from infected animals. Vertical transmission in mosquitoes and transmission among animals and mosquitoes allows RVFV to persist in endemic areas of Africa<sup>72</sup>. In East Africa the weather pattern, known as the El Nino Southern Oscillation cycle, often causes heavy rain. These periods of heavy rainfall promote transmission of RVFV among floodwater *Aedes* mosquitoes that thrive in such conditions. These cycles allow RVFV to continue endemic cycles, even during extreme drought<sup>30,73</sup>. *Aedes* mosquitoes lay their eggs in shallow wetlands called dambos, which dry up during periods of drought and refill when heavy rain falls. Following heavy

rains, infected eggs hatch and release RVFV-infected adults into the surrounding environment. Infected mosquitoes then feed on wild animals and local livestock, transmitting RVFV where it is then amplified in the animal host. The virus is then further transmitted by other mosquitoes into further animals or humans<sup>74</sup>. *Culex* mosquitoes feed on infected livestock and act as amplifying vectors by spreading RVFV to larger numbers of livestock and humans<sup>74</sup>. Though humans can be infected through mosquito bites, the handling of bodily fluids derived from infected animals appears to be the major route of infection<sup>74,75</sup>. Although RVF patients develop transient viremia, there has been no evidence of human-to-human transmission in RVF outbreaks. Vertical transmission of RVFV in humans may occur in rare cases, in which pregnant mothers transmit RVFV to their fetuses *in utero*<sup>76</sup>.

AMTV is also transmitted via mosquitoes; specifically, the *Culex antennatus* in the African continent and seroprevalence has been reported in sheep, humans, birds, and rodents. Other than these few facts, little is known about the pathogenesis of AMTV.

### **Viral life cycle of RVFV**

RVFV begins its life cycle with attachment to receptors expressed on host cells. RVFV has been reported to utilize the dendritic cell-specific intercellular adhesion molecule-3-grabbing non-integrin (DC-SIGN) and heparan sulfate as receptors for entry into a cell<sup>77,78</sup>. DC-SIGN is expressed on immature dendritic cells, which are major antigen-presenting cells of the immune system, and macrophages, and binds to carbohydrate chains attached to RVFV virions. Meanwhile, most cells express heparan sulfate on their surfaces, and the electrostatic interaction between negatively-charged heparan sulfate and positively-charged residues on the virion surface, support the broad cellular tropism of RVFV<sup>78</sup>. After attachment, RVFV enters the cells via

caveolae-mediated endocytosis<sup>79</sup>. RVFV then proceeds through the endosomal pathway, and the low pH within the late endosomal environment induces a structural change of Gc proteins, which exposes the fusion domain. The viral fusion domain inserts into the endosomal membrane, fusing the endosome and the viral envelope, resulting in the release of the RNP into the cytoplasm<sup>80,81</sup>. Upon being released into the cytoplasm, the L protein begins to transcribe the viral RNA to make viral mRNA. This is known as primary transcription. Following viral protein synthesis, further transcription from amplified genomic RNA (secondary transcription) can occur. Overall accumulations of viral L, M, and S-segment RNA as well as N, L, Gn, and Gc proteins lead to the assembly of viral structural components. The Gc proteins encode an endoplasmic reticulum (ER) localization signal and localizes to the ER by itself. The Gn encodes a Golgi retention signal, and the co-expression of Gn and Gc proteins lead to their co-localization to the Golgi apparatus<sup>82</sup>. After the localization of Gn and Gc proteins to the Golgi, the cytoplasmic tails of Gn and Gc are considered to recruit all L, M, and S-segment RNA, which are encapsidated with N proteins and attached to L proteins. Virions that bud into the Golgi lumens can be further matured via attachment and alteration of carbohydrate chains onto Gn and Gc proteins. Following all this, matured virions are allowed to be released from the cell.

### **RVF vaccines and the candidates**

Effective control of RVF outbreaks is important not only in endemic countries but also for non-endemic countries. One of the most important approaches to minimizing such impact of RVF outbreaks is through effective vaccination of susceptible animals and humans at risk of RVFV exposure<sup>83,84</sup>. In some countries in endemic regions, the Smithburn and/or the Clone 13 vaccines are available for vaccination of susceptible ruminants. The Smithburn strain, which is a live-

attenuated vaccine, was isolated from mosquitoes in Uganda and was developed via serial passages in mouse brains. The Clone 13 was isolated from a non-fatal human case of RVF and is a live-attenuated natural mutant carrying a large deletion in the NSs gene in the S segment (NSs). In the U.S., a live-attenuated MP-12 vaccine was conditionally licensed for veterinary use. The MP-12 strain was generated from serial passages of the ZH548 strain, which was previously isolated from a RVF patient during an outbreak in Egypt, in the presence of a chemical mutagen, 5-fluorouracil, in MRC-5 cells. The resulting strain encodes 23 mutations in the L-, M-, and S-segments. There are currently no licensed RVF vaccines or therapeutics available for humans. Live-attenuated RVF vaccines have shown strong protective efficacies in ruminants following a single dose without adjuvants. Since these vaccine strains replicate in vaccinated animals, residual virulence might be a concern for vulnerable populations, including pregnant or newborn animals<sup>83,85</sup>, whereas the formation of reassortants of the vaccine strain with wt RVFV or other phleboviruses might occur as well. Although subunit vaccines, DNA vaccines, viral vectors, and single-cycle RVF replicons are highly safe in animals due to a lack of viral spread, the vaccine immunogenicity of these novel candidates is not as high as live-attenuated vaccines, and a booster dose and/or the use of adjuvants might be required to induce long-term protective immunity<sup>86-89</sup>.

### **Specific Aims**

RVFV is a zoonotic arbovirus that causes significant morbidity and mortality in both humans and animals. Humans become infected with RVFV mainly through direct contact with bodily fluids as well as aerosols derived from infected animals or from the bite of an infected mosquito. The disease manifests itself as febrile illness, hemorrhagic fever, encephalitis, or retinitis. In ruminants, such as sheep, cattle, or goats, RVFV causes high rates of abortions and

fetal malformations<sup>30</sup>. Since the first RVF outbreak in 1930, there have been several major outbreaks, including the 1977 outbreak in Egypt with an estimated 600 human deaths<sup>31</sup>. Due to the significant impact on public health, RVFV is also classified as a Category A Priority Pathogen by the National Institutes of Health in the U.S., and an overlap Select Agent by the U.S. Departments of Health and Human Services and Agriculture<sup>30</sup>. As mentioned above, effective control of RVF outbreaks is important not only in endemic countries but also for non-endemic countries. In Africa, both inactivated and live-attenuated vaccines are available for vaccinations of susceptible ruminants. Although the latter provides prolonged protective immunity in ruminants with a single dose, residual virulence and the potential formation of reassortant strains with circulating pathogenic RVFV or other phleboviruses is a concern. In Burkina Faso, serological study revealed that sheep had antibodies specific to not only RVFV, but also other phleboviruses such as AMTV, ODRV, GFV, SAFV, and GORV<sup>61</sup>. Among these, AMTV and ODRV are transmitted by mosquitoes and are classified within the Salehabad species complex. AMTV is transmitted by *Cx. antennatus*, which is one of the highly competent vectors for RVFV, and thus, co-infection of RVFV and AMTV is expected to occur in mosquitoes<sup>63,64</sup>. Although RVFV can form reassortant strain via co-infection with different RVFV strains, interspecies reassortment has not been characterized for RVFV, and the potential of interspecies genetic reassortment upon vaccination using live-attenuated RVFV strains in endemic countries is important<sup>65</sup>. In the U.S., a live-attenuated MP-12 vaccine strain was conditionally licensed for animal use and is currently an Investigational New Drug under clinical trials in humans. In this study, I aim to characterize the genetic reassortment between MP-12 and the genetic variant, rMP12-GM50, and between MP-12 and AMTV. Although I hypothesize that the structural proteins, N, L and Gn/Gc, of AMTV cannot replace the functions of MP-12 strain for the formation of reassortants due to a lack of similarity, the UTR of genomic RNA is likely interchangeable among phlebovirus species. The 3'- and 5'-

termini of genomic RNA and the overall genome structure are highly conserved among phlebovirus species. The truncation of 5' UTR of RVFV M-segment is known to affect the co-packaging of L- and S-segment RNA, indicating a co-packaging signal located within the M-segment 5'-UTR<sup>90</sup>. I thus presume that a partial replacement of the MP-12 UTR with that of AMTV will alter the phenotype of MP-12 by reducing the efficiency of genomic RNA packaging. The resulting chimeric strain will be less replicable than parental MP-12 strain, due to a lack of an optimal surrogate function in AMTV UTR elements. Similarly, the replacement of MP-12 NSs gene with that of AMTV NSs gene will lead to less replicable strain than parental MP-12 strain, due to a lack of optimal antagonistic functions of the NSs protein.

Overall, my central hypothesis is that genetic reassortment or recombination between two phleboviruses can occur when a loss or swap of gene element does not deteriorate the viability of resulting viruses. The overall objective of this study is to analyze genetic reassortment or recombination between RVFV MP-12 strain and AMTV, using co-infection assays and reverse genetics. The long-term goal is to establish a universal method to develop a novel pseudotype chimeric virus system applicable for most pathogenic phleboviruses. To address the central hypothesis, the following three aims are proposed.

**Specific Aim 1: Characterization of genetic reassortment between MP-12 strain and the genetic variant, rMP12-GM50, and between MP-12 strain and Arumowot virus**

Hypothesis: Poor similarity of N, L, and Gn/Gc proteins between RVFV and AMTV limits the formation of genetic reassortants. Rationale: In Africa, due to the overlap in endemic regions and shared transmission pattern, humans and ruminants can be exposed to infected mosquitoes

harboring both RVFV and AMTV. Therefore, it is important to study the potential occurrence of genetic reassortment between MP-12 strain and AMTV, as well as between two RVFV strains.

**Specific Aim 2: Characterization of the attenuation and protective efficacy of rMP12-GM50 strain in mice.** Hypothesis: The rMP12-GM50 strain, which encodes a number of silent mutations, is highly attenuated and is similarly efficacious to parental MP-12 vaccine, with a number of gene markers to distinguish it from wt RVFV strains. Rationale: If MP-12 strain creates reassortant strains with wt RVFV, mutations unique to MP-12 strains will not serve as confirmative evidence to trace the origin of reassortant strains. The use of rMP12-GM50 strain with artificial gene markers will minimize the concern of spreading unknown reassortant strains in endemic areas.

**Specific Aim 3: Characterization of recombinant MP-12 strain with AMTV genetic elements.** Hypothesis: Recombinant MP-12 strains encoding a partial UTR or NSs gene of AMTV are viable, yet replicate less efficiently than parental MP-12 strain. Rationale: Although genetic reassortment may not readily occur between RVFV and AMTV, recombination between two phleboviruses may occur. Other than the exchange of structural proteins, genetic elements such as the UTR or the NSs gene may be interchangeable between RVFV and AMTV. Reverse genetics system likely generates recombinant chimeric MP-12 strains encoding AMTV UTR or NSs. Further understanding of interchangeable genetic elements will support the evaluation of potentially pathogenic chimeric strains.

Overall, the study will characterize potential occurrence of interspecies reassortment and recombination between RVFV and AMTV, and evaluate the significance of the presence of AMTV in RVF vaccination in endemic countries.

## **CHAPTER 2: Characterization of genetic reassortment between MP-12 strain and the genetic variant, rMP12-GM50, and between MP-12 strain and Arumowot virus**

### **Introduction**

The development and distribution of vaccines have led to significant public health accomplishments, including the eradication of smallpox and the near eradication of poliomyelitis<sup>91</sup>. The majority of viral diseases, however, have not been successfully prevented by vaccination due to either an absence of licensed vaccines or poor coverage of vaccination in susceptible populations. RVF is one of the most important zoonotic viral diseases in Africa and the Arabian Peninsula. RVFV infections cause high rates of abortion in pregnant sheep, cattle, goats, and camels, leading to devastating economic losses in the agricultural industry<sup>92</sup>. Most RVF patients suffer from febrile illness, whereas severely affected RVF patients exhibit hemorrhagic fever, encephalitis, or retinitis<sup>93,94</sup>. RVFV is naturally maintained via vertical transmission by the floodwater *Aedes* mosquitoes, whereas horizontal transmission via other mosquito species (e.g., *Culex* spp.), likely plays an important role in viral transmission to animals or humans<sup>74,95,96</sup>.

The viral genome consists of three single-stranded RNA segments: i.e., L-, M-, and S-segments. Co-infection of two different strains or species may thus lead to the generation of reassortant strains encoding one or more RNA segment(s) derived from heterologous viruses. Between 1997 and 1998, the Ngari virus was isolated from patients exhibiting hemorrhagic fever during an outbreak of RVF in Kenya, Tanzania, and Somalia<sup>97</sup>. Genetic analysis of the Ngari virus revealed that the S- and L-segments were related to those of the Bunyamwera virus, and the M-segment was closely related to that of the Batai virus, both of which are bunyaviruses<sup>66</sup>. The

nucleotide similarity between M-segments of the Batai virus and Bunyamwera virus was approximately 64%, which indicates that genetic reassortment between two different bunyavirus species is a concern, as it could generate novel pathogenic bunyaviruses. Little is known about the likelihood of RVFV to generate reassortant strains with heterologous phlebovirus species. Reassortant problem is particularly important if a live-attenuated vaccine strain were to be distributed widely in RVFV endemic area. The question would remain whether the vaccine is able to gain a pathogenic phenotype via genetic reassortment with a circulating pathogenic strain through co-infections when vaccinations are being carried out during an outbreak. In Africa, several phleboviruses are transmitted via multiple vector hosts: i.e., (i) sandfly-borne phleboviruses: Sandfly fever Sicilian virus (SFSV), Sandfly fever Naples phlebovirus (SFNV), Toscana virus (TOSV), and Punique virus, (ii) mosquito-borne phleboviruses: Arumowot virus (AMTV: transmitted by *Culex antennatus*), and Odrenisrou virus (ODRV: transmitted by *Culex albiventris*), and (iii) phleboviruses isolated from wild rodents: Gabek Forest virus (GFV), Gordil virus (GORV), and Saint Floris virus (SAFV)<sup>61,63,98,99</sup>. *Culex antennatus* is a potent vector for both AMTV and RVFV, and sheep was shown to be naturally exposed to AMTV, ODRV, and RVFV in Burkina Faso<sup>61,64</sup>. Experimental data revealed that transient fever occurs following infection of AMTV in sheep, but not by GORV, SAFV, or GFV<sup>70</sup>. AMTV shares overlapping endemic areas with RVFV and is distributed in at least Burkina Faso, Niger, Morocco, Senegal, Sierra Leone, Nigeria, Central African Republic, South Africa, Zimbabwe, Kenya, Uganda, Somalia, Ethiopia, Sudan, Egypt, and Tunisia<sup>62,70</sup>. Characterization of genetic reassortment between RVFV and other phleboviruses is required for identifying the potential environmental risk of vaccination using live-attenuated RVF vaccines, especially during outbreaks when infections are present in both mammalian and mosquito hosts. In this study, I aimed to characterize the formation of reassortant

strains between the RVFV MP-12 vaccine strain and AMTV. My hypothesis is that RVFV cannot form reassortant strains with AMTV due to a lack of compatibility among heterologous N, L, and/or Gn/Gc proteins. A minigenome system was utilized to evaluate the genetic compatibility of N, L, and Gn/Gc proteins. These results were followed by co-infection experiments in *Aedes albopictus* C6/36 cells, which support robust replication of both RVFV and AMTV, to detect the formation of reassortant strains.

## **Materials and Methods**

### **Media, cells, and viruses**

MRC-5 (ATCC CCL-171), VeroE6 (ATCC CRL-1586) and Vero cells (ATCC CCL-81) were kept in Dulbecco's modified minimum essential medium (DMEM) containing 10% fetal bovine serum (FBS), streptomycin (100 µg/ml), and penicillin (100 U/ml) at 37°C with 5% CO<sub>2</sub>. BHK/T7-9 cells, which stably express T7 RNA polymerase<sup>100</sup>, were kept in MEM-alpha containing 10% FBS, streptomycin (100 µg/ml), penicillin (100 U/ml), and hygromycin B (600 µg/ml) at 37°C with 5% CO<sub>2</sub>. C6/36 cells (ATCC CRL-1660) were kept in Leibovitz's L-15 medium containing 10% FBS, 10% tryptose phosphate broth (TPB), penicillin (100 U/ml), and streptomycin (100 µg/ml) at 28°C without CO<sub>2</sub>. All cells utilized in this study were verified to be mycoplasma free at the University of Texas Medical Branch (UTMB) Tissue Culture Core Facility.

The generation of rMP-12 and rMP-12 encoding an in-frame deletion of 69% of the NSs gene (rMP12-ΔNSs16/198: previous name of this virus was rMP12-C13type) have been

previously described<sup>101</sup>. Using reverse genetics, an rMP-12 variant encoding a cluster of silent mutations at every 50 nucleotides interval within each ORF was recovered and designated rMP12-GM50 (GenBank Accession No. MF593928, MF593929, and MF593930). Additionally, reassortant rMP-12 strains encoding either of the rMP12-GM50 L, M, or S-segment (RST-GM50-L, RST-GM50-M, RST-GM50-S, respectively), were rescued and used for the validation of genotypes. All rescued viruses were recovered from BHK/T7-9 cells and plaque-cloned once before further amplification in Vero cells. AMTV Ar 1286–64 strain (Sudan, 1963), which was kindly provided by Dr. Robert B. Tesh (UTMB), was plaque-cloned once in Vero cells and amplified three times. All viruses were titrated via plaque assay and sequenced before experimental use.

## **Plasmids**

Using the custom DNA synthesis service via GenScript Inc., plasmids encoding the positive-sense L-, M-, and S-segment of rMP12-GM50 downstream of the T7 promoter, were generated and named pProT7-vL(+)-GM50, pProT7-vM(+)-GM50, and pProT7-vS(+)-GM50, respectively. The pT7-RVFFV-M-rLuc(-) plasmid expressing the negative-sense M-segment minigenome of RVFFV was described previously. The pT7-AMTV-M-rLuc(-) plasmid expressing the negative-sense M-segment minigenome of AMTV was created using the gBlocks Gene Fragment synthesis service (Integrated DNA Technologies). Plasmids expressing the N, L, or Gn/Gc proteins of AMTV were generated via subcloning of inserts, synthesized using the custom DNA synthesis service (GenScript Inc.), into the pT7-IRES or pCAGGS plasmids: i.e, pCAGGS-AMTV-N, pT7-IRES-AMTV-L, or pCAGGS-AMTV-G, respectively<sup>102</sup>. Plasmids pT7-IRES-vN,

pT7-IRES-vL, or pCAGGS-vG, expressing the N, L, or Gn/Gc proteins of the RVFV MP-12 strain, respectively, were described previously<sup>101</sup>.

### **Adenovirus vectors**

Amplification of a PCR fragment from the pENTR4 plasmid (Thermo Fisher Scientific) was carried out to remove the *ccdB* gene and the chloramphenicol resistant gene. The PCR fragment, containing the attL1 and attL2 sites, was then recombined with a linearized pCAGGS-vG plasmid, which was cut with enzymes *SpeI* and *XhoI*, using Gibson assembly (New England BioLabs). Resulting plasmid encodes the CAG promoter and the M-segment ORF of the RVFV MP-12 strain (pENTR-CAG-vM). The pENTR-CAG-wL or pENTR-CAG-wN plasmids were then generated via replacement of the M-segment ORF of pENTR-CAG-vM plasmid with the L or N ORF of the RVFV ZH501 strain, respectively. Using Gateway Vector (Thermo Fisher Scientific), these pENTR plasmids were further recombined with pAd/PL-DEST via LR clonase. Recombined plasmids lacking resistant genes for chloramphenicol and kanamycin were selected for and linearized with the enzyme *PacI*. Recombinant human adenovirus 5 vectors lacking the entire E1 region and expressing the N or L protein of RVFV (rAd5-RVFV-N or rAd5-RVFV-L, respectively), were then rescued in 293A cells.

### **Replication kinetics of rMP-12 and rMP12-GM50**

Using a multiplicity of infection (MOI) of 0.01 or 1.0, Vero, MRC-5, and C6/36 cells were infected with either the rMP-12 or rMP12-GM50 strain for 1 hour at 37°C (Vero and MRC-5 cells) and 28°C (C6/36 cells). Cells were then washed three times with media, and culture supernatant

samples were collected at 1, 24, 48, 72, 96, and 144 hours post infection (hpi). Three independent experiments were carried out.

### **Co-infection with rMP-12 and rMP12-GM50 strains, or with rMP-12 and AMTV**

C6/36 cells were co-infected for 1 hour at 28°C, with the rMP-12 and rMP12-GM50 strain at an MOI of 2 and 3, respectively. The infectivity of both rMP-12 and rMP12-GM50 strain was confirmed using an indirect fluorescent assay (IFA) in C6/36 cells (Fig. 2.1), whereas viral titers were determined via plaque assays in VeroE6 cells. Similarly, using rMP-12 and AMTV at an MOI of 6 and 9, respectively, C6/36 cells were co-infected for 1 hour at 28°C. The majority of cells were infected with rMP-12 and AMTV with this amount of viral input (Fig. 2.1). After washing cells with media five times, cells were further incubated at 28°C. At 24 hpi, culture supernatants were collected and used for plaque isolation and genotype analysis.

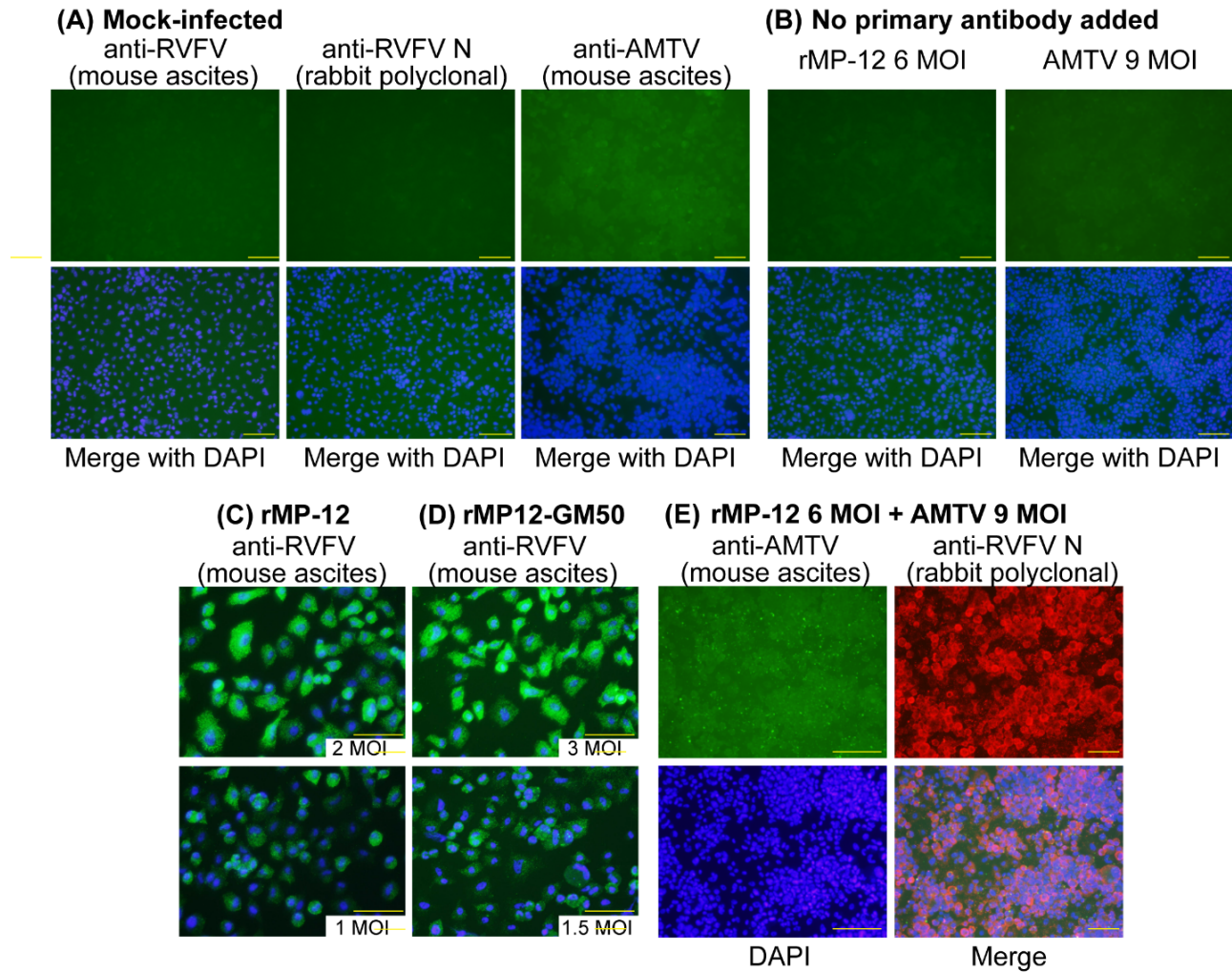


**Figure 2.1: Indirect fluorescent assay to test the infectivity of rMP-12, rMP12-GM50, and AMTV in C6/36 cells.**

C6/36 cells were infected with rMP-12, rMP12-GM50, and AMTV. At 8 hpi, cells were fixed with methanol and incubated with 1 in 800 dilution of either anti-RVFPV mouse ascites, anti-RVFPV N rabbit polyclonal antibody, or anti-AMTV mouse ascites. Secondary antibodies (1 in 800 dilutions) of either Alexa Fluor 488 goat anti-mouse IgG (H+L), Alexa Fluor 488 goat anti-rabbit IgG (H+L), or Alexa Fluor 594 goat anti-rabbit IgG (H+L) were utilized for the detection of specific signals. (A) mock-infected controls, (B) no primary antibody controls, (C) C6/36 cells infected with rMP-12 at 2 or 1 MOI, (D) C6/36 cells infected with rMP12-GM50 at 3 or 1.5 MOI, (E) C6/36 cells co-infected with rMP-12 (6 MOI) and AMTV (9 MOI). Nuclei were stained with 4,6-diamidino-2-phenylindole (blue). Scale bars represent 50  $\mu$ m. RVFPV and AMTV antigens were detected in the cytoplasm of infected cells.

Ly H et al. (2017) Risk analysis of inter-species reassortment through a Rift Valley fever phlebovirus MP-12 vaccine strain. PLoS ONE 12(9): e0185194. <https://doi.org/10.1371/journal.pone.0185194>

## Plaque isolation of virus

Supernatant from co-infected cells were collected, and used to infect fresh Vero cells in 10-cm dishes or six-well plates for 1 hour at 37°C, to isolate individual plaque clones. An overlay, which contains 0.6% noble agar, 1 x MEM, penicillin (50 U/ml), streptomycin (50 µg/ml) and 5% TPB, was then added over the cells<sup>103</sup>. A second overlay, which contains an additional 0.012% of neutral red solution, was added at 72 hpi. After incubation overnight, plaques were visible and those that were well isolated were slowly aspirated using a 20 – 200µl tip. The agar plug was then transferred into 1.7 ml Eppendorf tubes containing 200 µl of DMEM. Aliquots (50 µl) of plaque isolates were used for further amplification in Vero cells for 5 to 7 days at 37°C. Using the TRIzol reagent (Life Technologies), total RNA was extracted from infected Vero cells to determine the genotype of each reassortant.

### **PCR-restriction fragment length polymorphism (RFLP) analysis**

Using PCR-RFLP, genotyping of L-, M-, and S-segments from each plaque isolate was performed. The rMP-12 strain contains unique restriction enzyme sites in the L-, M-, and S-segments that are not present on the rMP12-GM50 strain. Primers for PCR flanking each restriction enzyme site on the L-, M-, and S-segment of the rMP-12 strain (L-segment PCR fragment: *Pst*I site; M- and S-segment PCR fragments: *Bam*HI site) were generated (Fig. 2.2). PCR primer sets were designed as follows: L-segment PCR–L1846F and L2362R; M-segment PCR–M19F and M456R; and S-segment PCR–S341F and S764R. Using SuperScript II Reverse Transcriptase (Life Technologies), first-stranded cDNA was synthesized with random hexamers according to manufacturer’s instructions. PCR reactions using Phusion High Fidelity DNA polymerase (New England BioLabs) was carried out according to manufacturer’s instruction. Purification of PCR products was carried out with the DNA Clean & Concentrator-5 Kit (Zymo

Research) and then digested with restriction enzymes (*Pst*I for L-segment PCR fragments and *Bam*HI for M- and S-segment PCR fragments) for 16 hours at 37°C. Two bands (185-bp and a 291-bp) could be generated from the PCR fragment (472 bp) generated from the rMP-12 S-segment after being digested with *Bam*HI. Two bands (306-bp and a 178-bp) could be generated from the PCR fragment (480 bp) from the rMP-12 M-segment after being digested with *Bam*HI. Lastly, two bands (121-bp and a 445-bp) could be generated from the PCR fragment (562 bp) from the rMP-12 L-segment after being digested with *Pst*I. The rMP12-GM50 strain do not encode the restriction enzyme sites for either *Bam*HI or *Pst*I. Genotyping was then carried out via electrophoresis on 2% agarose gels using cDNA samples derived from plaque clones.

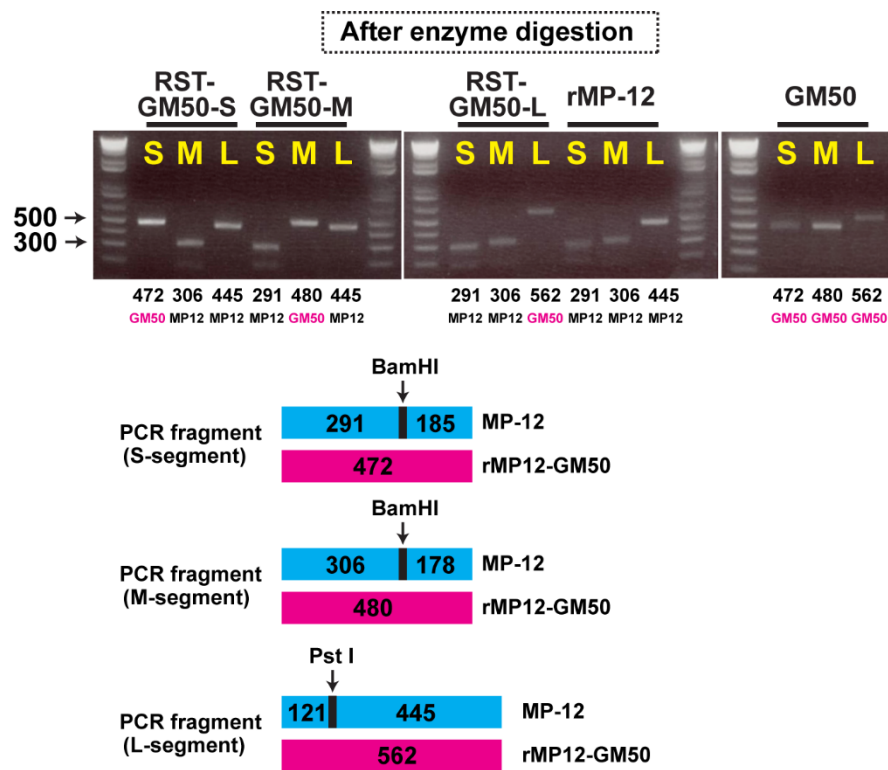


**Figure 2.2: PCR-RFLP analysis to genotype L-, M-, and S-segments of rMP-12 and rMP12-GM50 strains.**

To genotype each L-, M-, and S-segments, PCR primers flanking a *Bam*HI site unique to the MP-12 S- or M-segments, or a *Pst*I site unique to the MP-12 L-segment were utilized. To validate the products from PCR-RFLP, reverse genetics was carried out to generate reassortant rMP-12 strains encoding either the L-, M-, or S-segment of rMP12-GM50 (rMP12-RST-GM50-L, rMP12-RST-GM50-M, or rMP12-RST-GM50-S, respectively). Vero cells were then infected with either rMP-12, rMP12-GM50, rMP12-RST-GM50-L, rMP12-RST-GM50-M, or rMP12-RST-GM50-S at an MOI of 1. Total RNA was collected from infected cells at

24 hpi, and cDNA was synthesized using random hexamers. PCR-RFLP analysis on a 2% agarose gel demonstrated the expected size of each band representing the genotype of each segments.

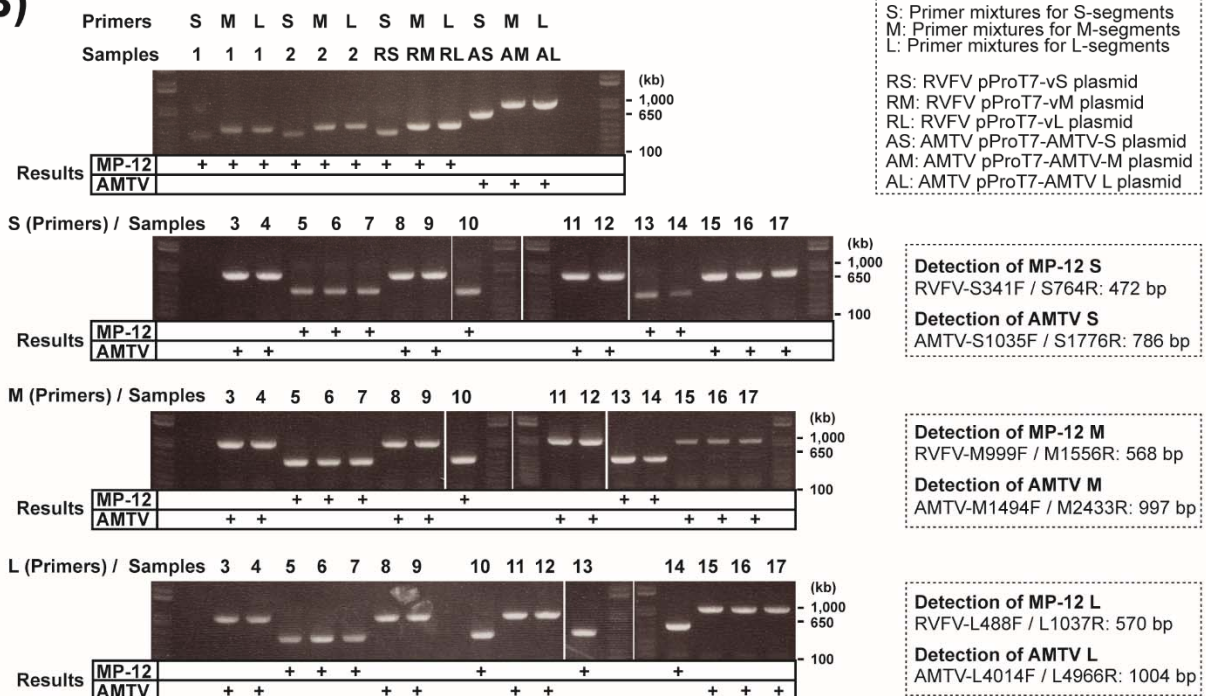
Ly H et al. (2017) Risk analysis of inter-species reassortment through a Rift Valley fever phlebovirus MP-12 vaccine strain. PLoS ONE 12(9): e0185194. <https://doi.org/10.1371/journal.pone.0185194>

### **Genotyping of L-, M-, and S-segments of AMTV and the rMP-12 strain via RT-PCR**

The cDNA samples derived from Vero cells that were infected with plaque isolates were used for genotyping. Since it was difficult to generate universal primers to amplify both AMTV and MP-12 DNA, the amplification was made via virus-specific primers: i.e., a mixture of virus-specific primers for MP-12 and AMTV in a PCR reaction (Fig. 2.3). For the L-segment, MP-12-specific 570 bp band was generated via RVFV-L488F and RVFV-L1037R, whereas AMTV-specific 1004 bp band was amplified via AMTV-L4014F and AMTV-L4966R. For the M-segment, MP-12-specific 568 bp band was generated via RVFV-M999F and RVFV-M1556R, whereas AMTV-specific 997 bp band was amplified via AMTV-M1494F and AMTV-M2433R. For the S-segment, MP-12-specific 472 bp band was generated via RVFV-S341F and RVFV-S764R, whereas AMTV-specific 786 bp band was amplified via AMTV-S1035F and AMTV-S1776R.

**(A)**

Plaque isolation from 1 dpi sup of C6/36 cells co-infected with rMP-12 and AMTV

**(B)**

**Figure 2.3: RT-PCR analysis to genotype L-, M-, and S-segments of the rMP-12 strain and AMTV.**

(A) C6/36 cells were co-infected with rMP-12 (6 MOI) and AMTV (9 MOI) at 28°C. Culture supernatant were then collected 24 hpi and used to infect Vero cells for plaque isolation. A total of 17 well isolated plaques were cloned. (B) Total RNA from infected Vero cells was used for RT-PCR to determine the genotypes of the L-, M-, and S-segment of each clone. PCR was performed separately for the L-segment (a mixture of RVFV-L488F, RVFV-L1037R, AMTV-L4014F, and AMTV-L4966R), M-segment (a mixture of RVFV-M999F, RVFV-M1556R, AMTV-M1494F, and AMTV-M2433R), and S-segment (a mixture of RVFV-S341F, RVFV-S764R, AMTV-S1035F, and AMTV-S1776R). The plasmids pProT7-vL, pProT7-vM, and pProT7-vS were used as positive controls for RVFV L-, M-, and S-segments and labeled as RL, RM, and RS, respectively. Similarly, the plasmids pProT7-

AMTV-L, pProT7-AMTV-M, and pProT7-AMTV-S were used as controls for AMTV L-, M-, and S-segments and labeled as AL, AM, and AS, respectively.

Ly H et al. (2017) Risk analysis of inter-species reassortment through a Rift Valley fever phlebovirus MP-12 vaccine strain. PLoS ONE 12(9): e0185194. <https://doi.org/10.1371/journal.pone.0185194>

## **Luciferase assay**

Using the TransIT-293 Transfection Kit (Mirus Bio), BHK/T7-9 cells were transfected with 0.8 µg of pT7-RVSV-M-rLuc(-), or pT7-AMTV-M-rLuc(-); 0.8 µg of pT7-IRES-vN, or pCAGGS-AMTV-N; 0.4 µg of pCAGGS-vG, or pCAGGS-AMTV-G; and 0.1 µg of pT7-IRES-vL, or pT7-IRES-AMTV-L, in 12-well plates. In addition, 0.01 µg of pT7-IRES-fLuc plasmid was co-transfected with each sample as a control<sup>102</sup>. At 72 hpi, cells were collected and the activity of luciferase was measured using the Dual-Luciferase Reporter Assay System (Promega Corporation), according to the manufacturer's instruction. To analyze the minigenome activities based on the constitutively expressed protein levels of fLuc, the activity values of rLuc were divided with the activity values of fLuc per samples. The activity values resulting from the Dual-Luciferase Reporter Assay System were shown as percentages: i.e., the median value of control samples, which express neither the N nor L protein, was set as 100%. Controls without N and L protein expression were set for each minigenome species, since background activities of rLuc varied among minigenomes of RVSV and AMTV. Alternatively, for the detection of the activity of rLuc without the activity of fLuc, measurement was carried out with the *Renilla* Luciferase Assay System (Promega Corporation).

## **Sequence alignment**

AMTV and MP-12 genome sequences were aligned using the CLC Genomics Workbench 7.5.2, via the following parameters: gap open cost, 10; gap extension cost, 1; and end gap cost, free.

### **Statistical analysis**

Using GraphPad Prism 6.05 (GraphPad Software Inc.), statistical analyses were carried out. For the comparison of two groups, viral titers at each time point were analyzed using the unpaired t-test. For the comparison of multiple groups, the arithmetic means of log<sub>10</sub> values were analyzed using one-way ANOVA, followed by the Tukey's multiple comparison test.

### **Results**

#### **Introduction of silent mutations into N, NSs, M, and L ORFs of the RVFV MP-12 strain**

Using the MP-12 vaccine strain, a total of 584 silent mutations were encoded into all ORFs, which resulted in the introduction of additional attenuations and gene markers without changing the functions of viral proteins. Overall, 326 mutations were introduced in the L-segment, 185 mutations in the M-segment, and 73 mutations in the S-segment. This MP-12 variant, named rMP12-GM50, was successfully rescued via the reverse genetics system. In order to retain the capability of viral replication in host cells, each introduced silent mutation was designed not to disturb the codon-pair bias and codon usage (Fig. 2.4)<sup>104</sup>. Within species, the codon pair bias represents the bias of the pairing frequency of two neighboring codons<sup>105,106</sup>. Previous study on codon pair bias used annotated human genes to calculate the codon pair bias score, where the underrepresented pair and overrepresented pair were shown as scores of <0 and >0, respectively<sup>104</sup>.

In the context of humans, the average codon pair bias score of rMP-12 was 0.018 and rMP12-GM50 was 0.189, whereas the codon adaptation index of rMP-12 was 0.72 and rMP12-GM50 was 0.73<sup>107,108</sup>. The homology at the nucleotide level between the MP-12 strain and the rMP12-GM50 strain is 94.9%, 95.2%, and 96.0% for the L-, M-, and S-segment, respectively. The replication kinetics of rMP-12 and rMP12-GM50 were evaluated in Vero cells and at 24, 48, and 72 hpi, the replication of rMP12-GM50 was less efficient than rMP-12, yet viral titers at 96 and 120 hpi had no significant difference (Fig. 2.5). Replication kinetics were also evaluated in MRC-5 cells, and the replication rMP12-GM50 were not significantly different than that from the rMP-12 strain (Fig. 2.5). These results demonstrate that the rMP12-GM50 strain retains the ability to replicate in mammalian cells.

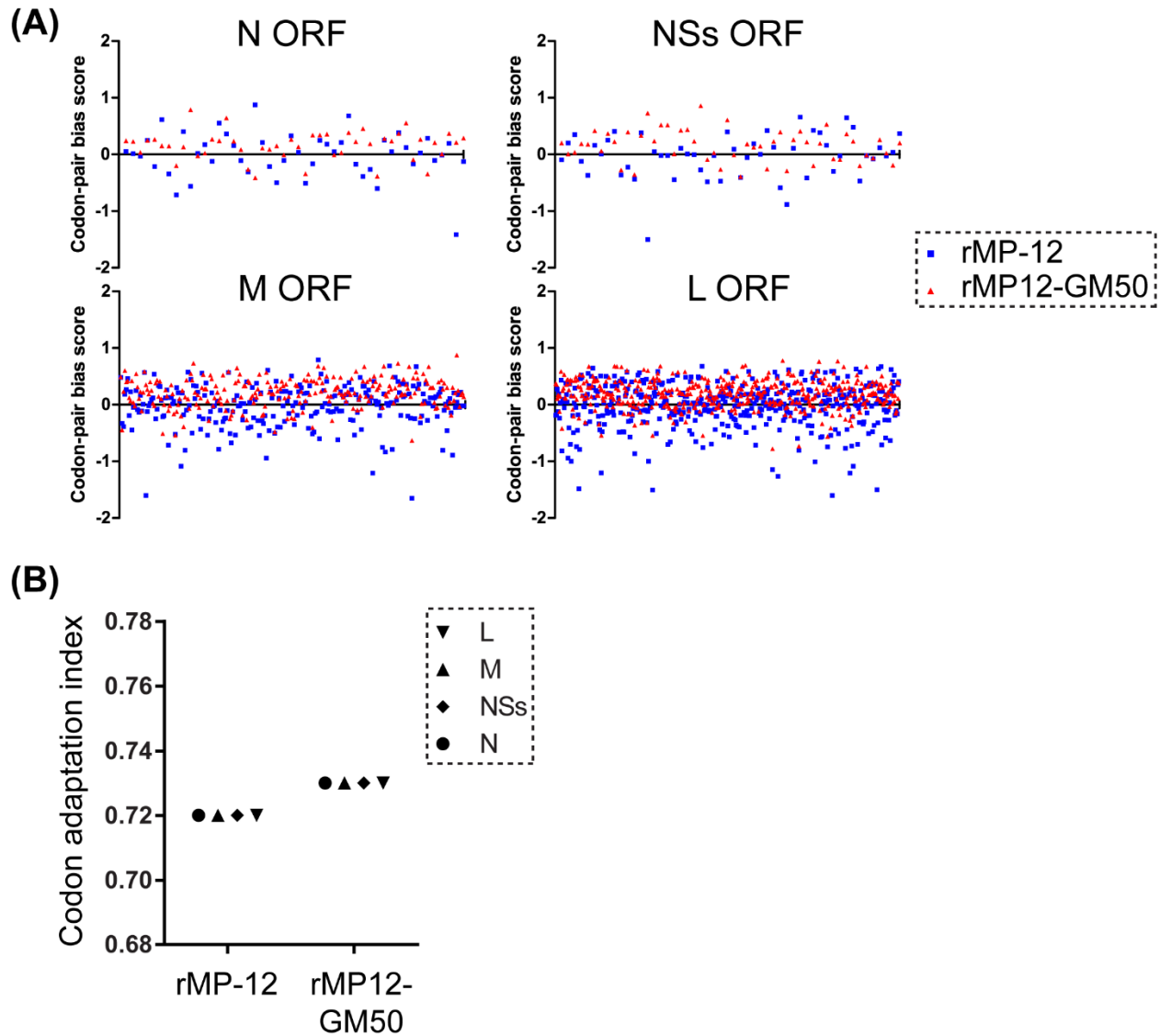


**Figure 2.4: Changes in codon pair bias and codon usage in rMP12-GM50 strain**

(A) Codon-pair bias scores for all altered codon-pair of rMP12-GM50 were compared with parental MP-12. The X-axis represents the nucleotide position numbers. Blue square = rMP-12; red triangle = rMP12-GM50. Human codon-pair bias score was obtained in Science, 2008, 320: 1784. (B) Codon usage was analyzed for human codon usage by GeneScript Rare Codon Analysis Tool software ([www.genscript.com](http://www.genscript.com)).

Ly H et al. (2017) Attenuation and protective efficacy of Rift Valley fever phlebovirus rMP12-GM50 strain. *Vaccine* 35(48): 6634-6642. <https://doi.org/10.1016/j.vaccine.2017.10.036>

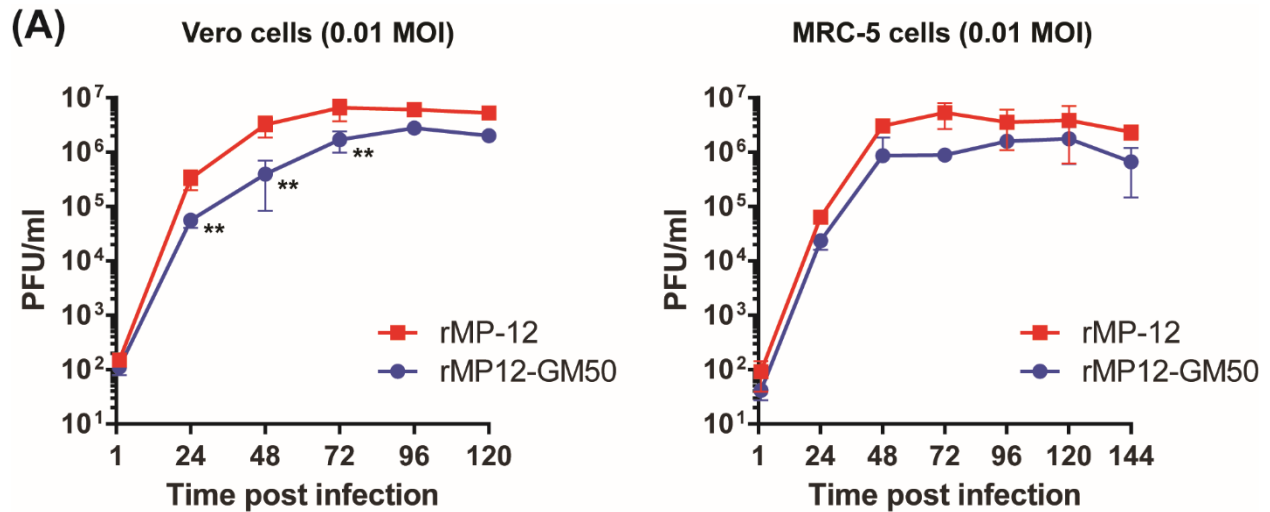


**Figure 2.5: Replication kinetics of rMP-12 and rMP12-GM50 in Vero cells and MRC-5 cells**

(A) Replication kinetics of rMP-12 and rMP12-GM50 in Vero cells (left panel) and MRC-5 cells (right panel) at an MOI of 0.01. Graph represents the means  $\pm$  standard deviations of three independent experiments. Statistical differences between the two strains were analyzed by unpaired t-test at each time point (\*\* $p < 0.01$ ). Red square = rMP-12; blue circle = rMP12-GM50.

Ly H et al. (2017) Attenuation and protective efficacy of Rift Valley fever phlebovirus rMP12-GM50 strain. *Vaccine* 35(48): 6634-6642. <https://doi.org/10.1016/j.vaccine.2017.10.036>

### Functional compatibility of RVFV N and L proteins for replication of AMTV M-segment minigenome

The L-, M-, and S-segment RNA of phleboviruses are complimentary at the 3'- and 5'- termini, and form panhandle structures that serve as promoters for RNA synthesis and encapsidation signals for N proteins<sup>5</sup>. Among phlebovirus species, these panhandle regions are highly conserved and it is possible that the N and L protein of RVFV can support the genome replication of other phleboviruses. The M-segment minigenome, encoding the entire ORF of the *Renilla* luciferase (rLuc) in place of the M-segment ORF, was constructed using the backbones of RVFV and AMTV (Fig. 2.6). The termini of both the M-segment of RVFV and AMTV share an identical 12-nucleotide sequence and the panhandle structure can be formed from just the terminal 10 nucleotides. BHK/T7-9 cells were transfected with plasmids expressing the N and L protein of

RVFV, and the M-segment minigenome of either RVFV or AMTV (RVFV-M-rLuc(-) and AMTV-M-rLuc(-), respectively), to determine whether the N and L proteins of RVFV can support the replication of the M-segment minigenome of AMTV. When compared to the background activity of rLuc in plasmids expressing RVFV L protein and minigenome RNA without RVFV N protein, the expression of RVFV N and L proteins increased the activities of rLuc for RVFV-M-rLuc(-) and AMTV-M-rLuc(-) by factors of 84 and 3.2, respectively, as shown in Fig. 2.6. Alternatively, BHK/T7-9 cells were transfected with plasmids expressing the N and L protein of AMTV, and either the RVFV-M-rLuc(-) or AMTV-M-rLuc(-) plasmid. When compared to the background rLuc activity in plasmids expressing the L protein and minigenome RNA of AMTV without the N protein, the N and L protein of AMTV increased the activities of rLuc for RVFV-M-rLuc(-) and AMTV-M-rLuc(-) by a factor of 98 and 17, respectively (Fig. 2.6). These results indicate that the N and L proteins from RVFV support the replication of the M-segment RNA of AMTV and the N and L proteins from AMTV support the replication of the M-segment RNA of RVFV. The detection of both a positive-sense AMTV minigenome RNA band and a fast migrating rLuc mRNA band in cells expressing the N and L protein of RVFV and AMTV M-segment minigenome in Northern blot, provides further evidence of viral AMTV minigenome RNA synthesis via RVFV N and L proteins (Fig. 2.6). The Northern blot result also indicated that the L protein of RVFV could recognize the transcription termination signal on the AMTV M-segment.

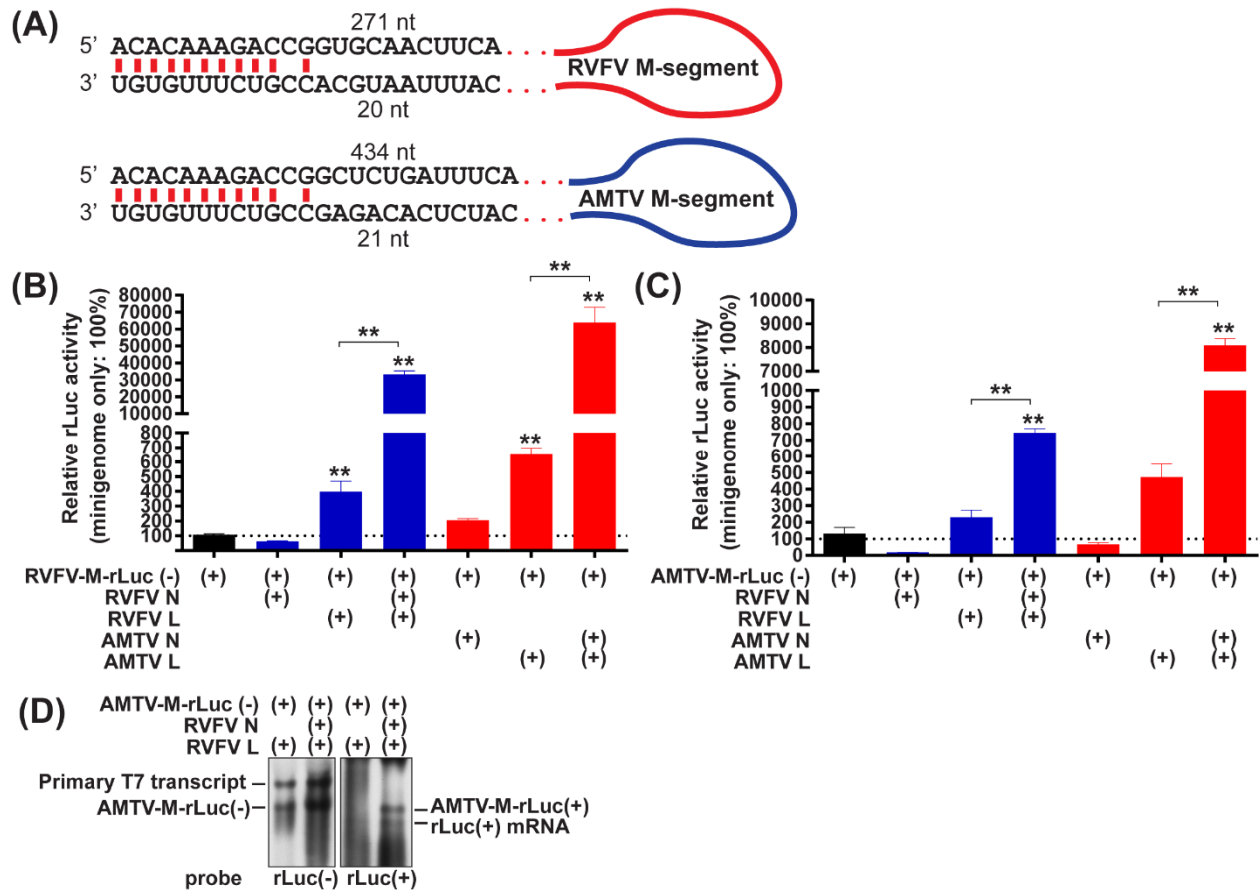


**Figure 2.6: Replication of the M-segment minigenomes of RVFV and AMTV in relation to co-expression of RVFV N and L proteins.**

(A) Schematic representation of panhandle sequences of RVFV and AMTV M-segments. (B) BHK/T7-9 cells were transfected with plasmids expressing the RVFV-M-rLuc(-) (M-segment minigenome RNA of RVFV), and (C) AMTV-M-rLuc(-) (M-segment minigenome RNA of AMTV). The ratio of Renilla luciferase (rLuc) activities to firefly luciferase (fLuc) activities derived from pT7-IRES-fLuc (control plasmid) was shown as percentage: i.e., the same type of minigenome without N and L expression was set as 100%. Bars represent means plus standard errors. Asterisks on error bars represent statistically significant increased value compared to samples expressing minigenome only (One-way ANOVA  $**p < 0.01$ ). Samples expressing minigenome, N proteins, and L proteins were also statistically compared with those expressing minigenome, and L proteins. ns, not significant. (D) Northern blot using total RNA derived from AMTV minigenome assay. Sense rLuc probe (left panels) and anti-sense rLuc probe (right panels) were utilized.

Ly H et al. (2017) Risk analysis of inter-species reassortment through a Rift Valley fever phlebovirus MP-12 vaccine strain. PLoS ONE 12(9): e0185194. <https://doi.org/10.1371/journal.pone.0185194>

## Functional compatibility of RVFV or AMTV N and L proteins for the replication of RNA minigenomes

Next, further analysis of genetic reassortment possibilities between RVFV and AMTV were carried out. From GenBank, the amino acid identities between the MP-12 strain (Accession numbers: DQ380154, DQ380208, and DQ375404) and the AMTV Ar 1286–64 strain (Accession numbers: MF593933, MF593932, and MF593931) were as follows: 57% for L protein, 22% for pre-Gn protein, 30% for Gn protein, 41% for Gc protein, 49% for N protein, and 25% for NSs protein. To characterize the compatibility of N and L proteins derived from RVFV and AMTV, a minigenome reporter assay was used (Fig. 2.7A). BHK/T7-9 cells were transfected with plasmids expressing N protein, L protein, or the minigenome RNA of RVFV or AMTV, and the activity level of rLuc were measured at 72 hpt. Co-expression of the N protein from AMTV and the L protein from RVFV, or that of RVFV N protein and AMTV L protein, did not significantly increase the activity level of rLuc for the AMTV-M-rLuc(-) when compared to the control sample that lacks both the N and L protein expression. Whereas there was a slight increase in the activity level of rLuc for RVFV-M-rLuc(-) by factors of 6.2 and 2.0, respectively, when compared to the activity level of rLuc using plasmids expressing RVFV minigenome RNA without RVFV N and L proteins. The raw luciferase activity level showed similar increases of the rLuc activity level, when minigenome RNA and L protein of RVFV were expressed (factor of 3.7), or when the minigenome RNA of RVFV and L protein of AMTV were expressed (factor of 6.1) (Fig. 2.7). The comparison of raw luciferase activity level did not show statistically significant differences between samples expressing the N protein of AMTV and L protein of RVFV, or between the samples expressing the N protein of RVFV and L protein of AMTV (Fig. 2.7B). These results demonstrated that AMTV N proteins and RVFV L proteins, or vice versa, do not support minigenome RNA replication.

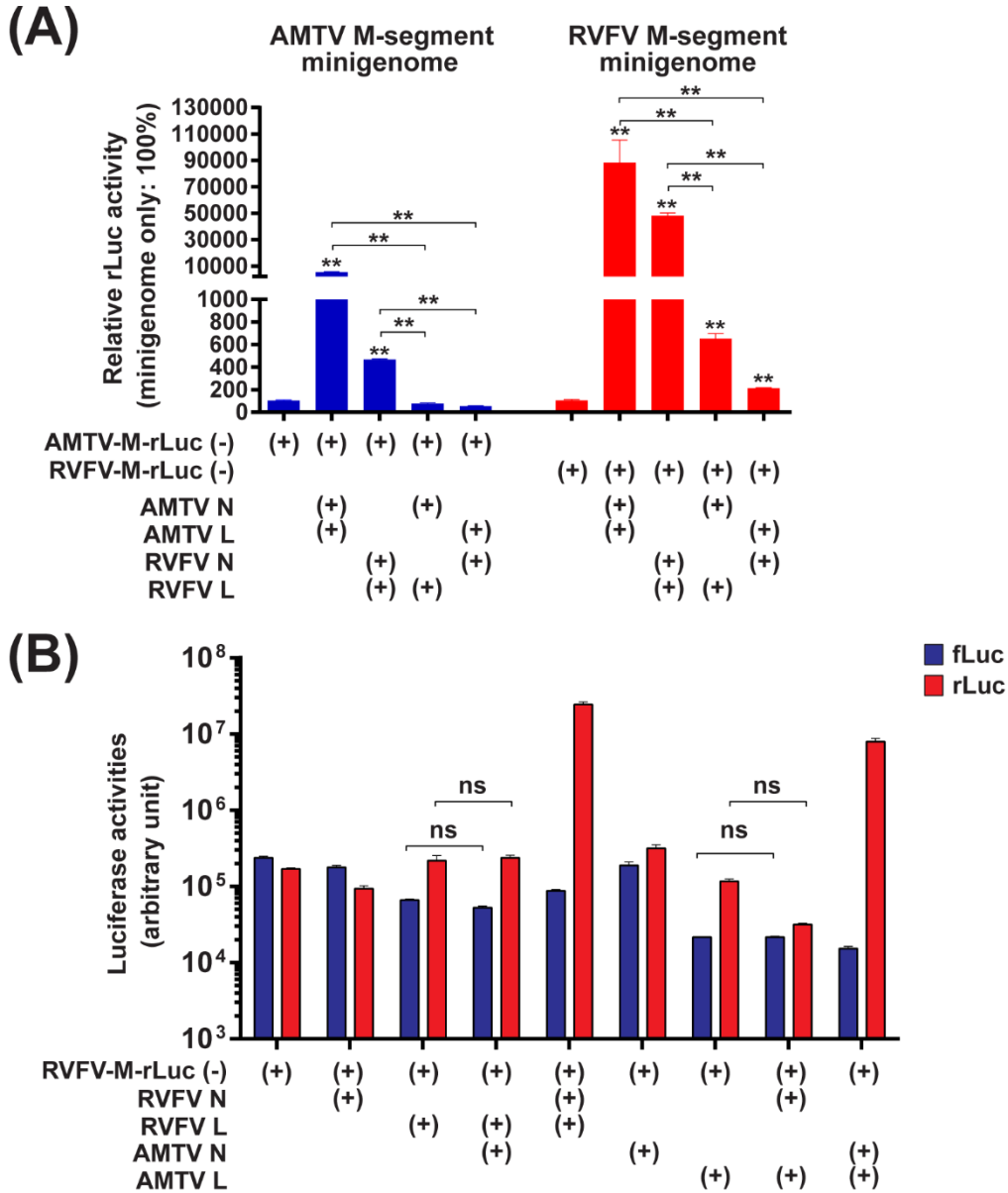


**Figure 2.7: Minigenome assays with expressions of N and L proteins derived from AMTV or RVFV.**

(A) BHK/T7-9 cells were transfected with the RVFV-M-rLuc(-) or AMTV-M-rLuc(-), and plasmid expressing N or L proteins derived from either AMTV or RVFV. Cell lysates were collected at 72 hpt, and the ratio of rLuc activities to fLuc activities derived from pT7-IRES-fLuc (control plasmid) was shown as percentage: i.e., the same type of minigenome without N and L expression was set as 100%. Bars represent means plus standard errors. Asterisks on error bars represent statistically significant increased values compared to samples expressing minigenome only (One-way ANOVA  $**p < 0.01$ ). (B) Raw luciferase activity values from minigenome assays. BHK/T7-9 cells were transfected with RVFV-M-rLuc(-) or AMTV-M-rLuc(-), and those expressing N or L proteins derived from either AMTV or RVFV. Cell lysates were collected at 72 hpt, and rLuc activity values and fLuc activity values are separately shown in the graph. The original fLuc value was divided with 100 so that the rLuc and fLuc values could be shown at a similar scale. Bars represent means plus standard errors. One-way ANOVA: ns, not significant.

Ly H et al. (2017) Risk analysis of inter-species reassortment through a Rift Valley fever phlebovirus MP-12 vaccine strain. PLoS ONE 12(9): e0185194. <https://doi.org/10.1371/journal.pone.0185194>

## **RVFV and AMTV Gn/Gc proteins ability to package minigenome RNA encapsidated with heterologous N proteins**

Next, the ability of the envelope Gn/Gc proteins to package the minigenome RNA, that is encapsidated with N proteins from either RVFV or AMTV, was evaluated through the production of infectious virus-like particles (VLP) carrying the minigenome of RVFV (Fig. 2.8). Plasmids encoding the minigenomes of RVFV or AMTV, and plasmids expressing the structural proteins N, L, and Gn/Gc of either RVFV or AMTV were used to transfect BHK/T7-9 cells. Indicator cells, or Vero cells, that were previously transduced with recombinant adenoviruses expressing either N or L proteins of RVFV, were incubated with the culture supernatant collected from BHK/T7-9 cells for 1 hour at 37°C. Lysates from Vero was collected and the activity of rLuc was analyzed at 36 hours post VLP infection.

The activity of rLuc measured from the minigenome of RVFV increased significantly in indicator Vero cells infected with VLP samples derived from transfected cells expressing N, L, and Gn/Gc proteins of RVFV, and in those expressing N, L, and Gn/Gc proteins of AMTV (Fig. 2.8). Similarly, the measured activity of rLuc from the minigenome of AMTV increased significantly in Vero cells infected with supernatant containing VLP that was collected from cells expressing N, L, and Gn/Gc proteins of RVFV, and in those expressing N, L, and Gn/Gc proteins in AMTV (Fig. 2.8). The activities of rLuc were not shown to be increased in cells incubated with culture supernatants collected from cells expressing RVFV N and L protein and AMTV Gn/Gc proteins, or in those expressing AMTV N and L protein and RVFV Gn/Gc proteins. These results demonstrate that the envelope Gn/Gc protein of RVFV are not capable of packaging the minigenome that is encapsidated with the N and L protein of AMTV, and vice versa. It was also

noted that when cells expressed either combination of N, L, and Gn/Gc proteins of RVFV, or that of N, L, and Gn/Gc proteins of AMTV, the activity level of rLuc increased significantly in transfected cells. The result demonstrate that VLP spread also occurred in cells that were transfected.

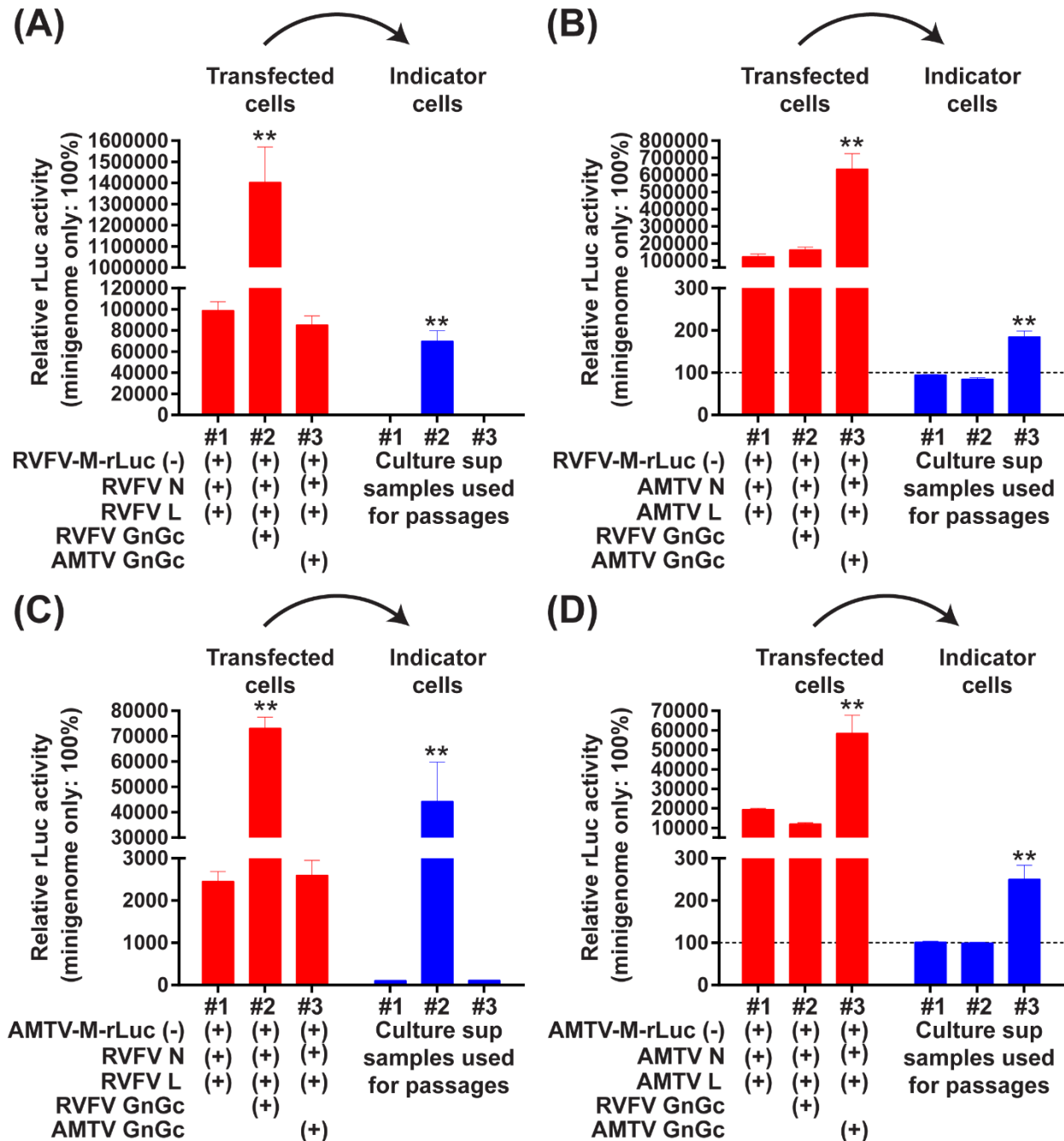


## **Figure 2.8: Minigenome assays with expressions of N, L, and Gn/Gc proteins derived from AMTV or RVFV.**

(A and B) BHK/T7-9 cells were transfected with plasmids expressing RVFV-M-rLuc(-). (C and D) BHK/T7-9 cells were transfected with plasmids expressing AMTV-M-rLuc(-). Cells were also co-transfected with plasmids expressing N and/or L derived from either RVFV (A and B) or AMTV (C and D), as well as those expressing Gn/Gc proteins derived from either AMTV or RVFV. The rLuc activity was measured at 72 hpt. Culture supernatants from transfected cells were transferred into fresh Vero cells transduced with adenovirus vectors expressing RVFV N and L proteins for 2 hours before incubation with supernatants. The rLuc activity was then measured 36 hours after incubation with culture supernatants. The ratio of rLuc activities to fLuc activities (transfected cells) or the rLuc activity values (indicator cells) were shown as percentage: i.e., minigenome without N and L expression was set as 100%. Bars represent means plus standard errors. Asterisks on error bars represent statistically significant increased values compared to samples expressing minigenome only (One-way ANOVA  $**p < 0.01$ ).

Ly H et al. (2017) Risk analysis of inter-species reassortment through a Rift Valley fever phlebovirus MP-12 vaccine strain. PLoS ONE 12(9): e0185194. <https://doi.org/10.1371/journal.pone.0185194>

## **Analysis of reassortant formation between rMP-12 and rMP12-GM50, and between rMP-12 and AMTV in C6/36 cells**

Using a co-infection assay with C6/36, the occurrence of genetic reassortment between the rMP-12 and AMTV strain was further analyzed. Conditions for reassortment analysis were initially evaluated through a co-infection assay with C6/36 cells using two different RVFV strains of MP-12 (i.e., rMP-12 and rMP12-GM50). As described above, the rMP12-GM50 strain encodes a cluster of silent mutations at every 50 nucleotide interval in each of the ORF (L, M, N, and NSs), resulting in a total of 584 mutations (Fig. 2.9). Although both the rMP-12 and rMP12-GM50 strain could replicate to similar viral titers in C6/36 cells after 4 dpi, rMP12-GM50 exhibited delayed growth kinetics before reaching plateau titers (Fig. 2.9).

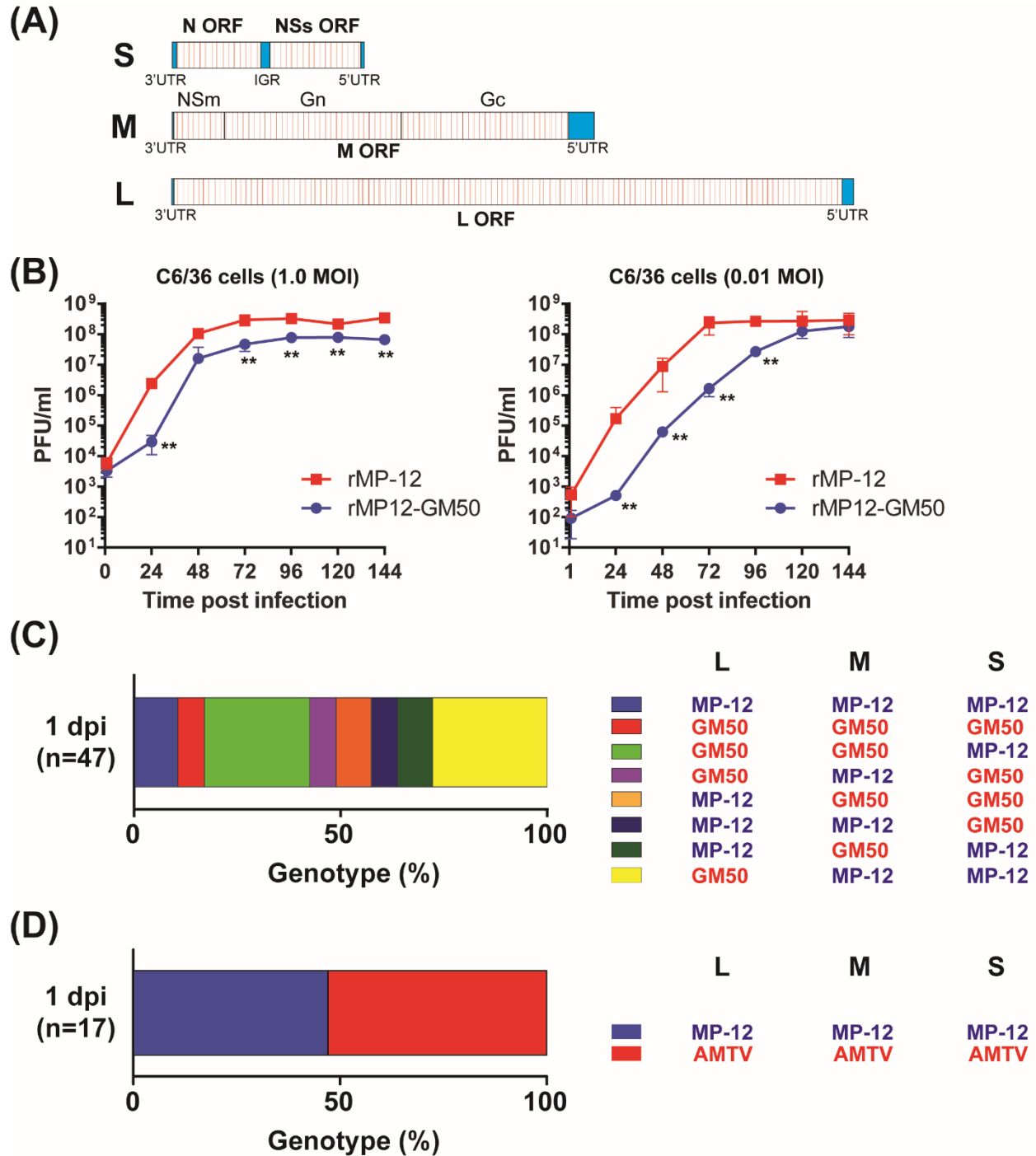


**Figure 2.9: Reassortant formation between rMP-12 and rMP12-GM50 strains, or between rMP-12 and AMTV.**

(A) Schematic representation of rMP12-GM50 L-, M-, and S-segments. The rMP12-GM50 strain encodes 326, 185, and 73 silent mutations throughout the ORF of the L-, M-, and S-segments, respectively. Individual silent mutations are shown in red. (B) Replication kinetics of rMP-12 and rMP12-GM50 strains in culture cells. C6/36 cells were infected with rMP-12 or rMP12-GM50 at an MOI of 0.01 or 1, and viral titers from culture supernatants were measured via plaque assay. The graph represents the mean  $\pm$  standard deviation of three independent experiments. Statistical differences between the two strains were analyzed by unpaired t-test at each time point (\*\* $p < 0.01$ ). (C) Genetic reassortants produced from C6/36 cells co-infected with rMP-12 and rMP12-

GM50 strains at 24 hpi. Genotypes for L-, M-, and S-segments of 47 plaque isolates from co-infected C6/36 cells were determined via PCR-RFLP analysis. (D) Genetic reassortants produced from C6/36 cells co-infected with rMP-12 and AMTV at 24 hpi. Genotypes for L-, M-, and S-segments of 17 plaque isolates from co-infected C6/36 cells were determined via RT-PCR analysis.

Ly H et al. (2017) Risk analysis of inter-species reassortment through a Rift Valley fever phlebovirus MP-12 vaccine strain. PLoS ONE 12(9): e0185194. <https://doi.org/10.1371/journal.pone.0185194>

For the co-infection assay, C6/36 cells were co-infected with rMP-12 and rMP12-GM50. Viral inputs, previously determined via IFA, were optimized, so that all C6/36 cells were infected (Figure 2.1). At 1 dpi, culture supernatants were collected, which would contain virions derived from cells co-infected with both rMP-12 and rMP12-GM50. A total of 47 well isolated plaques were identified in plaque assay, and plaque-cloning and subsequent amplification of each clone were performed. Vero cells were infected with each plaque clone, and total RNA was extracted for genotyping analysis via PCR-RFLP (Fig. 2.2). Genotyping analysis of L-, M-, and S-segments of collected plaque clones showed that 83% of them were reassortant strains, 10.6% were parental rMP-12, and 6.4% were parental rMP12-GM50. More specifically, 25.5% were G/G/M, 6.4% were G/M/G, 8.5% were M/G/G, 6.4% were M/M/G, 8.5% were M/G/M, and 27.7% were G/M/M reassortants (M = rMP-12, G = rMP12-GM50, order = L/M/S) (Fig. 2-9). These results demonstrated that this co-infection assay using C6/36 cells could generate all combinations of reassortant strains between rMP-12 and rMP12-GM50 strains.

Using a similar co-infection assay with C6/36 cells, the occurrence of genetic reassortment between the rMP-12 and AMTV strain was determined. At 1 dpi, 17 well isolated plaques were cloned and amplified in Vero cells (Fig. 2.3). The plaque morphology of both rMP12 and AMTV were similar and could not be distinguished based on plaque phenotypes. Total RNA was extracted from Vero cells and genotype analyses were carried via RT-PCR (Fig. 2.3). From the genotype analysis, no reassortant strains were identified between rMP-12 and AMTV, whereas 47% and 53% of the plaque clones were parental rMP-12 and parental AMTV, respectively (Fig. 2.9).

## Discussion

Implementation of routine vaccination program for susceptible livestock likely provides protection from severe diseases that are caused by RVFV infection, as well as preventing horizontal transmission of RVFV to mosquitoes. Freire et al. demonstrated that the genetic diversity of RVFV strains has gradually decreased since massive vaccination of livestock in the 1970s with the live-attenuated Smithburn vaccine<sup>65,109</sup>. Genetic reassortment has been reported to occur between the same RVFV species, whereas the exchange of genomic segments between two different bunyavirus species has also been shown<sup>110–113</sup>. For example, the Ngari virus, which is an unclassified orthobunyavirus within the family *Peribunyaviridae*, is a reassortant consisting of the L- and S-segment of the Bunyamwera virus, and the M-segment of the Batai virus. This reassortant strain was isolated during an outbreak of RVF in East Africa in 1997–1998 from hemorrhagic fever patients<sup>66,67</sup>. It is therefore critical to understand the likelihood of reassortant strain formation between RVFV vaccine strain and heterologous phlebovirus species in endemic regions. Within the *Phenuiviridae* family, AMTV is transmitted via mosquitoes in Africa<sup>62,63</sup>. In Burkina Faso, serological evidence of infection with either RVFV or AMTV was demonstrated in sheep<sup>61</sup>. AMTV induces transient fever in experimentally infected sheep, and shares mosquito vectors (*Culex antennatus*) with RVFV<sup>63,70</sup>. As of current, little is known regarding the ability of RVFV to incorporate RNA segments from other phleboviruses to generate infectious progeny virions. A past study characterized the RNA synthesis compatibility of the N and L protein of RVFV using a minigenome assay<sup>114</sup>. Using an S-like minigenome encoding the chloramphenicol acetyltransferase (CAT) with the backbone of RVFV or TOSV, the study demonstrated that the

co-expression of N and L proteins of RVFV or that of N and L proteins of TOSV supported the expression of CAT activity. The co-expression of the N protein of TOSV and L protein of RVFV also increased the activity level of CAT from the minigenome of RVFV, but not from the minigenome of TOSV. The co-expression of the N protein of RVFV and L protein of TOSV did not, however, increase the activity level of CAT from minigenomes of either RVFV and TOSV. The amino acid identities between RVFV and TOSV are 49% for the N protein and 54% for the L protein (GenBank accession number: KU925898 and KU925899), which is lower than the amino acid identities shown between RVFV and AMTV. Our results demonstrated that the co-expression of the N protein of RVFV and the L protein of AMTV, or vice versa, does not support the replication of the minigenome. In addition, the RVFV minigenome RNP consisting of RVFV N and L proteins cannot be packaged via the envelope Gn/Gc proteins of AMTV, and vice versa. Overall, the combinations of RVFV N and AMTV L, and vice versa, and the combinations of RVFV RNP and AMTV GnGc proteins, and vice versa, does not functionally support the viral life cycle. In further support, no reassortant strains between rMP-12 and AMTV could be identified in the co-infection assay using C6/36 cells after isolation of 17 well isolated plaques. This could be due to the small number of plaques isolated, however due to this incompatibility of the structural N, L, and Gn/Gc proteins, it was concluded that formation of genetic reassortant strains between RVFV and AMTV are most likely not viable. Similar approaches will be applicable to determine and characterize genetic compatibility and reassortment between other species of phleboviruses.

To characterize the potential formation of reassortant strains in co-infected cells, the rMP12-GM50 strain was newly generated via reverse genetics. This strain encodes a total of 584 silent mutations in the ORFs within the L-, M-, and S-segments; i.e., 326 mutations in the L-segment, 185 silent mutations in the M-segment, and 73 silent mutations in the S-segment. This

genetic variant encodes a unique pattern of silent mutations throughout the genomic RNA that is not found in nature. Additionally, the nucleotide difference of the genetic variant rMP12-GM50, is larger than the genetic diversity found among natural isolates of RVFV, which was reported to be 4-4.5%<sup>115</sup>. This rMP12-GM50 strain is thus useful not only for characterizing genetic reassortment, but also for studies pertaining to homologous recombination in species of RVFV. From the PCR-RFLP analysis, co-infection of C6/36 cells with the rMP-12 and rMP12-GM50 strains after 1 day produced all possible combinations of L-, M-, and S-segment reassortants, indicating that there is little bias when generating reassortants in mosquito cells. Maintenance of co-infected C6/36 cells, without adding fresh C6/36 cells, could result in the establishment of persistently-infected cells, which continuously generated infectious virions in culture supernatants. Characterization of viral genomic RNA from such persistently-infected C6/36 cells at 56 dpi did not indicate the formation of defective-interfering (DI) particles, whereas the full-genome sequencing of five plaque-clones did not encode evidence of recombination between rMP-12 and rMP12-GM50 (data not shown). Although RVFV RNA retained good integrity in C6/36 cells during persistent infection, genetic changes might be induced in other cell types, as a result of antiviral responses affecting viral replication. In this regard, the rMP12-GM50 strain will be an excellent tool to evaluate genetic exchanges during co-infections.

Pathogenic strains of RVFV and live-attenuated vaccine strains might form reassortant strains in co-infected cells in nature<sup>65</sup>. The MP-12 strain, however, has been reported to induce low level of viremia ( $10^{2.5}$  pfu/ml) in ruminants, and this is considered not sufficient enough to infect mosquitoes orally in laboratory studies<sup>116,117</sup>. Furthermore, the MP-12 strain is attenuated through several point mutations presented in each of the three segments; therefore, any generated reassortants encoding RNA segments of MP-12 will be further attenuated when compared to the

pathogenic strains of RVFV<sup>118</sup>. Taken together, this indicates that any reassortant of MP-12 with wt RVFV strains would not exhibit pathology more severe than parental RVFV infections.

## **CHAPTER 3: Characterization of the attenuation and protective efficacy of rMP12-GM50 strain in mice**

### **Introduction**

Since the first reported RVF outbreak in Kenya in 1930, the geographical distribution of RVFV has expanded into Saudi Arabia, Yemen, and many other countries in Africa<sup>32,33,115,119</sup>. Effective vaccination of susceptible animals and humans at high risk of viral exposure is one of the most important approaches to minimizing the impact of RVF outbreaks<sup>83,84</sup>. In some countries in endemic regions, live-attenuated vaccines and/or inactivated vaccines are commercially available for veterinary use<sup>120,121</sup>. Preparation of a national vaccine stockpile is just as important for neighboring non-endemic countries as it is for endemic countries. In the U.S., a live-attenuated MP-12 vaccine was conditionally licensed for veterinary use upon RVF outbreaks based on its protective efficacy and demonstrated safety in ruminants<sup>83,122-127</sup>. There are currently no licensed RVF vaccines or therapeutics available for humans. Live-attenuated RVF vaccines have shown strong protective efficacies in ruminants following a single dose without adjuvants. Since these vaccine strains replicate in vaccinated animals, residual virulence might be a concern in vulnerable populations, including pregnant or newborn animals<sup>85,128</sup>. Although subunit vaccines, DNA vaccines, viral vectors, and single-cycle RVF replicons are considered highly safe in animals due to a lack of viral spread, the vaccine immunogenicity of these novel candidates is not as high as traditional live-attenuated vaccines, and a booster dose and/or the use of adjuvants might be required to induce long-term protective immunity<sup>86-89</sup>. As introduced in the first aim, a recombinant MP-12 strain, which encodes hundreds of silent mutations throughout the ORFs of

genomic RNA (rMP12-GM50 strain) was newly generated<sup>129</sup>. The rMP12-GM50 strain is potentially valuable as a novel vaccine candidate, because numerous silent mutations might strengthen the attenuation profile of the MP-12 strain via the L-, M-, and S-segments, and also serve as genetic markers to be distinguished from other RVFV strains during or after the vaccination. This characteristic is a highly sought after feature for newly developed veterinary vaccines in endemic countries. In this study, I aim to characterize the attenuation profile and protective efficacy of rMP12-GM50 strain compared the parental MP-12 strain.

## **Materials and methods**

### **Media, cells, and viruses**

BHK/T7-9 cells, stably expressing T7 RNA polymerase<sup>100</sup>, were kept in MEM-alpha containing 10% FBS, streptomycin (100 µg/ml), penicillin (100 U/ml), and hygromycin B (600 µg/ml) at 37°C with 5% CO<sub>2</sub>. MRC-5 (ATCC CCL-171), Vero (ATCC CCL-81), and VeroE6 cells (ATCC CRL-1586) were kept in DMEM containing 10% FBS, penicillin (100 U/ml), and streptomycin (100 µg/ml) at 37 °C with 5% CO<sub>2</sub>. All cells were verified to be mycoplasma free with the UTMB Tissue Culture Core Facility, and the identity of MRC-5 cells was authenticated via Short Tandem Repeat analysis with the UTMB Molecular Genomics Core Facility. For this study, the MP-12 vaccine Lot 7-2-88 was amplified once in MRC-5 cells before experimental use. Using reverse genetics, recombinant ZH501 (rZH501) and rMP-12 strains were recovered from BHK/T7-9 cells and passaged once in VeroE6 cells in a BSL-4 Laboratory at UTMB<sup>101,103</sup>. As mentioned above, an rMP-12 variant encoding a total of 584 silent mutations within the L, M, N, and NSs ORFs named rMP12-GM50, was also recovered<sup>129</sup>. Using reverse genetics, reassortant

rZH501 strains encoding either the L-, M-, or S-segment of rMP12-GM50 (RST-GM50-L, RST-GM50-M, and RST-GM50-S, respectively) were rescued from BHK/T7-9 cells. All reassortant viruses were then amplified in Vero cells, and viral titers were carried out in VeroE6 cells via plaque assay<sup>103</sup>.

## **Plasmids**

Plasmids expressing the positive-sense RNA of the L, M-, and S-segments of rMP12-GM50 (pProT7-vL(+)-GM50, pProT7-vM(+)-GM50, and pProT7-vS(+)-GM50, respectively) were described previously<sup>129</sup>. Manually, silent mutations encoded in the rMP12-GM50 strain were designed and introduced one by one so as not to disturb the codon pair bias and codon usage in humans<sup>104,107</sup>. One or more silent mutations were introduced at every 50 nucleotide intervals serving as gene markers for this strain and was thus designated as gene marker 50 (GM50).

## **Mouse challenge experiments with rZH501 and the reassortant strains**

Five-week-old outbred CD1 mice (Charles River, North Franklin, CT) were inoculated via the intraperitoneal route (i.p.) with  $1 \times 10^3$  PFU of RST-GM50-L, RST-GM50-M, RST-GM50-S (n = 10 per group) or parental rZH501 (control, n = 5 per group). Clinical signs were recorded daily, whereas body weight was measured daily for seven days, followed by every three days until termination of study at 21 days post challenge. Mice displaying body weight loss of more than 20% and/or showing clinical signs of disease such as severe lethargy or viral encephalitis, were humanely euthanized. Remaining surviving mice were also humanely euthanized at 21 days post challenge. All experiments handling infectious rZH501 was performed at the Galveston National Laboratory or the Robert E. Shope BSL-4 laboratory at UTMB.

### **Protective efficacy experiment 1**

Five-week-old outbred CD1 mice were inoculated via the subcutaneous (s.c.) route with  $1 \times 10^4$  or  $1 \times 10^5$  PFU of parental MP-12 or the rMP12-GM50 strain ( $n = 10$  per group), or PBS (mock,  $n = 5$ ). At 43 days post vaccination (dpv), serum samples were collected via the retro-orbital vein. At 45 dpv, mice were then challenged via the i.p. route with  $1 \times 10^3$  PFU of pathogenic rZH501. Clinical signs were recorded daily, whereas body weight was measured daily for seven days, followed by every three days until termination of study at 21 days post challenge. At 21 days post rZH501 challenge, sera were collected via cardiac puncture from surviving mice. Using the GraphPad Prism 6.05 program (GraphPad Software Inc.), survival curves of mice were analyzed via the Kaplan-Meyer method.

### **Protective efficacy experiment 2**

Five-week-old outbred CD1 mice were inoculated via s.c. or intramuscular (i.m.) with  $5 \times 10^5$  PFU of parental MP-12 or the rMP12-GM50 strain (s.c.:  $n = 10$  per group; i.m.:  $n = 10$  per group), or PBS (s.c.:  $n = 5$ ; i.m.:  $n = 5$ ). At 42 dpv, serum samples were collected via the retro-orbital vein. As described previously for protective efficacy experiment 1, at 45 dpv, mice were then challenged via i.p. with  $1 \times 10^3$  PFU of pathogenic rZH501.

### **Plaque reduction neutralization test**

Titers, using the plaque reduction neutralization test (PRNT<sub>50</sub> and PRNT<sub>80</sub>), were determined as described previously<sup>130</sup>. Collected serum (20 $\mu$ l aliquot) from mice were serially diluted four-fold and transferred into flat-bottom 96-well plate containing the MP-12 virus, in

which 50 plaques were formed per well (final dilutions of sera mixed with viral input were 1:10, 1:40, 1:160, 1:640, 1:2560, and 1:10,240). After 1 hour of incubation at 37°C, 150µl of media was added to each well. Next, 150µl of the mixture was transferred to 24-well plates containing sub-confluent VeroE6 cells and incubated for 1 hour at 37°C. After removal of inocula, cells were further incubated for 72 hours with an overlay containing 1xMEM, 5% FBS, 5% TPB, streptomycin, penicillin, and 0.3% tragacanth gum. VeroE6 cells were then fixed with 25% formalin and 5% ethanol containing crystal violet. The average number of plaques from five different wells that contained mock-immunized mice sera was used to set the cut-off number of 50% or 80% reduction. To determine titers, the highest dilution of sera that inhibited plaque formation below the cut-off value was used.

### **Statistical analysis**

Using the GraphPad Prism 6.05 program (GraphPad Software Inc.), statistical analyses were carried out. The arithmetic means of  $\log_{10}$  values of viral titers were analyzed via one-way ANOVA followed by the Turkey's multiple comparison test. The Kaplan-Meier survival curve analysis was performed via the Log-rank (Mantel-Cox) test.

### **Results**

#### **Attenuation of pathogenic recombinant ZH501 strain through the L-, M-, or S-segments of the rMP12-GM50 strain.**

Although the MP-12 strain is attenuated through point mutations encoded in the L-, M-, and S-segment, each segment only partially contributes to the attenuation of RVFV. Previous study

showed that mice challenge via i.p. with  $1 \times 10^3$  PFU of reassortant rZH501 strain encoding either the L-, M-, or S-segment of the MP-12 strain (RST-MP12-L, RST-MP12-M, and RST-MP12-S) had a survival rate of 20%, 40%, and 0%, respectively<sup>118</sup>. Similarly, to determine attenuation of each segment of the rMP12-GM50 strain, reassortant rZH501 strains encoding either the L-, M-, or S-segment of the rMP12-GM50 strain (RST-GM50-L, RST-GM50-M, and RST-GM50-S) were generated. Outbred CD1 mice were challenged with rZH501, RST-GM50-L, RST-GM50-M, or RST-GM50-S. All mice challenged with the rZH501 strain died or were humanely euthanized due to severe clinical signs of disease within 5 days post challenge (Fig. 3.1). Out of the ten mice that was infected with RST-GM50-S, nine displayed a hunched back or scruffy coat from 5-12 dpi, and three mice showed neurological signs of disease, such as ataxia or paralysis at 7-8 dpi (Fig. 3.1). Similarly, out of the ten mice infected with RST-GST-M, nine mice showed a hunched back or scruffy coat from 3–8 dpi, and three mice displayed ataxia or paralysis at 7, 9, or 10 dpi (Fig. 3.1). In contrast, out of the ten mice infected with RST-GM50-L, three displayed a hunched back or a scruffy coat at 11 dpi, and one mouse died at 8 dpi (Fig. 3.1). Overall, mice infected with RST-GM50-L, RST-GM50-M, RST-GM50-S, and rZH501, had a survival rate of 90%, 50%, 30%, and 0% respectively (Fig. 3.1). The survival curves of RST-GM50-L, RST-GM50-M, or RST-GM50-S were significantly different when compared to the control group of rZH501 (Log-rank test,  $p < .0001$ ). Furthermore, the survival curves were also significantly different for the RST-GM50-L and RST-GM50-S groups (Log-rank test,  $p = .0073$ ).

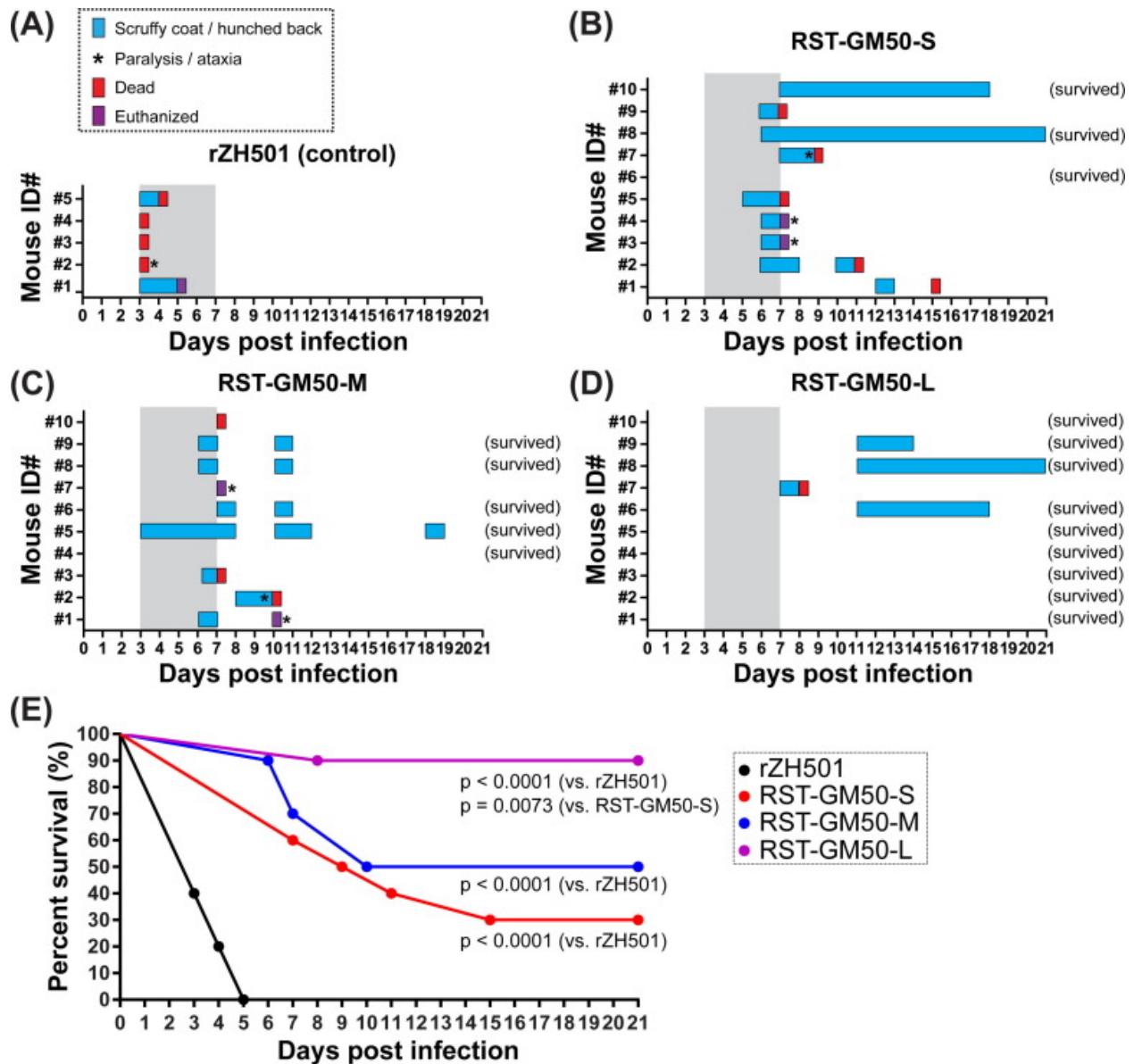


**Figure 3.1: Survival of mice infected with the parental rZH501 strain of Rift Valley fever virus or its reassortants with the rMP12-GM50 strain.**

(A – D) Outbred CD1 mice were mock-infected with PBS or infected with  $1 \times 10^3$  PFU of parental rZH501 ( $n = 5$ ), or reassortant strains RST-GM50-L, RST-GM50-M, or RST-GM50-S ( $n = 10$  per group) via i.p. Clinical signs of disease observed in each mouse infected with rZH501 (A), RST-GM50-S (B), RST-GM50-M (C), or RST-GM50-L (D) are shown. Blue = scruffy coat and/or hunched back; red = dead; purple = euthanized; asterisk = paralysis and/or ataxia; gray shadowing = typical period of disease in parental rZH501-infected mice. (E) The Kaplan-Meier survival curve of infected mice. Statistically significant differences based on log-rank testing among groups are shown.

Ly H et al. (2017) Attenuation and protective efficacy of Rift Valley fever phlebovirus rMP12-GM50 strain. *Vaccine* 35(48): 6634-6642. <https://doi.org/10.1016/j.vaccine.2017.10.036>

### **Protective efficacy of the rMP12-GM50 strain via the subcutaneous route**

The protective efficacy of the rMP12-GM50 strain was next evaluated and compared to the parental MP-12 strain. The protective efficacy of the MP-12 and rMP12-GM50 strains were first tested via the s.c. route using  $1 \times 10^4$  and  $1 \times 10^5$  PFU doses (Fig. 3.2), since previous efficacy experiments were carried out via the s.c. route using the MP-12 strain<sup>124,125,127,130,131</sup>. At 43 dpv, vaccination with  $1 \times 10^4$  or  $1 \times 10^5$  PFU doses of MP-12 resulted in an increase of PRNT<sub>50</sub> neutralizing antibody titers (1:40 or higher) in 30% or 100% of vaccinated mice, respectively (Fig. 3.3). While for PRNT<sub>80</sub>, vaccination with  $1 \times 10^4$  or  $1 \times 10^5$  PFU doses of MP-12 resulted in an increase of neutralizing antibody titers (1:40 or higher) in 20% or 40% of vaccinated mice, respectively. For rMP12-GM50, vaccination with  $1 \times 10^4$  or  $1 \times 10^5$  PFU doses resulted in an increase of PRNT<sub>50</sub> titers (1:40 or higher) in 30% or 60% of vaccinated mice, respectively. While for PRNT<sub>80</sub>, vaccination with  $1 \times 10^4$  or  $1 \times 10^5$  PFU doses resulted in an increase of neutralizing antibodies (1:40 or higher) in 10% or 50% of vaccinated mice, respectively. (Fig. 3.3). At 45 dpv, mice were challenge with pathogenic rZH501 strain, and four out of five (80%) mice that were mock-vaccinated with PBS died within 8 days post challenge (Fig. 3.2). Vaccination with  $1 \times 10^4$  or  $1 \times 10^5$  PFU of MP-12 resulted in 50% or 60% survival of mice after rZH501 challenge, respectively (Fig. 3.2). Vaccination of mice with  $1 \times 10^4$  or  $1 \times 10^5$  PFU of rMP12-GM50 resulted in 10% or 50% survival after rZH501 challenge, respectively (Fig. 3.2). Survival curves of the  $1 \times 10^5$  PFU dose group of MP-12 and the  $1 \times 10^5$  PFU dose group of rMP12-GM50 showed marginal differences when compared to the mock-vaccinated group (Log-rank test,  $p=.0376$  and  $p=.0493$ , respectively).

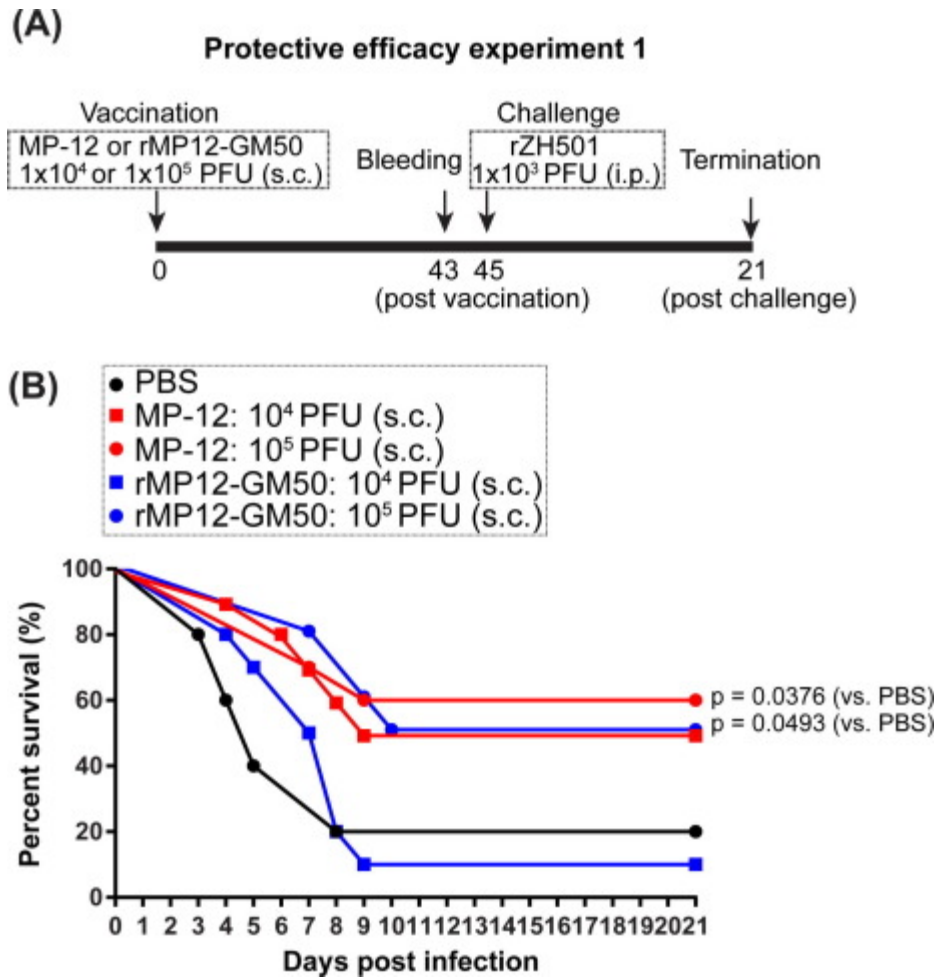


**Figure 3.2: Protective efficacy experiment #1: vaccination via subcutaneous route.**

(A) Schematic representation of vaccination and challenge schedule for the protective efficacy experiment #1. Outbred CD1 mice were mock-vaccinated via subcutaneous route (s.c.) with PBS ( $n = 5$ ), or vaccinated via s.c. with  $1 \times 10^4$  PFU or  $1 \times 10^5$  PFU of MP-12 ( $n = 10$  per group) or rMP12-GM50 ( $n = 10$  per group). (B) The Kaplan-Meier survival curve of infected mice is shown. Statistically significant differences based on log-rank testing between mock-vaccinated group and vaccinated group are also shown.

Ly H et al. (2017) Attenuation and protective efficacy of Rift Valley fever phlebovirus rMP12-GM50 strain. *Vaccine* 35(48): 6634-6642. <https://doi.org/10.1016/j.vaccine.2017.10.036>

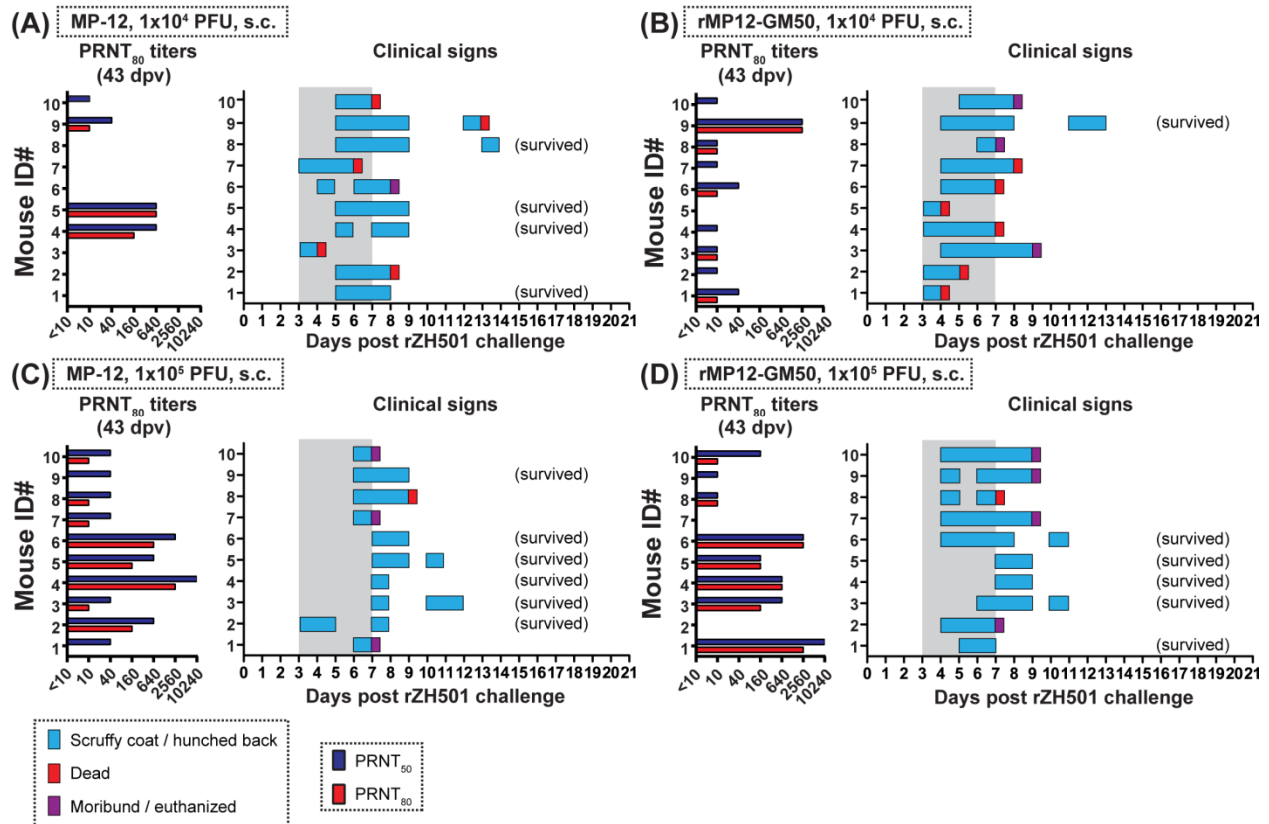


**Figure 3.3: Titrations of Plaque Reduction Neutralization Test (PRNT<sub>50</sub> and PRNT<sub>80</sub>) and clinical signs of disease observed in each mouse vaccinated via subcutaneous route.**

The PRNT<sub>50</sub>, PRNT<sub>80</sub>, and clinical signs of disease in mice vaccinated via s.c. with  $1 \times 10^4$  PFU (A and B) or  $1 \times 10^5$  PFU (C and D) of MP-12 ( $n=10$  per group, A and C) or rMP12-GM50 ( $n=10$  per group, B and D) are shown. Blue = scruffy coat and/or hunched back; asterisk = paralysis and/or ataxia, red = dead; purple = euthanized, gray shadowing = typical period of disease in parental rZH501 in mice.

Ly H et al. (2017) Attenuation and protective efficacy of Rift Valley fever phlebovirus rMP12-GM50 strain. *Vaccine* 35(48): 6634-6642. <https://doi.org/10.1016/j.vaccine.2017.10.036>

### Protective efficacy of the rMP12-GM50 strain via the intramuscular route

Since vaccinations via the s.c. route were not efficacious, even with  $1 \times 10^5$  PFU of the MP-12 or rMP12-GM50 strains, a higher dose of  $5 \times 10^5$  PFU via the s.c. or i.m. route was evaluated next (Fig. 3.4). At 42 dpv, 50% or 30% of mice vaccinated via s.c. with  $5 \times 10^5$  PFU of the MP-12 or rMP12-GM50 strains, respectively, had neutralizing antibodies with PRNT<sub>80</sub> 1:40 or higher. Whereas it was 50% or 70% of mice vaccinated via s.c. with  $5 \times 10^5$  PFU of the MP-12 or rMP12-

GM50 strains, respectively, had neutralizing antibodies with PRNT<sub>50</sub> 1:40 or higher (Fig. 3.4). The average neutralizing antibody titer of responders (PRNT<sub>80</sub> titers of 1:10 or higher) was 1:4375 against the MP-12 strain and 1:1840 against the rMP12-GM50 strain.

In contrast, improved immunogenicity for both MP-12 and rMP12-GM50 vaccine strains was shown from vaccination via the i.m. route. Neutralizing antibodies (PRNT<sub>50</sub> or PRNT<sub>80</sub> 1:40 or higher) were detected in 100% of mice vaccinated via i.m. with MP-12 and 90% of mice vaccinated via i.m. with rMP12-GM50. None of the mice in these groups displayed clinical signs of disease after rZH501 challenge for 21 days (Fig. 3.4). The average neutralizing antibody titers of responders via i.m. vaccination for PRNT<sub>80</sub> were 1:3712 against MP-12 and 1:853 against rMP12-GM50.

At 45 dpv, all mice were challenged with the pathogenic rZH501 strain. Mice vaccinated via the s.c. route with  $5 \times 10^5$  PFU of MP-12 or rMP12-GM50 resulted in a survival rate of 60% or 70%, respectively. Mice that died or was humanely euthanized due to clinical signs of disease, did not have neutralizing antibody of PRNT<sub>50</sub> or PRNT<sub>80</sub> higher than 1:40 (Fig. 3.4). The survival curves of mice vaccinated with  $5 \times 10^5$  PFU of MP-12 or rMP12-GM50 via s.c. were statistically significant when compared to the mock-vaccinated group (Log-rank test,  $p=0.0128$  or  $p=0.0313$ , respectively). In contrast, the survival rate was shown to be 100% for mice vaccinated via i.m. with  $5 \times 10^5$  PFU of MP-12 or rMP12-GM50, and the survival curves were significantly different when compared to the mock-vaccinated group (Log-rank test,  $p<0.0001$ ) (Fig. 3.4). Overall, these results demonstrated that the rMP12-GM50 strain has a protective efficacy similar to parental MP-12 strain in the mouse challenge model. In addition, vaccination via the i.m. route can induce better protection in mice from pathogenic RVFV challenge than vaccination via the s.c. route.

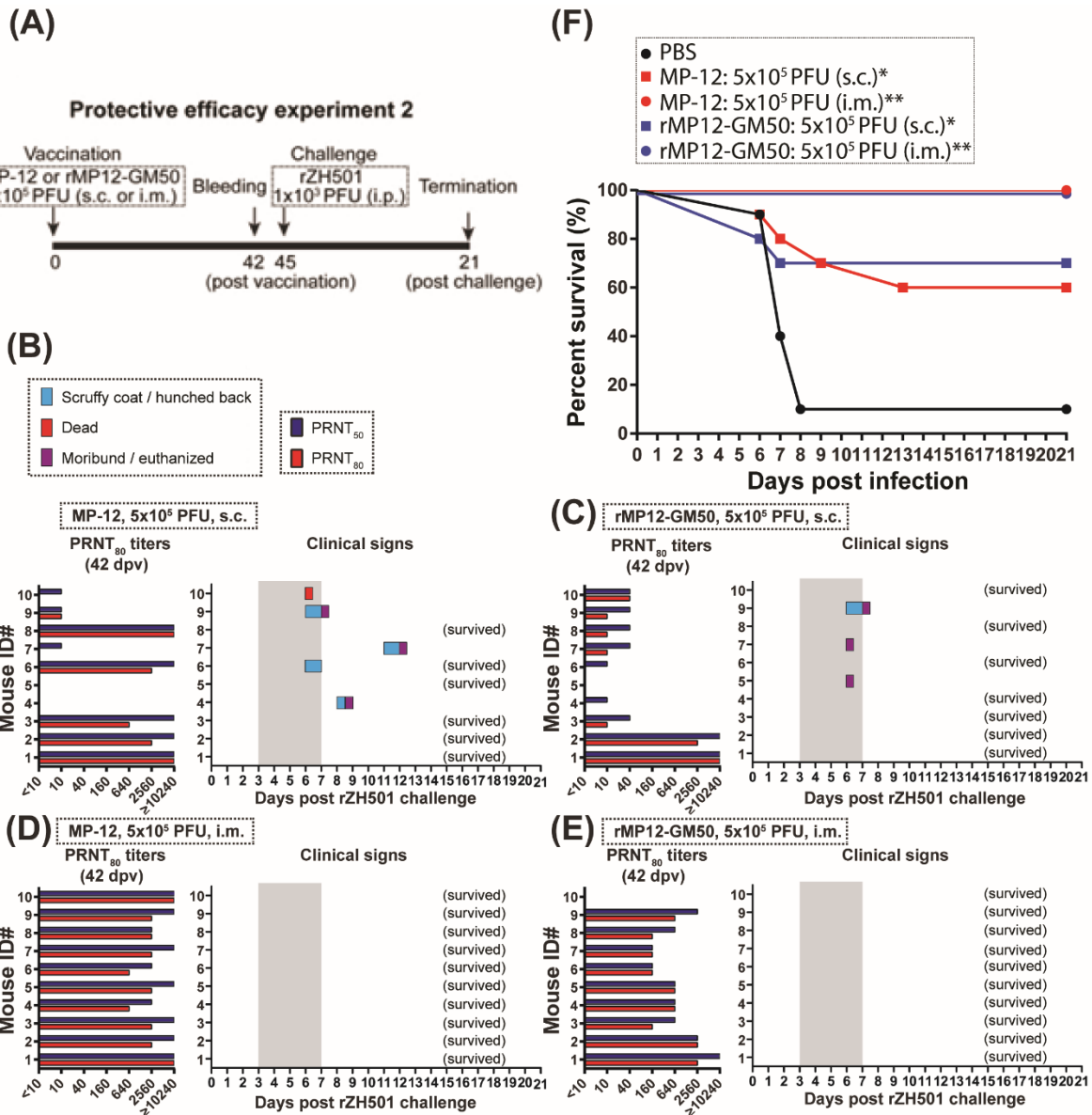


**Figure 3.4: Protective efficacy experiment #2: vaccination via subcutaneous or intramuscular route.**

(A) Schematic representation of vaccination and challenge schedule for the protective efficacy experiment #2. Outbred CD1 mice were mock-vaccinated via the s.c. or i.m. route with PBS ( $n = 5$  per route), or with  $5 \times 10^5$  PFU of MP-12 ( $n = 10$  per group) or rMP12-GM50 ( $n = 10$  per group). (B – E) The PRNT<sub>50</sub>, PRNT<sub>80</sub> and clinical signs of disease observed in each mouse infected with  $5 \times 10^5$  PFU of MP-12 or rMP12-GM50. Blue = scruffy coat and/or hunched back; red = dead; purple = euthanized; asterisk = paralysis and/or ataxia; gray shadow = typical period of disease in parental rZH501 in mice. (F) The Kaplan-Meier survival curve of infected mice is shown. Statistically significant differences based on log-rank testing between mock-vaccinated group and vaccinated group are also shown.

Ly H et al. (2017) Attenuation and protective efficacy of Rift Valley fever phlebovirus rMP12-GM50 strain. *Vaccine* 35(48): 6634-6642. <https://doi.org/10.1016/j.vaccine.2017.10.036>

## Discussion

In the U.S., the MP-12 vaccine has been conditionally licensed for veterinary use<sup>123</sup>. As mentioned above, the MP-12 strain was originally generated from the ZH548 strain that underwent serial passages in MRC-5 cells in the presences of 5-fluorouracil, which is a chemical mutagen<sup>122</sup>. This resulted in the introduction of 23 mutations into each of the L-, M-, and S-segments. Two amino acid substitutions (Gn-Y259H and Gc-R1182G) in the M-segment were reported to be independently responsible for the attenuation of MP-12<sup>118</sup>. These two mutations in the M-segment and two other amino acid substitutions (V172A and M1244I) in the L-segments, was reported to display a temperature-sensitive phenotype that results in the restriction of viral replication at 38°C and above<sup>132</sup>. Based on the virulence of reassortant ZH501 strains that encodes one of the L-, M-, or S-segments of MP-12, the degree or strength of attenuation of each segment were determined as M > L > S. The survival rate of mice infected via i.p. with  $1 \times 10^3$  PFU of RST-MP12-L, RST-MP12-M, or RST-MP12-S was 20%, 40%, or 0%, respectively<sup>118</sup>. Although the attenuation of the MP-12 strain through the S-segment was not evident based on the survival rate in mice, pathogenic strains of RVFV encoding the S-segment of MP-12 demonstrated prolonged survival times in mice<sup>118,133</sup>. To achieve further attenuation of the MP-12 S-segment, the truncation of the NSs gene (rMP12- $\Delta$ NSs16/198)<sup>101,130</sup> or the replacement of the NSs gene of MP-12 with the NSs gene of another phlebovirus could be accomplished<sup>131,134</sup>. Minimal attenuation of the M-segment could also be accomplished via truncation of the 78 kD/NSm gene (rMP12- $\Delta$ NSm21/384)<sup>25,135,136</sup>. The deletion of the 78 kD/NSm gene in the ZH501 strain (rZH501- $\Delta$ NSm21/384) was shown to be 100% lethal in mice, however in both mice and rats, the onset of disease was delayed<sup>134,137</sup>. This

indicated that truncation of the 78 kD/NSm gene had only a weak effect on attenuating the ZH501 strain. Due to a lack of rationale for any approach towards altering the functions of the L protein, modification of the L-segment has not been evaluated.

Further attenuation of MP-12 strain without affecting the immunogenicity is important, because parental MP-12 strain has residual virulence in pregnant ewes upon vaccination during the first trimester. Introduction of silent mutations throughout the ORFs of MP-12, via reverse genetics, generated the rMP12-GM50 strain in this study. Evaluation of viral replication kinetics in Vero cells demonstrated a significant reduction of the rMP12-GM50 strain early in infection. For MRC-5 cells, a slight decrease of the viral replication of rMP12-GM50 also occurred, yet this difference was not statistically significant. Mice infected with reassortant ZH501 strain encoding either the L-, M-, or S-segment of rMP12-GM50 strain showed 90%, 50%, or 30% survival, respectively. The result indicated that rMP12-GM50 strain is likely more attenuated than parental MP-12 strain via the L- and S-segment. Moreover, the protective efficacy experiment showed that mice vaccinated with rMP12-GM50 strain could induce high titers of neutralizing antibody, in particular through the i.m. route. Complete protection of vaccinated mice with rMP12-GM50 strain is a promising result for further characterization of this strain in vaccine research and development for RVF. It remains unknown how vaccination via the i.m. route with the MP-12 strain could produce high responders when compared to the s.c. route. Although there are evidences of better immune responses from vaccination via the i.m. route, vaccination with live-attenuated vaccines has been traditionally administered via the s.c. route<sup>138,139</sup>. Further evaluation of vaccination via the i.m. route may be important for the MP-12 vaccine strain as well as for other next generation vaccines for RVF.

Vaccination with live-attenuated Smithburn strain in South Africa resulted in a co-infection event with wild-type RVFV and the Smithburn strain in a human, which led to the isolation of an M-segment reassortant strain (SA184/10)<sup>110</sup>. Such unexpected events might occur in endemic countries via handling vaccines using the same syringes for both viremic and uninfected animals. In such a scenario, the formation of reassortant strain between circulating RVFV and MP-12 strain is likely. Although resulting reassortant strains are likely more attenuated than circulating pathogenic RVFV strains, it will be difficult to trace the RNA in nature due to a lack of notable genetic markers distinguishable between MP-12 strain and wild-type RVFV strains. For environmental surveillance of live-attenuated RVF vaccine in endemic countries, silent mutations in the rMP12-GM50 strain will serve as an excellent genetic marker to distinguish vaccine-derived RNA fragments from naturally circulating RVFV strains, upon the event of genetic reassortment or recombination in nature.

## CHAPTER 4: Characterization of recombinant MP-12 strain encoding a part of AMTV genome

### Introduction

Characterization of inter-species genetic recombination between RVFV and AMTV is important, because co-infection of susceptible animals or mosquitoes with RVFV and AMTV might lead to partial exchange of genetic materials in nature. RVFV is an arbovirus that is transmitted by many species of mosquitoes. Its continual presence in nature is possible through viral persistence for years in the eggs of infected *Aedes* spp. mosquitoes as well as transient amplifications of RVFV in susceptible animals, including African buffalos, livestock, rodents, or bats<sup>140</sup>. This vertical transmission partly explains why RVFV can reappear after long inter-epizootic periods, especially after excessive rainfalls during which hydration of *Aedes* eggs leads to the hatching of infected mosquitoes for new infections in susceptible animals. AMTV shares similar mosquito vectors and geographic regions endemic to RVF. It is an unclassified phlebovirus within the family *Phenuiviridae*, and is currently proposed as a member of the *Salehabad* species complex. AMTV has been isolated from wild mammals (mostly rodents) or birds in Africa. Although AMTV has not been isolated from humans or sheep, seroprevalence in humans and sheep in Africa indicates that AMTV infection does occur in these species. Other than what has been discussed previously in Chapter 1, little is known regarding the pathology of AMTV.

Due to a lack of functional compatibility between structural proteins, formation of genetic reassortant strains between RVFV and AMTV is unlikely, as discussed above. Meanwhile, it is unknown whether the RVFV strain encoding a part of AMTV genome, as a result of genetic recombination, is viable or not. AMTV genome, other than the ORF of structural proteins (N, L,

Gn, and Gc), might allow the generation of viable recombinant RVFV encoding AMTV sequence: e.g., UTR, NSs gene, NSm gene. Both RVFV and AMTV have a tripartite genome with each segment containing 3' and 5' UTR termini composed of a complementary 8 nt sequence, that is highly conserved among phleboviruses, to form a pan-handle structure (Fig 4.1). The UTR regions other than genomic termini are variable and the sequences and lengths are different among phleboviruses. The 5' UTR of the L- or M-segment, or the IGR of the S-segment are also responsible for mRNA termination. The L segment 5' UTR of RVFV contains a sequence forming a stem-loop structure, that is responsible for mRNA termination, whereas a pentanucleotide sequence, downstream of a homopolymeric tract of C or G sequences, are responsible for mRNA termination within the RVFV M- or S-segment<sup>141</sup>. Other than transcriptional termination, UTRs play a role in coordinated packaging of the L-, M-, and S-segments. Terasaki et al. demonstrated that the 5' UTR of the RVFV M-segment, functions in the co-packaging of the S-segment RNA, which then subsequently supports the packaging of the L- segment. RVFV M-segment could also be split into two segments via separating the Gn and Gc ORFs, leading to the production of a four-segmented RVFV, which was also shown to be highly attenuated<sup>90</sup>. The four-segmented RVFV failed to replicate efficiently in mosquito cells by an unknown mechanism<sup>142</sup>. By using a RVFV minigenome system, Gaudiard et al. indicated that the UTRs of L-, M- and S-segment function as signals for viral RNA packaging<sup>143</sup>. Recombinant LACV (genus *Orthobunyavirus*) encoding the chimeric M-segment consisting of the NSm, Gn, and Gc ORFs of Jamestown Canyon virus, flanked by the 5' and 3' UTRs of LACV M-segment, was viable in cell culture, yet also highly attenuated in mice<sup>144</sup>. These studies implied that viral UTR could be exchanged between different RNA segments or species, and may attenuate viral replication and virulence as a result of recombination.



## **Materials and methods**

### **Media, cells, and viruses**

Vero (ATCC CCL-81), VeroE6 (ATCC CRL-1586), MRC-5 (ATCC CCL-171), A549 (ATCC CCL-185), Hepa1-6 (ATCC CRL-1830), and BHK-21 (ATCC CCL-10) cells were maintained at 37°C with 5% CO<sub>2</sub> in DMEM containing 10% FBS, penicillin (100 U/ml), and streptomycin (100 µg/ml). BHK/T7-9 cells, which stably expresses T7 RNA polymerase<sup>100</sup>, were maintained at 37°C with 5% CO<sub>2</sub> in MEM alpha containing 10% FBS, penicillin (100 U/ml), streptomycin (100 µg/ml), and hygromycin B (600 µg/ml). *Aedes albopictus* C6/36 cells (ATCC CRL-1660) were maintained at 28°C without CO<sub>2</sub> in Leibovitz's L-15 medium containing 10% FBS, 10% TPB, penicillin (100 U/ml), and streptomycin (100 µg/ml). All cells used in this study were verified to be mycoplasma free at the UTMB Tissue Culture Core Facility, and the identities of MRC-5 and A549 cells were authenticated by Short Tandem Repeat analysis (UTMB Molecular Genomics Core Facility). The rMP-12 strain was recovered from BHK/T7-9 cells via reverse genetics, and passaged once in VeroE6 cells, as described previously<sup>101,103</sup>. AMTV Ar 1286-64 strain was kindly provided by Dr. Robert B. Tesh from the UTMB. AMTV was plaque-cloned once and then amplified three times in Vero cells before experimental use. An rMP-12 encoding an in-frame 69% deletion of the NSs gene (rMP12-ΔNSs16/198 or rMP12-C13type) has been previously described<sup>101</sup>.

### **Plasmids**

#### **Plasmids for chimeric MP-12 strain**

Plasmids expressing UTRs of AMTV were modified to encode MP-12 ORFs of L-, M-, or S-segments. PCR fragments encoding backbone plasmids plus the entire 3' and 5' UTRs of AMTV were amplified from either pProT7-AMTV-L(+), pProT7-AMTV-M(+), or pProT7-AMTV-S(+ plasmids. PCR fragments were also prepared to encode the N, M, or L ORFs of MP-12. Two PCR fragments were recombined via Gibson assembly, and the following plasmids were generated: pProT7-vL(+)-AMTVLUTR, pProT7-vM(+)-AMTVMUTR, pProT7-vS(+)-AMTVSUTR, which encodes L, M, or N ORF of MP-12 strain, in place of those of AMTV, respectively. To generate a plasmid encoding a partial 5' UTR of AMTV M-segment, a PCR fragment encoding the backbone vector plasmid plus the entire 3' UTR, M ORF, and 40 nt of 5' UTR termini of MP-12 was amplified from the pProT7-vM(+) plasmid. This was then recombined with the PCR fragment covering the AMTV M-segment 5' UTR lacking the 5' UTR 41 nt terminus via Gibson assembly. The resulting plasmid was designated as pProT7-vM(+)-AMTVM5'UTR.

### **Viral rescue of chimeric MP-12 strain**

To rescue chimeric MP-12 strain encoding full-length or partial UTR of AMTV in either L-, M-, or S-segment, BHK/T7-9 cells were transfected with following sets of plasmids: (i) pProT7-vS(+)-AMTVSUTR, pProT7-vM(+), pProT7-vL(+), pT7-IRES-vN, pT7-IRES-vL, and pCAGGS-vG (for rMP12-AM-SUTR), (ii) pProT7-vS(+), pProT7-vM(+)-AMTVMUTR, pProT7-vL(+), pT7-IRES-vN, pT7-IRES-vL, and pCAGGS-vG (for rMP12-AM-MUTR), or (iii) pProT7-vS(+), pProT7-vM(+), pProT7-vL(+)-AMTVLUTR, pT7-IRES-vN, pT7-IRES-vL, and pCAGGS-vG (for rMP12-AM-LUTR). From the initial attempt, rMP12-AM-SUTR virus could be successfully rescued, and rMP12-AM-MUTR or rMP12-AM-LUTR viruses could not. Next, the AMTV M-segment UTR was partially replaced. BHK/T7-9 cells were transfected with

pProT7-vS(+), pProT7-vM(+)-AMTVM5'UTR, pProT7-vL(+), pT7-IRES-vN, pT7-IRES-vL, and pCAGGS-vG (rMP12-AM-M5'UTR). Using this approach, viable rMP12-AM-M5'UTR could be rescued. To rescue the L-segment chimera, the S-segment NSs gene was replaced with the green fluorescent protein (GFP) gene, to efficiently detect recombinant viruses, which do not exhibit any CPE. BHK/T7-9 cells were then transfected with pProT7-vS(+)-GFP, pProT7-vM(+), pProT7-vL(+)-AMLUTR, pT7-IRES-vN, pT7-IRES-vL, and pCAGGS-vG (rMP12/GFP-AM-LUTR). Rescued of chimeric strains were further amplified in Vero cells and titrated for experimental use (PFU/ml, or FFU/ml for rMP12/GFP-AM-LUTR). Genome structures of rescued chimeric strains are shown in Figure 4.2.

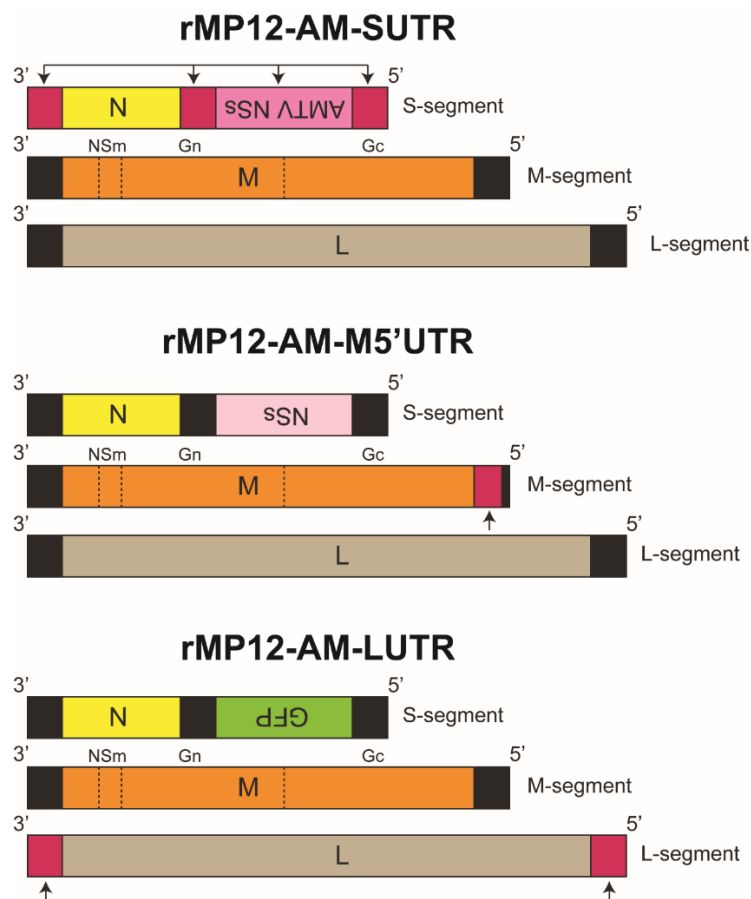


**Figure 4.2: Rescued chimeric strains genome**

Schematic representation of rMP12-AM-SUTR, rMP12-AM-M5'UTR, and rMP12/GFP-AM-LUTR chimeric virus. The rMP12-AM-SUTR encodes the entire 3' and 5' UTRs of the S-segment, IGR, and NSs of AMTV (red). The rMP12-AM-M5'UTR encodes only a partial 5' UTR of the M-segment of AMTV (red). The rMP12/GFP-AM-LUTR encodes the entire 3' and 5' UTR of the L-segment of AMTV (red). Arrows indicate replacement of rMP-12 with AMTV genetic elements.

### **Analysis of viral growth kinetics of chimeric MP-12 strains**

Vero cells were infected with rMP12-AM-SUTR, rMP12-AM-M5'UTR, rMP12/GFP-AM-LUTR, or parental rMP-12 strain (control) at an MOI of 0.01 for 1 hour at 37°C. After washing cells three times with PBS, cells were further incubated at 37°C. Culture supernatants were harvested at 1, 24, 48, 72, and 96 hpi, and viral titers were measured by plaque assay and focus-forming assay (FFA). C6/36 cells were infected with rMP12-AM-SUTR, rMP12-AM-M5'UTR, rMP12/GFP-AM-LUTR, or parental rMP-12 strain (control) at an MOI of 0.01 for 1 hour at 28°C. After washing cells three times with media, culture supernatant samples were collected at 1 hpi. Cells were further incubated at 28°C, and culture supernatants were collected at 24, 48, 72, and 96 hpi. Growth curves were calculated using means and standard deviations from three independent experiments.

### **Droplet digital polymerase chain reaction (ddPCR) analysis of rMP-12 chimeric strains**

Vero or C6/36 cells were mock-infected or infected with rMP12/GFP-AM-LUTR or rMP12-AM-SUTR. Total RNA was collected at 72 hpi, and the copy number of each L-, M-, and S-segment were analyzed by ddPCR using the QX100 droplet generator and reader (Bio-Rad Laboratories), as described previously<sup>148</sup>. Viral RNA was extracted using the RNeasy mini kit (Qiagen), according to the manufacturer's instructions. The concentration of extracted RNA was measured with the Qubit 2.0 Fluorometer (Thermo Fisher Scientific), and cDNA was synthesized using iScript (Bio-Rad Laboratory). PCR reactions were prepared as follow: 250 nM of TaqMan

probe, 900 nM of primer, ddPCR Supermix for Probes (Bio-Rad Laboratory), cDNA, and water (up to 25  $\mu$ l). PCR cycling parameters included an initial denaturation step (95°C for 10 minutes), followed by 40 cycles of 94°C for 30 seconds, 60°C for 1 minute, and a final denaturation step of 98°C for 10 minutes. For the measurement of RNA copy number, a probe and two primers for the detection of MP-12 L, M, and S RNA has been described previously<sup>148</sup>. The number of droplets with positive and negative signals was measured using the QX100 droplet reader. Data analysis was performed using QuantaSoft Version 1.4 (Bio-Rad Laboratory).

### **Analysis of L, M, S RNA ratios of virion RNA from rMP-12 chimeric strains**

Vero cells were infected with rMP-12, rMP12/GFP-AM-LUTR, rMP12-AM-M5'UTR, or rMP12-AM-SUTR at MOI 0.01. Sample supernatants were collected at 3 dpi, and spun down at 13,500 rpm for 10 minutes to remove cellular debris. Sample supernatant was then further incubated in benzonase nuclease for 1 hour at 37°C to remove non-virion RNA and then subsequently subjected to ultracentrifugation with 20% sucrose cushion at 38000 rpm for 2 hours in 4°C. Viral RNA was then mixed with Trizol reagent, together with *in vitro* transcribed GFP RNA (2  $\mu$ g) as a spike, and extracted using the Direct-zol (ZYMO Research), according to the manufacturer's instructions. The concentration of extracted RNA was measured with the Qubit 2.0 Fluorometer (Thermo Fisher Scientific), and cDNA was synthesized using iScript (Bio-Rad Laboratory). PCR reactions were prepared as follow: 250 nM of TaqMan probe, 900 nM of primer, ddPCR Supermix for Probes (Bio-Rad Laboratory), cDNA, and water (up to 25  $\mu$ l). PCR cycling parameters included an initial denaturation step (95°C for 10 minutes), followed by 40 cycles of 94°C for 30 seconds, 60°C for 1 minute, and a final denaturation step of 98°C for 10 minutes. For the measurement of RNA copy number, a probe and two primers for the detection of MP-12 L, M,

and S RNA has been described previously<sup>148</sup>. The number of droplets with positive and negative signals was measured using the QX100 droplet reader. Data analysis was performed using QuantaSoft Version 1.4 (Bio-Rad Laboratory).

### **Droplet digital polymerase chain reaction analysis of IFN- $\beta$ mRNA induced by chimeric MP-12 strains**

Hepa1-6 or MRC-5 cells were mock-infected or infected with rMP12-AMTVNSs or rMP12- $\Delta$ NSs16/198 at an MOI of 10. Total RNA was collected at 8 and 16 hpi, and copy numbers of human or murine IFN- $\beta$  mRNA were analyzed by ddPCR using the QX100 droplet generator and reader (Bio-Rad Laboratories), as described previously<sup>148</sup>. Viral RNA was extracted using the RNeasy mini kit (Qiagen), according to the manufacturer's instructions. The concentration of extracted RNA was measured with the Qubit 2.0 Fluorometer (Thermo Fisher Scientific), and cDNA was synthesized using iScript (Bio-Rad Laboratory). PCR reactions were prepared as follow: 250 nM of TaqMan probe, 900 nM of primer, ddPCR Supermix for Probes (Bio-Rad Laboratory), cDNA, and water (up to 25  $\mu$ l). PCR cycling parameters included an initial denaturation step (95°C for 10 minutes), followed by 40 cycles of 94°C for 30 seconds, 60°C for 1 minute, and a final denaturation step of 98°C for 10 minutes. For the measurement of human IFN- $\beta$  mRNA copy number, ddPCR was conducted using a Taqman probe, 5'-(5' Hexachloro-Fluorescein, HEX) CAA TTG AAT GGG AGG CTT GAA TAC (Black Hole Quencher 1, BHQ1)-3'; forward primer, 5'-TCA GTG TCA GAA GCT CCT GT-3'; and reverse primer, 5'-GTT CAT CCT GTC CTT GAG GC-3'. For the measurement of murine IFN- $\beta$  mRNA copy number, a different Taqman probe, 5'-(HEX) TGG AGA TGA CGG AGA TGC AGA (BHQ1)-3'; forward primer, 5'-TAC AGG GCG GAC TTC AAG AT-3'; and reverse primer, 5'-TGG CAA

AGG CAG TGT AAC TC-3', were used. The number of droplets with positive and negative signals was measured using the QX100 droplet reader. Data analysis was performed using QuantaSoft Version 1.4 (Bio-Rad Laboratory).

### **Statistical analysis.**

Statistical analyses were performed using GraphPad Prism 6.05 (GraphPad Software Inc.). To allow comparisons among multiple groups of viral titers or RNA copy numbers, arithmetic means of  $\log_{10}$  values were analyzed by one-way ANOVA, followed by Tukey's multiple comparison test.

### **Ethics statement**

The RVFV MP-12 strain, rMP-12 strain, and those recombinant DNA were used upon approval of the Notification of Use by the Institutional Biosafety Committee at UTMB.

### **Results**

#### **Rescue of chimeric strains via reverse genetics**

In this study, I initially attempted to rescue recombinant chimeric MP-12 strains encoding the entire 5' and 3' UTRs of AMTV in all 3 RNA segments (rMP12-AM-SMLUTR). The rMP12-AM-SMLUTR, however, could not be rescued after at least three independent attempts. Next, I tried to rescue chimeric MP-12 strains encoding the 5' and 3' UTRs of either AMTV S-, M-, or L-segment. In this initial attempt, rMP12-AM-SUTR could be successfully rescued, yet not rMP12-AM-MUTR or rMP12-AM-LUTR. To rescue the chimeric MP-12 strain encoding the M

UTR of AMTV, only a partial 5' UTR of the MP-12 M-segment, except for the terminal 40 nt, was replaced with that of AMTV M-segment 5' UTR (rMP12-AM-M5'UTR). As a result, rMP12-AM-M5'UTR was rescued and showed CPE in Vero cells. The rMP12-AM-LUTR also could not be rescued after several attempts, whereas when the NSs gene was replaced with the GFP gene in the S-segment, rMP12/GFP-AM-LUTR could be rescued. Replacement of the NSs gene with the GFP gene was carried out to facilitate the detection of rescued viruses under fluorescent microscope. Overall summary of the outcome of viral rescue is shown in Table 4.1.

<b>rMP-12 Chimeric Strain</b>	<b>S-segment UTRs</b>	<b>M-segment UTRs</b>	<b>L-segment UTRs</b>	<b>Other changes</b>	<b>Rescued</b>
rMP12-AM-SMLUTR	AMTV	AMTV	AMTV	AMTV NSs ORF in place of MP-12 NSs ORF	No
rMP12-AM-SUTR	AMTV	MP-12	MP-12	AMTV NSs ORF in place of MP-12 NSs ORF	Yes
rMP12-AM-MUTR	MP-12	AMTV	MP-12	None	No
rMP12-AM-M5'UTR	MP-12	MP-12 (3' UTR and 40nt of 5'UTR terminus) and AMTV (5' UTR other than 41 nt terminus)	MP-12	None	Yes
rMP12-AM-LUTR	MP-12	MP-12	AMTV	None	No
rMP12/GFP-AM-LUTR	MP-12	MP-12	AMTV	GFP ORF in place of MP-12 NSs ORF	Yes

**Table 4.1: Summary of rMP-12 Chimeric Strain rescue result.**

### **Analysis of viral replication of chimeric viruses**

Next, viral replication kinetics of all rescued chimeric viruses (rMP12-AM-SUTR, rMP12-AM-M5'UTR, and rMP12/GFP-AM-LUTR) were analyzed in Vero and C6/36 cells (Fig. 4.3). RVFV MP-12 strain encoding the entire 5' and 3' UTR, IGR and NSs gene of AMTV (rMP12-AM-SUTR) replicated efficiently in Vero and C6/36 cells. The chimeric MP-12 strain, rMP12-AM-M5'UTR, which encodes a partial 5' UTR of the AMTV M-segment, replicated less efficiently than parental rMP-12 in Vero and C6/36 cells. The chimeric MP-12 strain encoding the entire UTR of AMTV L-segment (rMP12/GFP-AM-LUTR) replicated less efficiently than parental rMP-12 in Vero cells, whereas infectious viral titers of rMP12/GFP-AM-LUTR did not show any increase in C6/36 cells.

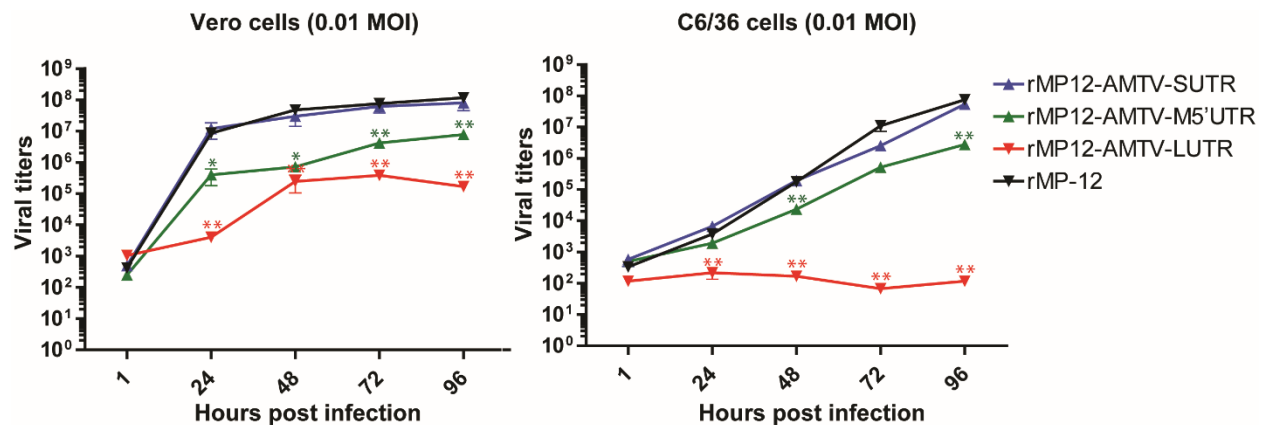


**Figure 4.3: Replication kinetics of chimeric strains in Vero and C6/36 cells**

Replication kinetics of rMP12-AM-SUTR, rMP12-AM-M5'UTR, rMP12/GFP-AM-LUTR, and rMP12 were analyzed in Vero (left panel) or C6/36 cells (right panel). Cells were infected with rMP12-AM-SUTR, rMP12-AM-M5'UTR, rMP12/GFP-AM-LUTR, or rMP12 at an MOI of 0.01. After washing, culture supernatants were collected at 1, 24, 48, 72, and 96 hpi. Experiments were performed in triplicate, and means +/- standard errors are shown. Arithmetic means of log<sub>10</sub> values were analyzed via unpaired t-test (chimeric strain vs rMP12). Asterisks represent statistical differences among viral titers at corresponding time points (\*p < 0.05, \*\*p < 0.01).

### Viral RNA accumulation of chimeric MP-12 viruses

To further analyze the occurrence of viral RNA replication, droplet digital PCR was performed to measure RNA copy numbers of each segment from cells infected with rMP12/GFP-

AM-LUTR. Less abundant viral RNA was detected from Vero or C6/36 cells infected with rMP12/GFP-AM-LUTR than those infected with rMP-12. In C6/36 cells, rMP12/GFP-AM-LUTR infection induced 118, 241, and 50 copies of S, M, and L segment, respectively, at 72 hpi, in comparison to 6118151, 165109, and 176290 copies of S, M, and L segment of parental rMP-12 (Fig. 4.4A). This indicated that mosquito C6/36 cells did not support the replication of rMP12/GFP-AM-LUTR even after 72 hpi. In Vero cells, rMP12/GFP-AM-LUTR infection induced 8573, 30203, and 6813 RNA copies of S, M, and L segment, respectively, at 72 hpi, in comparison to 276323, 212175, and 244297 copies of S, M, and L segment of rMP-12 (Fig. 4.4B). Droplet digital PCR was also performed with rMP12-AM-SUTR to compare the difference of RNA accumulation from that seen with rMP12/GFP-AM-LUTR. As expected, infection with rMP12-AM-SUTR showed RNA copy numbers similar to those of parental rMP-12 at 1, 24, 48, and 72 hpi (Fig. 4.5). High level of viral RNA were detected at 24, 48, and 72 hpi in both C6/36 and Vero cells, demonstrating that the RNA replication of rMP12-AM-SUTR is as efficient as parental rMP-12 strain in both C6/36 and Vero cells.

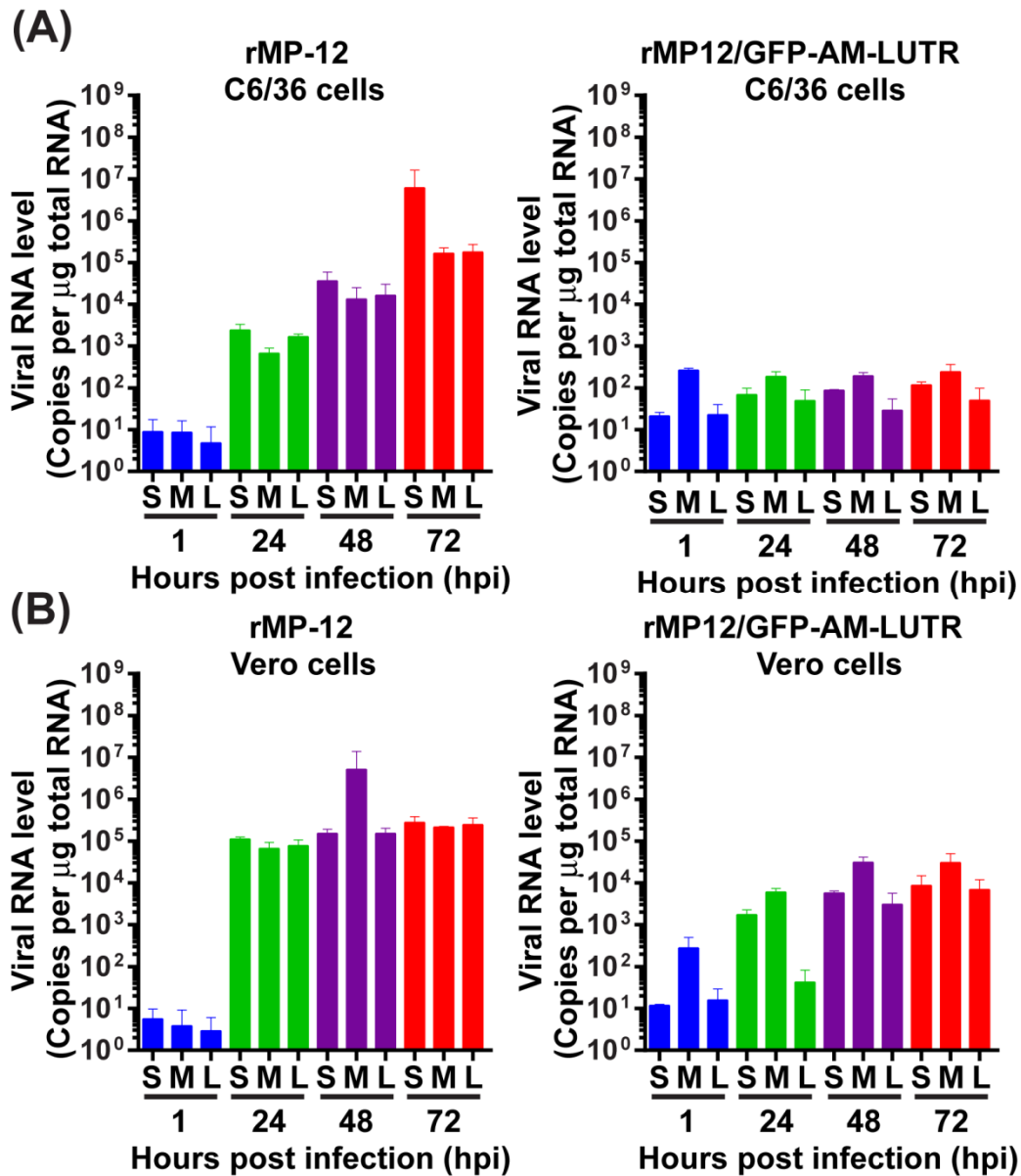


**Figure 4.4: Viral RNA accumulation of chimeric MP-12 viruses (rMP-12 vs rMP12/GFP-AM-LUTR)**

C6/36 cells (A) or Vero cells (B) were infected with rMP-12 (left panel) or rMP12/GFP-AM-LUTR (right panel) at an MOI of 0.01. Total RNA was extracted at 1, 24, 48, and 72 hpi, and ddPCR analysis was performed using probes designed to detect MP-12 S, M, or L segments. The X-axis represents collected time points after infection and the Y-axis represents the RNA copy number per  $\mu\text{g}$  of total RNA. Experiments were performed in triplicate, and means  $\pm$  standard errors are shown.

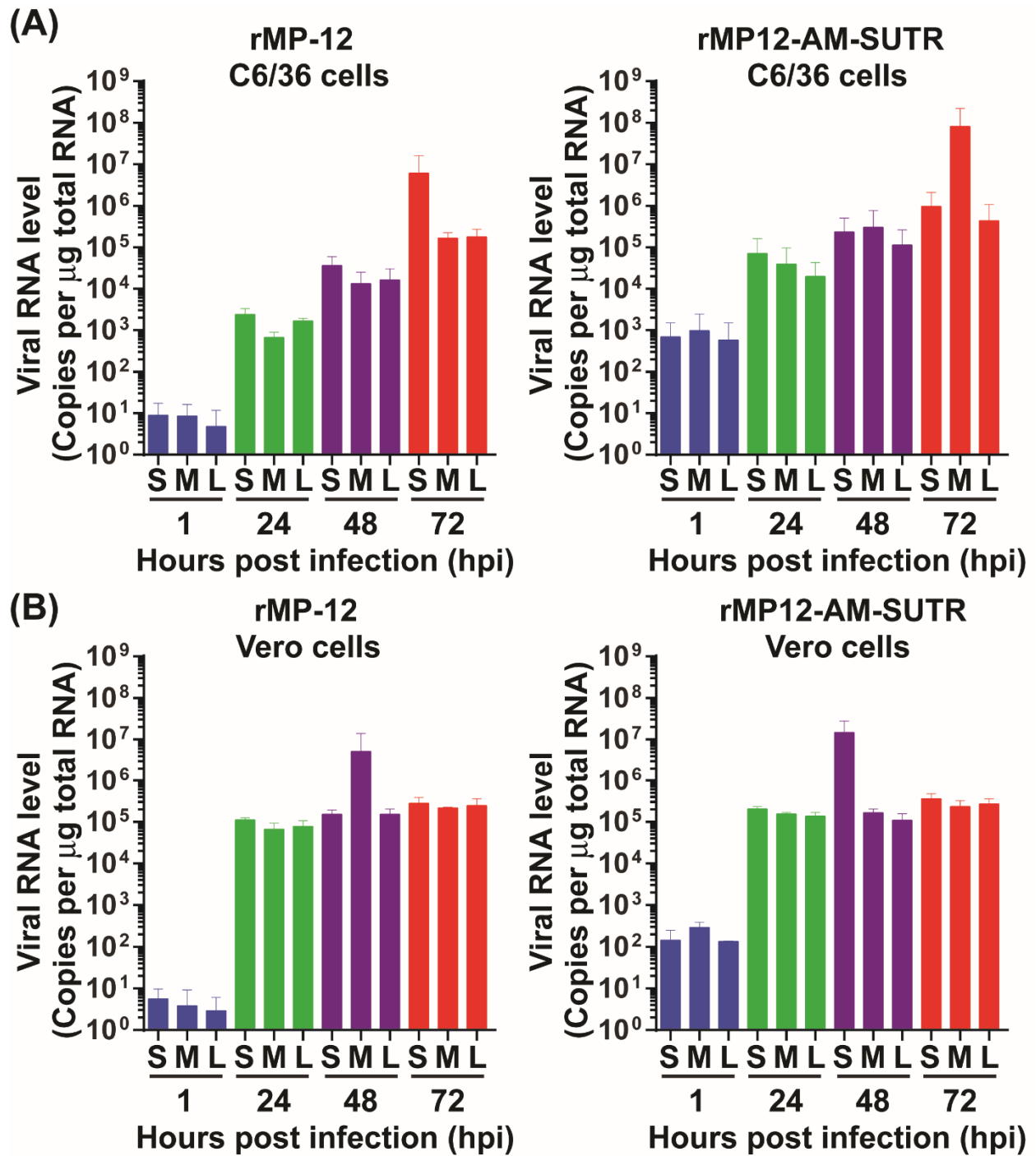


**Figure 4.5: Viral RNA accumulation of chimeric MP-12 viruses (rMP-12 vs rMP12-AM-SUTR)**

C6/36 cells (A) or Vero cells (B) were infected with rMP-12 (left panel) or rMP12-AM-SUTR (right panel) at an MOI of 0.01. Total RNA were extracted at 1, 24, 48, and 72 hpi, and ddPCR analysis was performed using probes designed to detect MP-12 S, M, or L segments. The X-axis represents collected time points after infection and the Y-axis represents the RNA copy number per µg of total RNA. Experiments were performed in triplicate, and means +/- standard errors are shown.

### **Characterization of L/ M/ S RNA ratios of virion RNA from rMP-12 chimeric strains**

It was hypothesized that alteration of MP-12 UTR affects the packaging of viral RNA into virions. Thus, the RNA copy number of virion-derived RNA was next determined. To minimize the contamination of cell-derived viral RNA, culture supernatants were first treated with nuclease, and then, virions were collected via ultracentrifugation. Viron-derived RNA collected from the pellet was analyzed by droplet digital PCR using probes specific to L-, M-, or S-segment. As shown in Figure 4.6, the L/M/S ratio of parental rMP-12 virion RNA was 1:1.4:3.1. The L/M/S ratio of virion RNA for the rMP12-AMTV-SUTR, rMP12-AMTV-M5'UTR, or rMP12-AMTV-LUTR were 1:2:12.2, 1:10.8:18.8, or 1:3.2:6.6, respectively. This result demonstrates that exchange of rMP-12 UTR leads to alteration of L/M/S ratio of virion-derived RNA.

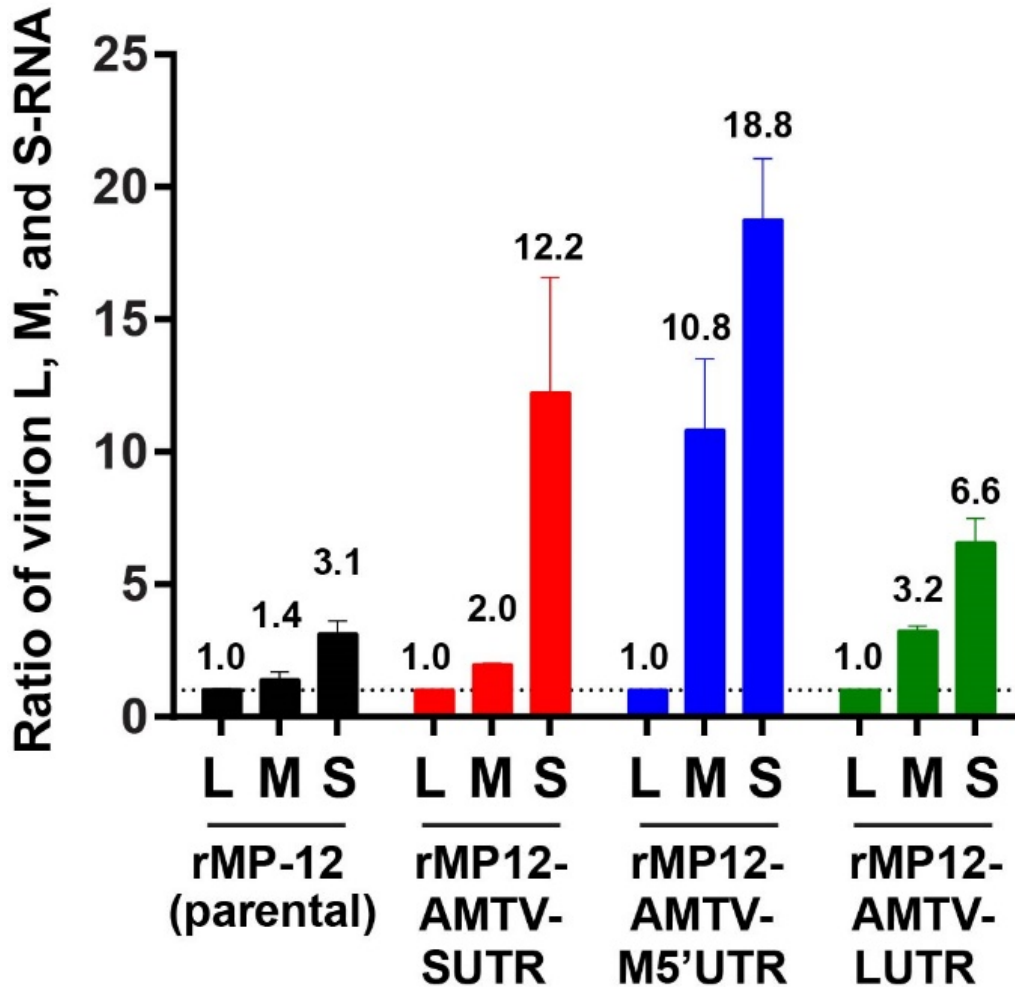


**Figure 4.6: Alteration of L, M, S RNA ratios in virions via UTR exchanges**

Vero cells were infected with rMP12, rMP12-AM-SUTR, rMP12-AM-M5'UTR, and rMP12/GFP-AM-LUTR. Culture supernatant was collected at 3 dpi for ultracentrifugation and virion RNA was extracted and ddPCR analysis using probes designed to detect MP-12 S, M, or L segments was used. The X-axis represents chimeric rMP-12 strain used with respective L, M, and S segments and the Y-axis represents the ratio of virion L, M, and S RNA. Experiments were performed in triplicate.

### **Characterization of recombinant MP-12 strain encoding AMTV NSs gene**

Since the rMP12-AM-SUTR encodes not only AMTV S-segment UTRs, but also AMTV NSs ORF, it is possible that the chimeric virus could display different phenotypes in type-I IFN-competent human cells. Little is known about the biological functions of AMTV NSs proteins. Thus, the impact of the replacement of the MP-12 NSs gene with that of the AMTV NSs gene was next evaluated. If AMTV NSs protein can functionally counteract host antiviral responses as

RVFV NSs protein does, then the rMP12-AMTVNSs should replicate robustly in type-I IFN-competent cells. The replication kinetics of rMP-12, rMP12-AMTVNSs, or rMP12- $\Delta$ NSs16/198 was then carried out in MRC-5 and Hepa1-6 as shown in Figure 4.7. The rMP12-AMTVNSs replicated efficiently in murine Hepa1-6 cells, and not in human MRC-5 cells. This result indicated that AMTV NSs proteins likely inhibit antiviral responses in Hepa1-6 cells, but not in MRC-5 cells.

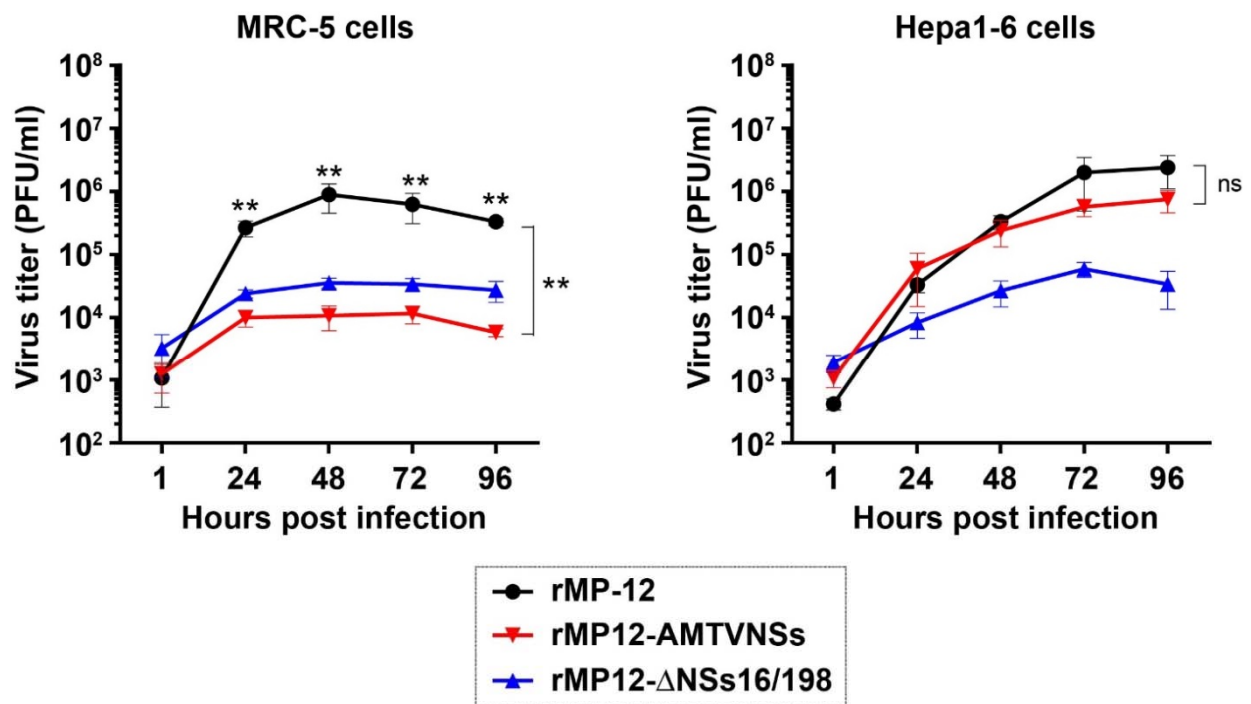


**Figure 4.7: The replication kinetics of rMP-12, rMP12-AMTVNSs, or rMP12- $\Delta$ NSs16/198 in MRC-5 and Hepa1-6**

Replication kinetics of rMP-12, rMP12-AMTVNSs, or rMP12- $\Delta$ NSs16/198 in MRC-5 and Hepa1-6. Cells were infected with rMP-12, rMP12-AMTVNSs, or rMP12- $\Delta$ NSs16/198 at 0.01 MOI. After washing, culture supernatants were collected at 1, 24, 48, 72, and 96 hpi. Experiments were performed in triplicate, and means  $\pm$  standard errors are shown. Asterisks represent statistical differences among viral titers at corresponding time points.

## Role of AMTV NSs proteins in interferon- $\beta$ mRNA up-regulation in MRC-5 and Hepa1-6 cells

To further confirm this, the induction of IFN- $\beta$  mRNA in MRC-5 or Hepa1-6 cells were analyzed by ddPCR (Fig. 4.8). In MRC-5 cells, rMP12-AMTVNSs induced 27,383 copies of human IFN- $\beta$  mRNA at 8 hpi, which was 57 times more than mock-infected cells. Infection with rMP12- $\Delta$ NSs16/198 induced slightly more human IFN- $\beta$  mRNA than rMP12-AMTVNSs at 8 hpi, but the difference at 16 hpi was no longer significant. In Hepa1-6 cells the rMP12- $\Delta$ NSs16/198 induced murine IFN- $\beta$  mRNA 138 and 93 times more than rMP12-AMTVNSs at 8 and 16 hpi, respectively. These results indicated that AMTV NSs expression can significantly inhibit the induction of murine IFN- $\beta$  mRNA. Viral S-segment RNA and N mRNA copies were also measured in Hepa1-6 and MRC-5 cells at 8 hpi (data not shown). Viral RNA levels of rMP12-AMTVNSs or rMP12- $\Delta$ NSs16/198 were abundantly detected at 8 hpi in Hepa1-6 and MRC-5 cells (100,000 to 1,000,000 copies per total RNA  $\mu$ g).

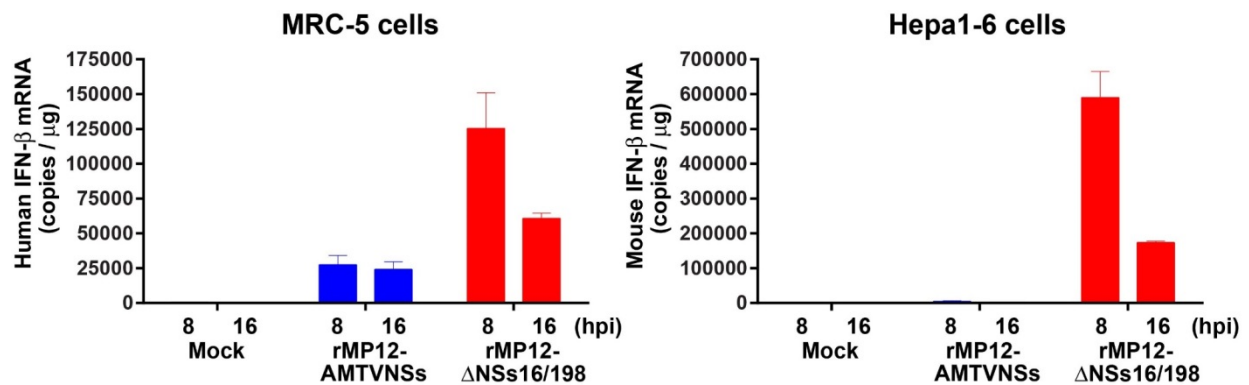


**Figure 4.8: Induction of interferon- $\beta$  mRNA in MRC-5 cells or Hepa1-6**

MRC-5 or Hepa1-6 cells were mock-infected, or infected with rMP12-AMTVNSs or rMP12- $\Delta$ NSs16/198 (rMP12- $\Delta$ NSs) at an MOI of 10. Total RNA was extracted at 8 or 16 hpi, and ddPCR analysis was performed using a human IFN- $\beta$  probe (left panel) or a murine IFN- $\beta$  probe (right panel). The Y-axis represents the RNA copy number per  $\mu$ g of total RNA. Experiments were performed in triplicate, and means  $\pm$  standard errors are shown.

## Discussion

AMTV and several other phleboviruses, such as Adana virus, Adria Virus, Alcube virus, Edrine virus, Medjerda Valley virus, Odrenisrou virus, Olbia virus, and Ponticelli virus<sup>149–156</sup>, are clustered into a phylogenetic clade that is closely related to the Salehabad species complex. Currently, there is little evidence of human diseases associated with viruses within this species complex, with the exception of Adria virus, whose genome was partially detected from a child who was hospitalized in Greece due to febrile seizure and nausea<sup>157</sup>. In addition, there are some evidences of human infections by phleboviruses within the Salehabad species complex. For example, in Tunisia, human sera (1.35%; 1:10 – 1:160) showed detectable neutralizing antibodies against Medjerda virus<sup>149</sup>, whereas human sera from Italy (4.6%; 1:10 – 1:20) showed neutralizing antibodies to Arbia virus<sup>150</sup>. Human sera have also shown detectable neutralizing antibodies against AMTV in Egypt (1.6 – 8.3%;  $\geq 1:10$ ), Sudan (1.4 – 80%;  $\geq 1:10$ ), and Somalia (2.1%;  $\geq 1:10$ )<sup>69</sup>. Past isolations of AMTV, however, were mainly from rodents, such as African grass rats, wild rats, typical striped grass mice, gerbils, and shrews<sup>68</sup>. It is thus important to evaluate whether or not the Salehabad species complex, AMTV in particular, can interact with RVFV to generate potentially pathogenic chimeric strains.

In previous chapter, it was demonstrated that the structural proteins, N, L and Gn/Gc, are not interchangeable between RVFV and AMTV. It is thus unlikely that RVFV and AMTV can form reassortant strains from co-infected cells. Meanwhile, there are no sufficient evidences to exclude the capability of genetic recombination between RVFV and AMTV. Thus the exchange of genetic elements, such as the UTRs of the S-, M-, and L-segments or the NSs protein, of AMTV can functionally act as a surrogate to those of RVFV. Although genetic recombination between RVFV and AMTV may not easily occur in nature, the use of reverse genetics might allow creations

of various chimeric strains between them. Further characterization of virological phenotypes of chimeric strains might predict the outcome of genetic recombination between RVFV and AMTV, which would be useful for the evaluation of the potential recombination impact of MP-12 vaccine use in endemic countries.

The exchange of the L UTR of rMP-12 with that of AMTV (i.e., rMP12/GFP-AM-LUTR) resulted in a significant decrease in viral replication when compared to rMP12-AM-M5'UTR, rMP12-AM-SUTR, or rMP-12 in Vero cells. Interestingly, the rMP12/GFP-AM-LUTR did not show productive RNA replication in C6/36 cells. This result indicates that the exchange of MP-12 L 3' and 5' UTR with that of AMTV L 3' and 5' UTR could have a major impact in viral replication in C6/36 cells. Analysis of viral RNA copy numbers of L-, M-, and S-segment of rMP12/GFP-AM-LUTR virions purified from Vero cells showed decreased L-segment RNA copy numbers relative to S- and M-segment, indicating less efficient replication or packaging of chimeric L-segment in Vero cells. Moreover, mosquito C6/36 cells may not be able to support the AMTV L-segment replication using RVFV N and L proteins by an unknown mechanism. The replacement of the entire M segment UTR of rMP-12 with AMTV did not result in a viable chimeric strain. Alternatively, a partial M segment 5' UTR of rMP-12 was replaced with that of AMTV and a recombinant chimeric strain (rMP12-AM0M5'UTR) was successfully rescued. It was shown that a AMTV 5' UTR in the MP-12 M-segment affects efficient viral RNA replication in both Vero and C6/36 cells, when compared to that of parental rMP-12. The replacement of the 5' and 3' S UTRs, IGR and NSs of rMP-12 with those of AMTV did not show negative impact on the viral replication in Vero cells or C6/36 cells. It was thus concluded that the 3' and/or 5' UTRs of MP-12 strain could be exchanged with those of AMTV, yet such changes affects efficient viral replication, except for the exchange of S-segment UTRs or NSs gene.

This study also demonstrated that exchanges of UTRs of MP-12 with those of AMTV led to alteration of L/M/S ratio of virion-derived RNA. The L/M/S ratio of virion RNA for the parental rMP-12, rMP12-AMTV-SUTR, rMP12-AMTV-M5'UTR, or rMP12-AMTV-LUTR were 1:1.4:3.1, 1:2:12.2, 1:10.8:18.8, or 1:3.2:6.6, respectively. Thus, an exchanges in the UTR might have significant impact on the coordinated genome RNA packaging. A previous study estimated the L/M/S ratio of RVFV C13 strain virion as 1:3.9:3.9<sup>143</sup>. Although observed 1:1.4:3.1 ratio for rMP-12 was similar to the reported L/M/S ratio of RVFV virions, increases of S-segment RNA copy numbers for rMP12-AMTV-SUTR in virions might be due to exchanges of S-segment 3'- and 5'-UTRs as well as IGR and NSs gene. Potential disruption of presumable coordinated packaging of chimeric S-segment RNA via MP-12 M-segment might result in independent release of S-segment RNA as non-infectious virus-like particle (VLP)s. Similarly, a lack of MP-12 M-segment 5'UTR might lead to abolishment of coordinated packaging via the MP-12 M-segment. As a result, both M- and S-segments of rMP12-AMTV-M5'UTR might be released into VLP virions without synergic packaging of L-, M-, and S-segments. Moreover, the L-segment of rMP12-AMTV-LUTR might be less efficiently packaged into virions, which increased relative abundance of M- and S-segment RNA in virion. Those hypotheses will need to be further validated in future experiments.

Although the rMP12-AM-SUTR was viable and efficiently replicated in Vero and C6/36 cells, it is possible that the AMTV NSs gene expressed from this chimeric strain could not be functional in counteracting host type-I IFN responses. Although many pathogenic phleboviruses encode NSs gene, which inhibit the induction of human IFN- $\beta$  mRNA, little is known about the biological functions of AMTV NSs protein in this regard. Accordingly, the induction of human IFN- $\beta$  mRNA was analyzed in MRC-5 cells infected with rMP12-AMTVNSs. Human IFN- $\beta$

mRNA upregulation occurred in MRC-5 cells in response to the replication of rMP12-AMTVNSs, indicating that AMTV NSs protein does not inhibit the IFN- $\beta$  induction/signaling pathways in human cells. In contrast, the rMP12-AMTVNSs inhibited the induction of murine IFN- $\beta$  mRNA in Hepa1-6 cells. Nevertheless, AMTV NSs functions in human or murine cells remains largely uncharacterized, which should be addressed in future studies. Meanwhile, AMTV has been isolated in rodents in Africa. Since AMTV NSs proteins can inhibit murine IFN- $\beta$  gene, it is likely that it can also inhibit such pathways in other wild rodents. If rodents serve as reservoir for AMTV, AMTV NSs proteins may support amplification of AMTV *in vivo*.

In summary, none of the artificial chimeric MP-12 strain encoding AMTV UTRs or NSs gene showed significantly increased replication in culture cells and the NSs gene failed to counteract with IFN- $\beta$  gene up-regulation in human cells. Based on the characterization of three chimeric MP-12 strains encoding AMTV gene fragments derived from either L-, M-, or S-segment, the chimeric MP-12 strains encoding AMTV genetic element are considered less pathogenic than parental MP-12 strain. Although it is not clear how the homologous recombination can occur between RVFV and AMTV in nature, this experimental finding will provide fundamental knowledge of basic chimeric strains to predict the concerns of potential viability or virulence of other genetic recombinants of MP-12 vaccine with AMTV during the field trials.

## CHAPTER 5: Epilogue

Although the live-attenuated MP-12 vaccine has never been used for field trials in Africa, the rMP12- $\Delta$ NSm21/384, a genetic variant of MP-12, has been introduced into Tanzania, and the safety and immunogenicity has been tested<sup>158</sup>. Further evaluation of rMP12- $\Delta$ NSm21/384 in field trials will expose vaccinated animals to vector mosquitoes in nature. My immediate concern was the spillover of vaccine strain to environment and subsequent genetic exchanges with circulating wt RVFV in mosquito vectors. Fortunately, the rMP12- $\Delta$ NSm21/384 lacks the 78kD/NSm gene, which most likely abolish viral potential to disseminate via midgut of mosquitoes<sup>22</sup>. It is however important to address potential concerns occurring via MP-12 vaccine for field use in endemic countries. For example, Smithburn vaccine and wt RVFV generated a reassortant strain in a human, which led to the isolation of SA184/10, which encodes the vaccine strain M-segment and S- and L-segments of SA54/10 strain. In my Aim 1 study, MP-12 strain was shown to randomly reassort with other RVFV genotype. It is thus likely that reassortant strains carrying the S- and/or L-segment of rMP12- $\Delta$ NSm21/384 and the M-segment of wt RVFV may be transmitted via mosquitoes. The S- or L-segment of rMP12- $\Delta$ NSm21/384 encode only weak attenuation phenotype, and thus such reassortants likely retain some virulence to humans or animals. In Aim 2, the experiment demonstrated that the S- and L-segments of rMP12-GM50 was more attenuated than those of parental MP-12. Moreover, the rMP12-GM50 encode more than 500 silent mutations throughout the genome. In this regard, any reassortants derived from rMP12-GM50 strain will be highly attenuated, whereas such reassortant strains encode genetic markers to be distinguished from wt RVFV. It is even likely that such attenuated RVFV reassortants may serve as a natural vaccine to immune wild animals. Accurate surveillance of the distribution of vaccine strain or the

reassortants will thus be important to understand environmental impact of vaccination in endemic countries.

Another concern was the formation of any reassortant or recombinant MP-12 strains via interspecies genetic exchanges. Mosquito-borne phleboviruses have not been extensively characterized in Africa, yet at least AMTV is widely distributed there. AMTV is transmitted via *C. antennatus*, which is also a vector for RVFV. Seroprevalence for AMTV was shown in humans and ruminants in Africa, indicating mosquito-borne exposure of AMTV to humans or animals in nature. Historically, AMTV has not been pathogenic to humans, whereas AMTV NSs proteins did not inhibit IFN- $\beta$  mRNA up-regulations in an Aim 3 experiment. In Aim 1 study, MP-12 and AMTV did not form any viable reassortants, due to functional incompatibility of N, L, and GnGc proteins between them. Based on those results, it will be less likely to have an emergence of viable reassortant virus derived from RVFV and AMTV. Potential limitation of current study was the use of C6/36 cells, which lacks functional antiviral functions<sup>159</sup>. Under selective pressures with robust antiviral responses in animals or vector mosquitoes, additional genetic mutations might be introduced into RVFV and AMTV genome, which might lead to viral fitness to survive better using those genetic materials. Such unpredictable concerns should be addressed in future studies.

Homologous recombination does not frequently occur among negative-stranded RNA viruses. It was however reported that hantaviral RNA could recombine in persistently-infected cells<sup>160</sup>. In this regard, I initially tested the occurrence of homologous recombination between MP-12 and rMP12-GM50 in persistently-infected C6/36 cells, yet no clues of homologous recombination could be obtained. I also tested homologous recombination between rMP12- $\Delta$ NSs16/198 and rMP12-GM50 lacking the NSs gene in persistently-infected Vero cells. It demonstrated generation of defective-interfering (DI) RNA, yet no isolation of recombined MP-

12 strain was made. To clarify whether the chimeras between MP-12 and AMTV could be highly viable, I used reverse genetics and designed the favorable incorporation of AMTV UTR or NSs gene into MP-12 genome. An exchange of partial or full UTRs in the L-, M-, or S-segment abolished authentic L/M/S RNA ratio in virions, and affected efficient viral replication in Vero, C6/36, or MRC-5 cells. It is thus less likely that MP-12 strain encoding AMTV UTR or NSs gene will surpass the residual virulence of MP-12 strain. It is however difficult to exclude the possibility that further optimized incorporation of AMTV genetic elements might lead to revert the attenuation phenotype of MP-12 strain.

In conclusion, this study characterized potential formation of genetic reassortants and recombinants between MP-12 and AMTV. Without further viral adaptation, it is not likely that MP-12 and AMTV form viable reassortants. In contrast, MP-12 chimeras encoding AMTV UTR or NSs gene could be generated artificially by using reverse genetics. It is however uncertain whether homologous recombination can occur and create such ideal chimeras in naturally co-infected cells. Nevertheless, it will be ideal to minimize the spillover of vaccine strains into mosquito populations. Further attenuation of L-, M-, and S-segment or incorporation of genetic markers such as rMP12-GM50 will benefit future RVF vaccination in endemic countries.



## BIBLIOGRAPHY

1. Jonsson, C. B., Cole, K. S., Roy, C. J., Perlin, D. S. & Byrne, G. Challenges and Practices in Building and Implementing Biosafety and Biosecurity Programs to Enable Basic and Translational Research with Select Agents. *J Bioterror Biodef Suppl* **3**, 12634 (2013).
2. Ikegami, T., Won, S., Peters, C. J. & Makino, S. Characterization of Rift Valley Fever Virus Transcriptional Terminations. *J. Virol.* **81**, 8421–8438 (2007).
3. Albariño, C. G., Bird, B. H. & Nichol, S. T. A shared transcription termination signal on negative and ambisense RNA genome segments of Rift Valley fever, sandfly fever Sicilian, and Toscana viruses. *J. Virol.* **81**, 5246–5256 (2007).
4. Lara, E., Billecocq, A., Leger, P. & Bouloy, M. Characterization of Wild-Type and Alternate Transcription Termination Signals in the Rift Valley Fever Virus Genome. *J. Virol.* **85**, 12134–12145 (2011).
5. Schmaljohn C, Nichol ST. Bunyaviridae. In: Knipe DM, Howley PM, Griffin DE, Lamb RA, Martin MA, Roizman B, Straus SE, ed.
6. Ferron, F. *et al.* The Hexamer Structure of the Rift Valley Fever Virus Nucleoprotein Suggests a Mechanism for its Assembly into Ribonucleoprotein Complexes. *PLOS Pathogens* **7**, e1002030 (2011).
7. Barski, M. *et al.* Rift Valley fever phlebovirus NSs protein core domain structure suggests molecular basis for nuclear filaments. *eLife Sciences* **6**, e29236 (2017).
8. Bouloy, M. *et al.* Genetic evidence for an interferon-antagonistic function of rift valley fever virus nonstructural protein NSs. *J. Virol.* **75**, 1371–1377 (2001).

9. Muller, R. *et al.* Characterization of clone 13, a naturally attenuated avirulent isolate of Rift Valley fever virus, which is altered in the small segment. *Am. J. Trop. Med. Hyg.* **53**, 405–411 (1995).
10. Le May, N. *et al.* A SAP30 complex inhibits IFN-beta expression in Rift Valley fever virus infected cells. *PLoS Pathog.* **4**, e13 (2008).
11. Weill, L., Shestakova, E. & Bonnefoy, E. Transcription factor YY1 binds to the murine beta interferon promoter and regulates its transcriptional capacity with a dual activator/repressor role. *J. Virol.* **77**, 2903–2914 (2003).
12. Billecocq, A. *et al.* NSs Protein of Rift Valley Fever Virus Blocks Interferon Production by Inhibiting Host Gene Transcription. *J. Virol.* **78**, 9798–9806 (2004).
13. Le May, N. *et al.* TFIIF transcription factor, a target for the Rift Valley hemorrhagic fever virus. *Cell* **116**, 541–550 (2004).
14. Compe, E. & Egly, J.-M. TFIIF: when transcription met DNA repair. *Nat. Rev. Mol. Cell Biol.* **13**, 343–354 (2012).
15. Ikegami, T. *et al.* Rift Valley Fever Virus NSs Protein Promotes Post-Transcriptional Downregulation of Protein Kinase PKR and Inhibits eIF2 $\alpha$  Phosphorylation. *PLOS Pathogens* **5**, e1000287 (2009).
16. Habjan, M. *et al.* NSs protein of rift valley fever virus induces the specific degradation of the double-stranded RNA-dependent protein kinase. *J. Virol.* **83**, 4365–4375 (2009).
17. García, M. A., Meurs, E. F. & Esteban, M. The dsRNA protein kinase PKR: virus and cell control. *Biochimie* **89**, 799–811 (2007).
18. Kalveram, B. *et al.* Rift Valley fever virus NSs inhibits host transcription independently of the degradation of dsRNA-dependent Protein Kinase PKR. *Virology* **435**, 415–424 (2013).

19. Gori-Savellini, G., Valentini, M. & Cusi, M. G. Toscana virus NSs protein inhibits the induction of type I interferon by interacting with RIG-I. *J. Virol.* **87**, 6660–6667 (2013).
20. Gerrard, S. R. & Nichol, S. T. Synthesis, proteolytic processing and complex formation of N-terminally nested precursor proteins of the Rift Valley fever virus glycoproteins. *Virology* **357**, 124–133 (2007).
21. Weingartl, H. M. *et al.* Rift Valley Fever Virus Incorporates the 78 kDa Glycoprotein into Virions Matured in Mosquito C6/36 Cells. *PLOS ONE* **9**, e87385 (2014).
22. Kreher, F. *et al.* The Rift Valley fever accessory proteins NSm and P78/NSm-GN are distinct determinants of virus propagation in vertebrate and invertebrate hosts. *Emerg Microbes Infect* **3**, e71 (2014).
23. Kading, R. C. *et al.* Deletion of the NSm Virulence Gene of Rift Valley Fever Virus Inhibits Virus Replication in and Dissemination from the Midgut of *Aedes aegypti* Mosquitoes. *PLOS Neglected Tropical Diseases* **8**, e2670 (2014).
24. Crabtree, M. B. *et al.* Infection and Transmission of Rift Valley Fever Viruses Lacking the NSs and/or NSm Genes in Mosquitoes: Potential Role for NSm in Mosquito Infection. *PLOS Neglected Tropical Diseases* **6**, e1639 (2012).
25. Won, S., Ikegami, T., Peters, C. J. & Makino, S. NSm Protein of Rift Valley Fever Virus Suppresses Virus-Induced Apoptosis. *J. Virol.* **81**, 13335–13345 (2007).
26. Terasaki, K., Won, S. & Makino, S. The C-Terminal Region of Rift Valley Fever Virus NSm Protein Targets the Protein to the Mitochondrial Outer Membrane and Exerts Antiapoptotic Function. *J Virol* **87**, 676–682 (2013).
27. Bouloy, M. & Weber, F. Molecular Biology of Rift Valley Fever Virus. *Open Virol J* **4**, 8–14 (2010).

28. Klemm, C. *et al.* Systems To Establish Bunyavirus Genome Replication in the Absence of Transcription. *J. Virol.* **87**, 8205–8212 (2013).
29. Reguera, J., Weber, F. & Cusack, S. Bunyaviridae RNA polymerases (L-protein) have an N-terminal, influenza-like endonuclease domain, essential for viral cap-dependent transcription. *PLoS Pathog.* **6**, e1001101 (2010).
30. Bird, B. H., Ksiazek, T. G., Nichol, S. T. & Maclachlan, N. J. Rift Valley fever virus. *J. Am. Vet. Med. Assoc.* **234**, 883–893 (2009).
31. Meegan, J. M., Hoogstraal, H. & Moussa, M. I. An epizootic of Rift Valley fever in Egypt in 1977. *Vet. Rec.* **105**, 124–125 (1979).
32. Madani, T. A. *et al.* Rift Valley fever epidemic in Saudi Arabia: epidemiological, clinical, and laboratory characteristics. *Clin. Infect. Dis.* **37**, 1084–1092 (2003).
33. Enzootic hepatitis or rift valley fever. An undescribed virus disease of sheep cattle and man from east africa - Daubney - 1931 - The Journal of Pathology and Bacteriology - Wiley Online Library. Available at: <https://onlinelibrary.wiley.com/doi/abs/10.1002/path.1700340418>. (Accessed: 26th July 2018)
34. Easterday, B. C. Rift valley fever. *Adv Vet Sci* **10**, 65–127 (1965).
35. Van der Lugt, J. J., Coetzer, J. A. & Smit, M. M. Distribution of viral antigen in tissues of new-born lambs infected with Rift Valley fever virus. *Onderstepoort J. Vet. Res.* **63**, 341–347 (1996).
36. Coetzer, J. A. W. & Tustin, R. C. *Infectious Diseases of Livestock*. (Oxford University Press, 2004).
37. Busquets, N. *et al.* Experimental infection of young adult European breed sheep with Rift Valley fever virus field isolates. *Vector Borne Zoonotic Dis.* **10**, 689–696 (2010).

38. Olaleye, O. D., Tomori, O. & Schmitz, H. Rift Valley fever in Nigeria: infections in domestic animals. *Rev. - Off. Int. Epizoot.* **15**, 937–946 (1996).
39. Findlay, G. M. Rift valley fever or enzootic hepatitis. *Trans R Soc Trop Med Hyg* **25**, 229–262 (1932).
40. Walker, J. S. *et al.* The clinical aspects of Rift Valley Fever virus in household pets. I. Susceptibility of the dog. *J. Infect. Dis.* **121**, 9–18 (1970).
41. Walker, J. S. *et al.* The Clinical Aspects of Rift Valley Fever Virus in Household Pets. II. Susceptibility of the Cat. *The Journal of Infectious Diseases* **121**, 19–24 (1970).
42. Keefer, G. V., Zebarth, G. L. & Allen, W. P. Susceptibility of Dogs and Cats to Rift Valley Fever by Inhalation or Ingestion of Virus. *The Journal of Infectious Diseases* **125**, 307–309 (1972).
43. Swai, E. S. & Sindato, C. Seroprevalence of Rift Valley fever virus infection in camels (dromedaries) in northern Tanzania. *Trop Anim Health Prod* **47**, 347–352 (2015).
44. Easterday BC, Murphy LC, Bennett DG. Experimental Rift Valley fever in calves, goats, and pigs. *Am J Vet Res.*
45. Francis, T. & Magill, T. P. RIFT VALLEY FEVER. *J Exp Med* **62**, 433–448 (1935).
46. Gear, J., De Meillon, B., Measroch, V., Davis, D. H. S. & Harwin, H. Rift valley fever in South Africa. 2. The occurrence of human cases in the Orange Free State, the North-Western Cape Province, the Western and Southern Transvaal. B. Field and laboratory investigation. *S. Afr. Med. J.* **25**, 908–912 (1951).
47. Kitchen, S. F. Laboratory Infections with the Virus of Rift Valley Fever<sup>1</sup>. *The American Journal of Tropical Medicine and Hygiene* **s1-14**, 547–564 (1934).

48. Mundel, B. & Gear, J. Rift valley fever; I. The occurrence of human cases in Johannesburg. *S. Afr. Med. J.* **25**, 797–800 (1951).
49. Smithburn, K. C. Rift Valley fever; the neurotropic adaptation of the virus and the experimental use of this modified virus as a vaccine. *Br J Exp Pathol* **30**, 1–16 (1949).
50. Abdel-Wahab, K. S. *et al.* Rift Valley Fever virus infections in Egypt: Pathological and virological findings in man. *Trans. R. Soc. Trop. Med. Hyg.* **72**, 392–396 (1978).
51. Yassin, W. Clinico-pathological picture in five human cases died with Rift Valley fever. *J Egypt Public Health Assoc* **53**, 191–193 (1978).
52. Swanepoel, R., Manning, B. & Watt, J. A. Fatal Rift Valley fever of man in Rhodesia. *Cent Afr J Med* **25**, 1–8 (1979).
53. Alrajhi, A. A., Al-Semari, A. & Al-Watban, J. Rift Valley Fever Encephalitis. *Emerg Infect Dis* **10**, 554–555 (2004).
54. Laughlin, L. W. *et al.* Clinical studies on Rift Valley fever. Part 2: Ophthalmologic and central nervous system complications. *J Egypt Public Health Assoc* **53**, 183–184 (1978).
55. van Velden, D. J., Meyer, J. D., Olivier, J., Gear, J. H. & McIntosh, B. Rift Valley fever affecting humans in South Africa: a clinicopathological study. *S. Afr. Med. J.* **51**, 867–871 (1977).
56. Deutman, A. F. & Klomp, H. J. Rift Valley Fever Retinitis. *American Journal of Ophthalmology* **92**, 38–42 (1981).
57. Salib, M. & Sobhy, M. I. Epidemic maculopathy. *Bull Ophthalmol Soc Egypt* **71**, 103–106 (1978).
58. Siam, A. L., Meegan, J. M. & Gharbawi, K. F. Rift Valley fever ocular manifestations: observations during the 1977 epidemic in Egypt. *Br J Ophthalmol* **64**, 366–374 (1980).

59. Al-Hazmi, A. *et al.* Ocular complications of Rift Valley fever outbreak in Saudi Arabia. *Ophthalmology* **112**, 313–318 (2005).
60. Schrire, L. Macular changes in rift valley fever. *S. Afr. Med. J.* **25**, 926–930 (1951).
61. Gonzalez, J. P., Le Guenno, B., Some, M. J. & Akakpo, J. A. Serological evidence in sheep suggesting phlebovirus circulation in a Rift Valley fever enzootic area in Burkina Faso. *Trans. R. Soc. Trop. Med. Hyg.* **86**, 680–682 (1992).
62. Inc, G. I. & Berger, D. S. *Rift Valley Fever: Global Status: 2018 edition.* (GIDEON Informatics Inc, 2018).
63. Berthet, N., Nakouné, E., Gessain, A., Manuguerra, J.-C. & Kazanji, M. Complete Genome Characterization of the Arumowot Virus (Unclassified Phlebovirus) Isolated from *Turdus libonyanus* Birds in the Central African Republic. *Vector Borne Zoonotic Dis.* **16**, 139–143 (2016).
64. Gad, A. M., Hassan, M. M., el Said, S., Moussa, M. I. & Wood, O. L. Rift Valley fever virus transmission by different Egyptian mosquito species. *Trans. R. Soc. Trop. Med. Hyg.* **81**, 694–698 (1987).
65. Grobbelaar, A. A. *et al.* Molecular Epidemiology of Rift Valley Fever Virus. *Emerging Infectious Diseases* **17**, 2270–2276 (2011).
66. Briese, T., Bird, B., Kapoor, V., Nichol, S. T. & Lipkin, W. I. Batai and Ngari Viruses: M Segment Reassortment and Association with Severe Febrile Disease Outbreaks in East Africa. *J. Virol.* **80**, 5627–5630 (2006).
67. Gerrard, S. R., Li, L., Barrett, A. D. & Nichol, S. T. Ngari virus is a Bunyamwera virus reassortant that can be associated with large outbreaks of hemorrhagic fever in Africa. *J. Virol.* **78**, 8922–8926 (2004).

68. Kemp, G. E., Causey, O. R., Setzer, H. W. & Moore, D. L. ISOLATION OF VIRUSES FROM WILD MAMMALS IN WEST AFRICA, 1966-1970. *Journal of Wildlife Diseases* **10**, 279–293 (1974).
69. Tesh, R. B., Saidi, S., Gajdamovič, S. J., Rodhain, F. & Vesenjāk-Hirjan, J. Serological studies of the epidemiology of sandfly fever in the Old World. *Bull World Health Organ* **54**, 663–674 (1976).
70. Swanepoel, R. *et al.* Comparative pathogenicity and antigenic cross-reactivity of Rift Valley fever and other African phleboviruses in sheep. *J Hyg (Lond)* **97**, 331–346 (1986).
71. Tesh, R. B. & Duboise, S. M. Viremia and immune response with sequential phlebovirus infections. *Am. J. Trop. Med. Hyg.* **36**, 662–668 (1987).
72. Olive, M.-M., Goodman, S. M. & Reynes, J.-M. The role of wild mammals in the maintenance of Rift Valley fever virus. *J. Wildl. Dis.* **48**, 241–266 (2012).
73. Linthicum, K. J. *et al.* Climate and satellite indicators to forecast Rift Valley fever epidemics in Kenya. *Science* **285**, 397–400 (1999).
74. Pepin, M., Bouloy, M., Bird, B. H., Kemp, A. & Paweska, J. Rift Valley fever virus (Bunyaviridae: Phlebovirus): an update on pathogenesis, molecular epidemiology, vectors, diagnostics and prevention. *Vet Res* **41**, (2010).
75. Chambers, P. G. & Swanepoel, R. Rift valley fever in abattoir workers. *Cent Afr J Med* **26**, 122–126 (1980).
76. Arishi, H. M., Aqeel, A. Y. & Al Hazmi, M. M. Vertical transmission of fatal Rift Valley fever in a newborn. *Ann Trop Paediatr* **26**, 251–253 (2006).
77. Lozach, P.-Y. *et al.* DC-SIGN as a receptor for phleboviruses. *Cell Host Microbe* **10**, 75–88 (2011).

78. Boer, S. M. de *et al.* Heparan Sulfate Facilitates Rift Valley Fever Virus Entry into the Cell. *J. Virol.* **86**, 13767–13771 (2012).
79. Harmon, B. *et al.* Rift Valley fever virus strain MP-12 enters mammalian host cells via caveola-mediated endocytosis. *J. Virol.* **86**, 12954–12970 (2012).
80. Filone, C. M., Heise, M., Doms, R. W. & Bertolotti-Ciarlet, A. Development and characterization of a Rift Valley fever virus cell-cell fusion assay using alphavirus replicon vectors. *Virology* **356**, 155–164 (2006).
81. Lozach, P.-Y. *et al.* Entry of bunyaviruses into mammalian cells. *Cell Host Microbe* **7**, 488–499 (2010).
82. Gerrard, S. R. & Nichol, S. T. Characterization of the Golgi Retention Motif of Rift Valley Fever Virus GN Glycoprotein. *J. Virol.* **76**, 12200–12210 (2002).
83. Ikegami, T. & Makino, S. Rift Valley fever vaccines. *Vaccine* **27S4**, D69–D72 (2009).
84. Kortekaas, J. One Health approach to Rift Valley fever vaccine development. *Antiviral Research* **106**, 24–32 (2014).
85. Botros, B. *et al.* Adverse response of non-indigenous cattle of European breeds to live attenuated Smithburn Rift Valley fever vaccine. *J. Med. Virol.* **78**, 787–791 (2006).
86. Indran, S. V. & Ikegami, T. Novel approaches to develop Rift Valley fever vaccines. *Front Cell Infect Microbiol* **2**, 131 (2012).
87. Terasaki, K., Tercero, B. R. & Makino, S. Single-cycle replicable Rift Valley fever virus mutants as safe vaccine candidates. *Virus Res.* **216**, 55–65 (2016).
88. Warimwe, G. M. *et al.* Chimpanzee Adenovirus Vaccine Provides Multispecies Protection against Rift Valley Fever. *Scientific Reports* **6**, 20617 (2016).

89. Faburay, B. *et al.* A Recombinant Rift Valley Fever Virus Glycoprotein Subunit Vaccine Confers Full Protection against Rift Valley Fever Challenge in Sheep. *Scientific Reports* **6**, 27719 (2016).
90. Terasaki, K., Murakami, S., Lokugamage, K. G. & Makino, S. Mechanism of tripartite RNA genome packaging in Rift Valley fever virus. *PNAS* **108**, 804–809 (2011).
91. Minor, P. D. Live attenuated vaccines: Historical successes and current challenges. *Virology* **479–480**, 379–392 (2015).
92. Muga, G. O., Onyango-Ouma, W., Sang, R. & Affognon, H. Sociocultural and economic dimensions of Rift Valley fever. *Am. J. Trop. Med. Hyg.* **92**, 730–738 (2015).
93. 01\_rift\_valley\_fever\_complete.pdf.
94. Ikegami, T. & Makino, S. The Pathogenesis of Rift Valley Fever. *Viruses* **3**, 493–519 (2011).
95. Linthicum, K. J., Davies, F. G., Kairo, A. & Bailey, C. L. Rift Valley fever virus (family Bunyaviridae, genus Phlebovirus). Isolations from Diptera collected during an inter-epizootic period in Kenya. *J Hyg (Lond)* **95**, 197–209 (1985).
96. Seufi, A. M. & Galal, F. H. Role of Culex and Anopheles mosquito species as potential vectors of rift valley fever virus in Sudan outbreak, 2007. *BMC Infect Dis* **10**, 65 (2010).
97. Bowen, M. D. *et al.* A reassortant bunyavirus isolated from acute hemorrhagic fever cases in Kenya and Somalia. *Virology* **291**, 185–190 (2001).
98. Alkan, C. *et al.* Sandfly-borne phleboviruses of Eurasia and Africa: epidemiology, genetic diversity, geographic range, control measures. *Antiviral Res.* **100**, 54–74 (2013).
99. Tesh, R. B. The genus Phlebovirus and its vectors. *Annu. Rev. Entomol.* **33**, 169–181 (1988).

100. Ito, N. *et al.* Improved recovery of rabies virus from cloned cDNA using a vaccinia virus-free reverse genetics system. *Microbiol. Immunol.* **47**, 613–617 (2003).
101. Ikegami, T., Won, S., Peters, C. J. & Makino, S. Rescue of infectious rift valley fever virus entirely from cDNA, analysis of virus lacking the NSs gene, and expression of a foreign gene. *J. Virol.* **80**, 2933–2940 (2006).
102. Ikegami, T., Peters, C. J. & Makino, S. Rift Valley Fever Virus Nonstructural Protein NSs Promotes Viral RNA Replication and Transcription in a Minigenome System. *J. Virol.* **79**, 5606–5615 (2005).
103. Kalveram, B., Lihoradova, O., Indran, S. V. & Ikegami, T. Using reverse genetics to manipulate the NSs gene of the Rift Valley fever virus MP-12 strain to improve vaccine safety and efficacy. *J Vis Exp* e3400 (2011). doi:10.3791/3400
104. Coleman, J. R. *et al.* Virus attenuation by genome-scale changes in codon pair bias. *Science* **320**, 1784–1787 (2008).
105. Gutman, G. A. & Hatfield, G. W. Nonrandom utilization of codon pairs in *Escherichia coli*. *Proc. Natl. Acad. Sci. U.S.A.* **86**, 3699–3703 (1989).
106. Moura, G. *et al.* Comparative context analysis of codon pairs on an ORFeome scale. *Genome Biol* **6**, R28 (2005).
107. Rare Codon Analysis Tool. Available at: <https://www.genscript.com/tools/rare-codon-analysis>. (Accessed: 30th July 2018)
108. Puigbò, P., Bravo, I. G. & Garcia-Vallve, S. CAIcal: A combined set of tools to assess codon usage adaptation. *Biology Direct* **3**, 38 (2008).
109. Freire, C. C. M. *et al.* Reassortment and distinct evolutionary dynamics of Rift Valley Fever virus genomic segments. *Sci Rep* **5**, (2015).

110. Sall, A. A. *et al.* Genetic Reassortment of Rift Valley Fever Virus in Nature. *J. Virol.* **73**, 8196–8200 (1999).
111. Fields, B. N., Henderson, B. E., Coleman, P. H. & Work, T. H. Pahayokee and Shark River, two new arboviruses related to Patois and Zegla from the Florida everglades. *Am. J. Epidemiol.* **89**, 222–226 (1969).
112. Klimas, R. A. *et al.* GENOTYPIC VARIETIES OF LA CROSSE VIRUS ISOLATED FROM DIFFERENT GEOGRAPHIC REGIONS OF THE CONTINENTAL UNITED STATES AND EVIDENCE FOR A NATURALLY OCCURRING INTERTYPIC RECOMBINANT LA CROSSE VIRUS. *Am J Epidemiol* **114**, 112–131 (1981).
113. Ushijima, H., Clerx-Van Haaster, C. M. & Bishop, D. H. L. Analyses of patois group bunyaviruses: Evidence for naturally occurring recombinant bunyaviruses and existence of immune precipitable and nonprecipitable nonvirion proteins induced in bunyavirus-infected cells. *Virology* **110**, 318–332 (1981).
114. Accardi, L. *et al.* Activity of Toscana and Rift Valley fever virus transcription complexes on heterologous templates. *J. Gen. Virol.* **82**, 781–785 (2001).
115. Bird, B. H., Khristova, M. L., Rollin, P. E., Ksiazek, T. G. & Nichol, S. T. Complete genome analysis of 33 ecologically and biologically diverse Rift Valley fever virus strains reveals widespread virus movement and low genetic diversity due to recent common ancestry. *J. Virol.* **81**, 2805–2816 (2007).
116. Miller, M. M. *et al.* Evaluation of the Efficacy, Potential for Vector Transmission, and Duration of Immunity of MP-12, an Attenuated Rift Valley Fever Virus Vaccine Candidate, in Sheep. *Clin. Vaccine Immunol.* **22**, 930–937 (2015).

117. Turell, M. J. & Rossi, C. A. Potential for mosquito transmission of attenuated strains of Rift Valley fever virus. *Am. J. Trop. Med. Hyg.* **44**, 278–282 (1991).
118. Ikegami, T. *et al.* Rift Valley Fever Virus MP-12 Vaccine Is Fully Attenuated by a Combination of Partial Attenuations in the S, M, and L Segments. *J. Virol.* **89**, 7262–7276 (2015).
119. Carroll, S. A. *et al.* Genetic evidence for Rift Valley fever outbreaks in Madagascar resulting from virus introductions from the East African mainland rather than enzootic maintenance. *J. Virol.* **85**, 6162–6167 (2011).
120. Alhaj, M. Safety and Efficacy Profile of Commercial Veterinary Vaccines against Rift Valley Fever: A Review Study. *Journal of Immunology Research* (2016). doi:10.1155/2016/7346294
121. The use of veterinary vaccines for prevention and control of Rift Valley fever: Memorandum from a WHO/FAO Meeting. *Bull World Health Organ* **61**, 261–268 (1983).
122. Caplen, H., Peters, C. J. & Bishop, D. H. Mutagen-directed attenuation of Rift Valley fever virus as a method for vaccine development. *J. Gen. Virol.* **66 ( Pt 10)**, 2271–2277 (1985).
123. NOTICE: CVB Notice 13-12 Conditional License Issuance. *USDA Animal and Plant Health Inspection Service Available at: <https://content.govdelivery.com/accounts/USDAAPHIS/bulletins/8a8a59>*. (Accessed: 30th July 2018)
124. Morrill, J. C. *et al.* Further evaluation of a mutagen-attenuated Rift Valley fever vaccine in sheep. *Vaccine* **9**, 35–41 (1991).
125. Morrill, J. C. *et al.* Pathogenicity and immunogenicity of a mutagen-attenuated Rift Valley fever virus immunogen in pregnant ewes. *Am. J. Vet. Res.* **48**, 1042–1047 (1987).

126. Morrill, J. C., Mebus, C. A. & Peters, C. J. Safety of a mutagen-attenuated Rift Valley fever virus vaccine in fetal and neonatal bovids. *Am. J. Vet. Res.* **58**, 1110–1114 (1997).
127. Morrill, J. C., Mebus, C. A. & Peters, C. J. Safety and efficacy of a mutagen-attenuated Rift Valley fever virus vaccine in cattle. *Am. J. Vet. Res.* **58**, 1104–1109 (1997).
128. Ikegami, T. Rift Valley fever vaccines: an overview of the safety and efficacy of the live-attenuated MP-12 vaccine candidate. *Expert Rev Vaccines* **16**, 601–611 (2017).
129. Ly, H. J., Lokugamage, N., Nishiyama, S. & Ikegami, T. Risk analysis of inter-species reassortment through a Rift Valley fever phlebovirus MP-12 vaccine strain. *PLOS ONE* **12**, e0185194 (2017).
130. Lihoradova, O. *et al.* The Dominant-Negative Inhibition of Double-Stranded RNA-Dependent Protein Kinase PKR Increases the Efficacy of Rift Valley Fever Virus MP-12 Vaccine. *J. Virol.* **86**, 7650–7661 (2012).
131. Lihoradova, O. A. *et al.* Characterization of Rift Valley fever virus MP-12 strain encoding NSs of Punta Toro virus or sandfly fever Sicilian virus. *PLoS Negl Trop Dis* **7**, e2181 (2013).
132. Nishiyama, S., Lokugamage, N. & Ikegami, T. The L, M, and S Segments of Rift Valley Fever Virus MP-12 Vaccine Independently Contribute to a Temperature-Sensitive Phenotype. *J. Virol.* **90**, 3735–3744 (2016).
133. Billecocq, A. *et al.* RNA polymerase I-mediated expression of viral RNA for the rescue of infectious virulent and avirulent Rift Valley fever viruses. *Virology* **378**, 377–384 (2008).
134. Nishiyama, S. *et al.* Attenuation of pathogenic Rift Valley fever virus strain through the chimeric S-segment encoding sandfly fever phlebovirus NSs or a dominant-negative PKR. *Virulence* **7**, 871–881 (2016).

135. Morrill, J. C. *et al.* Safety and immunogenicity of recombinant Rift Valley fever MP-12 vaccine candidates in sheep. *Vaccine* **31**, 559–565 (2013).
136. Morrill, J. C. *et al.* Immunogenicity of a Recombinant Rift Valley Fever MP-12-NSm Deletion Vaccine Candidate in Calves. *Vaccine* **31**, (2013).
137. Bird, B. H., Albariño, C. G. & Nichol, S. T. Rift Valley fever virus lacking NSm proteins retains high virulence in vivo and may provide a model of human delayed onset neurologic disease. *Virology* **362**, 10–15 (2007).
138. Cook, I. F. Evidence based route of administration of vaccines. *Hum Vaccin* **4**, 67–73 (2008).
139. Herzog, C. Influence of parenteral administration routes and additional factors on vaccine safety and immunogenicity: a review of recent literature. *Expert Rev Vaccines* **13**, 399–415 (2014).
140. LaBeaud, A. D., Cross, P. C., Getz, W. M., Glinka, A. & King, C. H. Rift Valley Fever Virus Infection in African Buffalo (*Syncerus caffer*) Herds in Rural South Africa: Evidence of Interepidemic Transmission. *Am J Trop Med Hyg* **84**, 641–646 (2011).
141. Ikegami, T., Won, S., Peters, C. J. & Makino, S. Characterization of Rift Valley Fever Virus Transcriptional Terminations. *J Virol* **81**, 8421–8438 (2007).
142. Schreur, P. J. W., Oreshkova, N., Moormann, R. J. M. & Kortekaas, J. Creation of Rift Valley Fever Viruses with Four-Segmented Genomes Reveals Flexibility in Bunyavirus Genome Packaging. *J. Virol.* **88**, 10883–10893 (2014).
143. Gaudiard, N., Billecocq, A., Flick, R. & Bouloy, M. Rift Valley fever virus noncoding regions of L, M and S segments regulate RNA synthesis. *Virology* **351**, 170–179 (2006).

144. Bennett, R. S., Gresko, A. K., Nelson, J. T., Murphy, B. R. & Whitehead, S. S. A Recombinant Chimeric La Crosse Virus Expressing the Surface Glycoproteins of Jamestown Canyon Virus Is Immunogenic and Protective against Challenge with either Parental Virus in Mice or Monkeys. *Journal of Virology* **86**, 420–426 (2012).
145. Ly, H. J. & Ikegami, T. Rift Valley fever virus NSs protein functions and the similarity to other bunyavirus NSs proteins. *Virol J* **13**, (2016).
146. Wuerth, J. D. & Weber, F. Phleboviruses and the Type I Interferon Response. *Viruses* **8**, (2016).
147. Ikegami, T., Won, S., Peters, C. J. & Makino, S. Rift Valley Fever Virus NSs mRNA Is Transcribed from an Incoming Anti-Viral-Sense S RNA Segment. *Journal of Virology* **79**, 12106–12111 (2005).
148. Ly, H. J., Lokugamage, N. & Ikegami, T. Application of Droplet Digital PCR to Validate Rift Valley Fever Vaccines. *Methods Mol. Biol.* **1403**, 207–220 (2016).
149. Bichaud, L. *et al.* Isolation, full genomic characterization and neutralization-based human seroprevalence of Medjerda Valley virus, a novel sandfly-borne phlebovirus belonging to the Salehabad virus complex in northern Tunisia. *J. Gen. Virol.* **97**, 602–610 (2016).
150. Verani, P. *et al.* Ecology of viruses isolated from sand flies in Italy and characterized of a new Phlebovirus (Arabia virus). *Am. J. Trop. Med. Hyg.* **38**, 433–439 (1988).
151. Palacios, G. *et al.* Characterization of the Salehabad virus species complex of the genus Phlebovirus (Bunyaviridae). *J Gen Virol* **94**, 837–842 (2013).
152. Papa, A., Velo, E. & Bino, S. A novel phlebovirus in Albanian sandflies. *Clinical Microbiology and Infection* **17**, 585–587 (2011).

153. Alkan, C. *et al.* Isolation, Genetic Characterization, and Seroprevalence of Adana Virus, a Novel Phlebovirus Belonging to the Salehabad Virus Complex, in Turkey. *J Virol* **89**, 4080–4091 (2015).
154. Amaro, F. *et al.* Co-circulation of a novel phlebovirus and Massilia virus in sandflies, Portugal. *Virol. J.* **12**, 174 (2015).
155. Calzolari, M. *et al.* Isolation of three novel reassortant phleboviruses, Ponticelli I, II, III, and of Toscana virus from field-collected sand flies in Italy. *Parasit Vectors* **11**, 84 (2018).
156. Peyrefitte, C. N. *et al.* Diversity of Phlebotomus perniciosus in Provence, southeastern France: Detection of two putative new phlebovirus sequences. *Vector Borne Zoonotic Dis.* **13**, 630–636 (2013).
157. Anagnostou, V., Pardalos, G., Athanasiou-Metaxa, M. & Papa, A. Novel Phlebovirus in Febrile Child, Greece. *Emerg Infect Dis* **17**, 940–941 (2011).
158. Nyundo, S. *et al.* Safety and immunogenicity of Rift Valley fever MP-12 and arMP-12ΔNSm21/384 vaccine candidates in goats (*Capra aegagrus hircus*) from Tanzania. *Onderstepoort J Vet Res* **86**, (2019).
159. Brackney, D. E. *et al.* C6/36 *Aedes albopictus* Cells Have a Dysfunctional Antiviral RNA Interference Response. *PLoS Negl Trop Dis* **4**, (2010).
160. Sibold, C. *et al.* Recombination in Tula hantavirus evolution: analysis of genetic lineages from Slovakia. *J. Virol.* **73**, 667–675 (1999).

## VITAE

**NAME** **Hoai Jaclyn Hallam (Ly)**

**PRESENT POSITION** Graduate Student Research Assistant  
Department of Experimental Pathology  
Graduate School of Biomedical Science  
University of Texas Medical Branch  
301 University Boulevard, Galveston, TX 77555  
Phone: 409-747-8158  
Email: [hjly@utmb.edu](mailto:hjly@utmb.edu)

### EDUCATION

In Progress	Ph.D in Experimental Pathology	University of Texas Medical Branch Galveston, TX
2014	MPH in Epidemiology	Texas A&M University College Station, TX
2012	B.S. in Microbiology	The University of Texas Austin, TX

### HONORS

#### Predocctoral Scholarship

2018	Recipient, Jeane B. Kempner Award, The University of Texas Medical Branch at Galveston
2017	Recipient, SCVD Predocctoral Fellowship

#### GSBS Scholarship

2018	Recipient, Robert Shope Endowed Scholarship, The University of Texas Medical Branch at Galveston
2017	Recipient, Robert Shope Endowed Scholarship, The University of Texas Medical Branch at Galveston
2016	Recipient, Robert Shope Endowed Scholarship, The University of Texas Medical Branch at Galveston
2015	Recipient, GSBS Associates Scholarship, The University of Texas Medical Branch at Galveston
2015	Recipient, Harold T. Sanders Endowed Fellowship in Vaccine Development, The University of Texas Medical Branch at Galveston

#### Travel award

2018	Recipient, SIVS Travel award, The 12 <sup>th</sup> Vaccine Congress, Budapest, Hungary
------	--

- 2018 Recipient, SCVD Travel award, 2018 21<sup>st</sup> Annual Conference on Vaccine Research, Bethesda, Maryland
- 2017 Recipient, SCVD Travel award, The International Society for Vaccine Annual Congress, Paris, France
- 2017 Recipient, SCVD Travel award, The 11th Vaccine Meeting, San Diego, CA
- 2017 Recipient, SCVD Travel award, 20th Annual Conference on Vaccine Research, Bethesda, Maryland
- 2016 Recipient, Sealy Center of Vaccine Development (SCVD) travel award, The 10th Vaccine Congress, Amsterdam, The Netherlands
- 2015 Recipient, Travel award, the 34th Annual Meeting, American Society for Virology, Western Ontario, Canada

Poster award

Other awards

- 2013 Recipient, Public Health in China at Nanjing Medical University International Education Scholarship, Texas A&M University
- 2012 Participant, Research Experience for Undergraduate, National Science Foundation
- 2011 Recipient, Undergraduate Research Fellowship, The University of Texas at Austin
- 2009 Recipient, Texas Exes Local Chapter Scholarship, The University of Texas at Austin
- 2008 Recipient, Knights of Columbus Scholarship, The University of Texas at Austin
- 2008 Recipient, Gabriel Lester Memorial, Republican Club of Washington County Scholarship, The University of Texas at Austin

**PROFESSIONAL WORK HISTORY**

Academic Positions

- 2017 Intern – Mentor: Dr. Alan Barrett  
World Health Organization Collaboration Center  
The University of Texas Medical Branch  
Galveston, TX
- 2013 – 2014 Research Technician – Mentor: Dr. Tetsuro Ikegami  
The University of Texas Medical Branch  
Galveston, TX
- 2013 Graduate Research Assistant Intern – Mentor: Dr. Xifeng Wu  
MD Anderson Cancer Center  
Houston, TX
- 2012 – 2014 Research Assistant – Mentor: Dr. Aline Rodrigues-Hoffmann  
Texas A&M University  
College Station, TX
- 2011 – 2012 Student Researcher – Mentors: Drs. Quinn McFrederick, and Ulrich Mueller  
The University of Texas at Austin

Austin, TX  
2010 – 2011 Undergraduate Research Assistant – Mentor: Dr. Rasika Harshey  
The University of Texas at Austin  
Austin, TX

## RESEARCH ACTIVITIES

Area of Research: My long-term goal is to be an independent researcher in the field of infectious diseases and to handle globally important public health problems through vaccinations and antivirals. I am open in my future career path; government, academia, or industry, however, I have a strong desire to take on further research training at the postdoctoral level after my PhD, and expand my professional network through my own publications and projects. During the graduate program, I gained the following skills to further assist me towards my future career: i.e., experimental design, analysis of data, publication of manuscripts, grant writing, oral presentations, and other career development activities. I have a strong interest in learning molecular virology, in particular highly pathogenic RNA viruses with public health importance. My project at Dr. Ikegami's lab was to characterize reassortments formed through Rift Valley fever phlebovirus (RVFV). I was able to rescue a recombinant MP-12 strain encoding more than 500 silent mutations throughout the genome, which inspired my scientific interest in the role of those genetic changes in viral replication and attenuation. I also rescued the recombinant Arumowot virus via the reverse genetics system, which was the first among the Salehabad species complex among the phlebovirus genus.

## MEMBERSHIP IN SCIENTIFIC SOCIETIES/PROFESSIONAL ORGANIZATIONS:

2018-present	Success Networking Team Coordinator, The National Society of Leadership and Success
2016-present	Associate Member, American Association for the Advancement of Science
2015-present	Associate Member, American Society for Virology
2015-present	Associate Member, Institute for Human Infections & Immunity
2012-13	Social Chair, Epidemiology Student Organization – Texas A&M University
2012-present	Member, Association of Public Health Laboratories
2009-13	Vice President of Public Relations (2011-2012), Sigma Alpha Lambda National Leadership and Honors Organization – The University of Texas at Austin Chapter
2008-present	Member, Texas Exes Member

## PUBLICATIONS

### A. ARTICLES IN PEER-REVIEWED JOURNALS:

1. **Hallam HJ**, Hallam S, Rodriguez SE, Barrett A, Beasley D, Chua A, Ksiazek TG, Milligan GN, Sathiyamoorthy V, Reece LM. 2018. Baseline mapping of Lassa fever virology, epidemiology and vaccine research and development. *npj Vaccines*, 3: 11.
2. **Ly HJ**, Nishiyama S, Lokugamage N, Smith JK, Zhang L, Perez D, Juelich TL, Freiberg AN, Ikegami T. Attenuation and protective efficacy of Rift Valley fever phlebovirus

rMP12-GM50 strain. *Vaccine*. 2017; 35: 6634-6642. PubMed PMID: 29061350; PubMed Central PMCID: PMC5696010.

3. **Ly HJ**, Lokugamage N, Nishiyama S, Ikegami T. Risk analysis of inter-species reassortment through a Rift Valley fever phlebovirus MP-12 vaccine strain. *PLoS One*. 2017;12(9):e0185194. PubMed PMID: 28926632; PubMed Central PMCID: PMC5604998.
4. **Ly HJ**, Ikegami T. Rift Valley fever virus NSs protein functions and the similarity to other bunyavirus NSs proteins. *Viol. J.* 13: 118. 2016. PMCID: PMC4930582.
5. Ikegami T, Hill TE, Smith JK, Zhang L, Juelich TL, Gong B, Slack OA, **Ly HJ**, Lokugamage N, Freiberg AN. Rift Valley fever virus MP-12 vaccine is fully attenuated by a combination of partial attenuations in the S-, M- and L-segments. *J. Virol.* 89: 7262-76. 2015. PMCID: PMC4473576.
6. Zychowski K, Elmore S, Rychlik K, **Ly H**, Pierezan F, Isaiah A, Suchodolski J, Rodrigues Hoffmann A, Romoser A, Phillips T. Mitigation of colitis with NovaSil clay therapy. *Digestive Diseases and Sciences*, 60(2): 382-92. 2014. PMID: 25240298.
7. Rodrigues Hoffmann A, Patterson A, Diesel A, **Ly H**, Elkins C, Mansell J, Steiner J, Dowd S, Olivry T, Suchodolski J. The Skin Microbiome in Healthy and Allergic Dogs. *PLoS ONE*, 9(1): e83197. 2013. PMCID: PMC3885435.
8. Zychowski K, Rodrigues Hoffmann A, **Ly H**, Buentello A, Romoser A, Gatlin D, Phillips T. The effect of Aflatoxin-B1 on red drum (*Sciaenops ocellatus*) and assessment of dietary supplementation of NovaSil for the prevention of aflatoxicosis. *Toxins*, 5(9): 1555-1573. 2013. PMCID: PMC37988873.

## B. OTHER:

### Book Chapters

1. **Ly HJ**, Lokugamage N, Ikegami T. Application of droplet digital PCR to validate Rift Valley fever vaccines. In *Vaccine Design: Methods and Protocols*, Methods in Molecular Biology, 1403: 207-220. Springer, NY. 2016. PMID: 27076132.

## C. ABSTRACTS:

1. **Hallam H**, Lokugamage N, Ikegami T. "Characterization of the genetic compatibility between a Rift Valley fever virus MP-12 vaccine strain and the Arumowot virus". 12th Vaccine Congress, Budapest, Hungary, 2018
2. **Hallam H**, Lokugamage N, Ikegami T. "Characterization of the genetic compatibility between Rift Valley fever virus and Arumowot virus". National Foundation for Infectious Diseases 21st Annual Conference on Vaccine, Bethesda, Maryland, 2018
3. **Ly H**, Lokugamage N, Ikegami T. "Arumowot Virus NSs Proteins Inhibit the Upregulation of Murine but not Human Interferon Beta". IHII/McLaughlin Colloquium on Infection & Immunity, UTMB, Galveston, 2017
4. **Ly H**, Lokugamage N, Ikegami T. "Characterization of inter-species reassortment through a Rift Valley fever virus MP-12 vaccine strain" International Society of Vaccine Annual Congress, Paris, France, 2017
5. **Ly H**, Lokugamage N, Ikegami T. "Characterization of the genetic compatibility between Rift Valley fever virus MP-12 strain and Arumowot virus for the reassortant risk

- analysis". 11th Vaccine Congress, San Diego, CA, 2017
6. **Ly H**, Lokugamage N, Ikegami T. "Characterization of Defective Interfering RNA Generated in Cells Persistently Co-infected with Rift Valley Fever Virus MP-12 Strain and the Variant". National Foundation for Infectious Diseases 20th Annual Conference on Vaccine, Bethesda, Maryland, 2017
  7. **Ly H**, Lokugamage N, Ikegami T. "Characterization of mosquito and mammalian cells persistently co-infected with Rift Valley fever virus MP-12 strain and the genetic variant". 10th Vaccine Congress, Amsterdam, The Netherlands, 2016
  8. **Ly H**, Lokugamage N, Ikegami T. "Characterization of persistently infected C6/36 cells with Rift Valley fever virus MP-12 strains". IHII/McLaughlin Colloquium on Infection & Immunity, UTMB, Galveston, 2016
  9. **Ly H**, Lokugamage N, Ikegami T. "Characterization of persistently infected C6/36 cells with Rift Valley fever virus MP-12 strains". 22nd Annual Pathology Trainee Research, UTMB, Galveston, 2016
  10. **Ly H**, Lokugamage N, Ikegami T. "Characterization of persistently infected C6/36 cells with Rift Valley fever virus MP-12 strains". 35th Annual Meeting of the American Society for Virology, Virginia Tech, Blacksburg, Virginia, 2016
  11. **Ly H**, Lokugamage N, Ikegami T. "Development of Rift Valley Fever Virus MP-12 Vaccine with Silent Mutation Markers for Reassortment and Recombination Analyses between RVFV Strains". IHII/McLaughlin Colloquium on Infection & Immunity, UTMB, Galveston, 2015
  12. **Ly H**, Lokugamage N, Ikegami T. "Development of Rift Valley Fever Virus MP-12 Vaccine with Silent Mutation Markers for Reassortment and Recombination Analyses between RVFV Strains". 21st Annual Pathology Trainee Research, UTMB, Galveston, 2015
  13. **Ly H**, Lokugamage N, Ikegami T. "Development of Rift Valley Fever Virus MP-12 Vaccine with Silent Mutation Markers for Reassortment and Recombination Analyses between RVFV Strains". 34th Annual Meeting of the American Society for Virology, Western University London ON, Canada, 2015
  14. **Ly H**, Lokugamage N, Ikegami T. "Rift Valley fever virus MP-12 vaccine with silent mutation markers for reassortment and recombination analyses between RVFV strains". National Foundation for Infectious Diseases 18th Annual Conference on Vaccine, Bethesda, Maryland, 2015